The Minimal Scale Invariant Extension of the Standard Model

A thesis submitted to the University of Manchester for the degree of

Doctor of Philosophy

in the Faculty of Engineering and Physical Sciences

2010

Lisa Pamela Alexander-Nunneley

School of Physics and Astronomy

Contents

Total word count: 24036

List of Tables

List of Figures

Abstract

The Minimal Scale Invariant Extension of the Standard Model

The Minimal Scale Invariant extension of the Standard Model (MSISM) is a model of low-energy particle physics which is identical to the Standard Model except for the inclusion of an additional complex singlet scalar and tree-level scale invariance. Scale invariance is a classical symmetry which is explicitly broken by quantum corrections whose interplay with the quartic couplings can be used to trigger electroweak symmetry breaking. The scale invariant Standard Model suffers from a number of problems, however the inclusion of a complex singlet scalar results in a perturbative and phenomenologically viable theory.

We present a thorough and systematic investigation of the MSISM for a number of representative scenarios along two of its three classified types of flat direction. In these scenarios we determine the permitted quartic coupling parameter space, using both theoretical and experimental constraints, and apply these limits to make predictions of the scalar mass spectrum and the energy scale at which scale invariance is broken. We calculate the one-loop effective potential and the one-loop β functions of the pertinent couplings of the MSISM specifically for this purpose. We also discuss the phenomenological implications of these scenarios, in particular, whether they realise explicit or spontaneous CP violation, contain neutrino masses or provide dark matter candidates. Of particular importance is the discovery of a new minimal scale invariant model which provides maximal spontaneous CP violation, can naturally incorporate neutrino masses, produces a massive stable scalar dark matter candidate and can remain perturbative up to the Planck scale. It can be argued that the last property, along with the classical scale invariance, can potentially solve the gauge hierarchy problem for this model.

Lisa Pamela Alexander-Nunneley
The University of Manchester

For the degree of Doctor of Philosophy
September 2010

Declaration

No portion of the work referred to in this thesis has been submitted in support of an application for another degree or qualification of this or any other university or other institution of learning.

Lisa Pamela Alexander-Nunneley
School of Physics and Astronomy
The University of Manchester
Oxford Road
Manchester
M13 9PL
September 2010

Copyright

aboutus/regulations) and in The Universitys policy on presentation of Theses.

Acknowledgements

My first thank-you goes to my supervisor Professor Apostolos Pilaftsis for his guidance throughout the past four years and for choosing an interesting and challenging project for me to focus my thesis on. I would also like to thank everybody at the University of Manchester particle physics group who have helped me along the way, especially those who have answered my many questions. For her continued post-Durham support and advice, my thanks go to Silvia Pascoli. I would also like Tim, Neil, Pete and Phil to know that I greatly appreciate them taking the time to read draft copies of my thesis. For solving all my computer worries, including saving all my first and second year work from a virus, I would like to thank Sabah and Stuart.

I would also like to thank the participants of the Workshop on Multi-Higgs Models in Lisbon, Portugal (16^{th} – 18^{th} September 2009), for their comments and suggestions on my presentation.

On a more person note, my thanks go to Jenna, Graham, Chris and Tom for being in the same boat at the same time and for being there to trade PhD stories, both the good ones and the bad ones. I would also like to thank my family for all their support, encouragement and pride in what I'm attempting to achieve.

Finally, for being the best husband I could ever want or need, my biggest thank-you deservedly goes to my husband Pete.

Chapter 1

Introduction

Understanding the nature of electroweak symmetry breaking is one of the most important challenges of particle physics today. The solution to this puzzle will not only answer the fundamental question of where the masses of the elementary particles come from, but will undoubtedly require an extension to the current theory of particle physics: the Standard Model (SM). The SM[1] is a renormalisable gauge field theory with a minimal particle content that includes both the electroweak theory of Glashow, Weinberg and Salam [4], described by the $SU(2)_L \times U(1)_Y$ gauge groups, and Quantum Chromodynamics (QCD) which is based on the $SU(3)_c$ colour gauge group [5]. After rigorous testing at the LEP collider, Tevatron and a number of low energy experiments [6], the SM appears to describe the fundamental interactions up to energies of the order of 100 GeV remarkably well and with very high precision. For example, prior to its experimental detection, successful predictions of the top quark mass were made based on quantum fluctuations to within 10% of the physical value eventually measured at the CDF and D0 detectors at Tevatron [7]. Given the experimental successes of the rest of particle physics, it is particularly surprising how little is known about the nature of electroweak symmetry breaking.

In the SM, the electroweak symmetry is thought to be broken spontaneously

[1] For reviews of the SM see for example [1, 2, 3].

and the $W^{\pm}$ and Z boson masses generated via the Higgs mechanism [8]. For this to happen, a complex scalar doublet field with a negative mass squared parameter $-m^2$ ($m^2 > 0$), a quartic self-coupling λ and a non-zero vacuum expectation value (VEV) needs to be included in the model. Once the scalar field is postulated, it can also be used to generate the fermion masses. Thus the SM predicts the existence of an additional massive scalar to the known particle content: the Higgs boson (H_{SM}). However, to-date, this Higgs boson has evaded all experimental searches. This non-detection has not been fruitless but has provided strong experimental constraints on the mass of the SM Higgs: the LEP2 Higgs mass limit requires $m_{H_{SM}} > 114.4\,\mathrm{GeV}$ [9], whilst recent results from the Tevatron exclude masses in the region $158\,\mathrm{GeV} < m_{H_{SM}} < 175\,\mathrm{GeV}$ [10]. These limits are not inconsistent with the theoretical limits from unitarity, triviality and vacuum stability. Unitarity places an upper bound of $m_{H_{\mathrm{SM}}} \leq 1$ TeV [11], beyond which perturbative unitarity cannot be maintained. The triviality bound provides an upper limit on $m_{H_{\mathrm{SM}}}$ by pushing the Landau pole beyond a specific energy scale Q. Requiring vacuum stability gives a lower bound on the Higgs mass by demanding that the potential stay bounded from below (BFB) or $\lambda(Q) \geq 0$. These last two constraints are commonly displayed on a "chimney plot" (for example see Figure 6 of [12]) and assuming Q is of the order of the Planck scale $M_{\mathrm{Planck}} \approx 10^{19}$ GeV then $m_{H_{\mathrm{SM}}} \sim 160 - 170$ GeV [12].

As well as the currently undetected Higgs boson, the SM also suffers from the infamous gauge hierarchy problem [13] as a result of the negative mass squared parameter. In the SM, the fermions and gauge bosons are massless before electroweak spontaneous symmetry breaking (EWSSB) due to the chiral and gauge symmetries respectively. This means that any masses they obtain after EWSSB are protected from quantum corrections. However, the Higgs boson has no such symmetry to protect its mass from the large quantum corrections which contain quadratically divergent terms proportional to Λ^2, where Λ is an ultra-violet (UV)

cut-off scale. This UV cut-off scale is usually associated with the scale of a possible higher-energy theory in which the SM is embedded, such as a Grand Unified Theory (GUT), which occur at scales $M_{\rm GUT} \approx 10^{16}$ GeV. In the SM, which has no intermediate mass scale or theory between the electroweak (EW) and Planck scale, the cancellation of the divergent terms requires an excessive amount of fine-tuning to give a Higgs mass of the order of the EW scale. Many beyond the SM theories have been postulated with the aim of trying to avoid the gauge hierarchy problem, these include Supersymmetry (SUSY). In SUSY this problem is naturally solved provided the SUSY-breaking scale, $M_{\rm SUSY}$, stays close to the EW scale ($M_{\rm SUSY} \lesssim 1$ TeV). In this thesis, we propose a different and very minimal approach that could solve the gauge hierarchy problem: imposing tree-level scale invariance.

A classically scale invariant (SI) theory naturally excludes any dimensionful parameters, including the negative scalar mass squared parameter, from the Higgs potential. The removal of the $-m^2$ term does not solve the gauge hierarchy problem in itself, as Λ^2 terms can still be generated by quantum corrections in a regularisation scheme with a UV cut-off. However, the quadratic divergences introduced by the UV cut-off regularisation scheme explicitly violate the symmetry of scale invariance. One may argue that if two regularisation schemes provide different answers for observable quantities, which usually results from one or both violating a symmetry of the theory, and if the symmetry is taken to be fundamental, a new axiom of the theory, then the regularisation scheme which preserves the symmetry must be applied. Following the arguments of [14, 15, 16], the quadratic divergences in a SI theory are considered to be only spurious effects of the regularisation process and to remove them one has to simply adopt a regularisation scheme which does not break the classical symmetries of the local classical action, in this case scale invariance. Dimensional regularisation (DR) [17] is such a SI scheme within which the vanishing of the mass squared parameter is maintained to all orders in perturbation theory. A further two requirements are suggested

by [16]; firstly, that the theory has no intermediate scales between the EW and Planck scale and secondly, that the running couplings have neither Landau poles nor instabilities before the Planck scale. Consequently, provided DR is used as the renormalisation scheme and the above criteria are met, the gauge hierarchy problem can be considered to be removed in SI theories.

We should mention that SI models are not without their own problems. An inherent field-theoretic difficulty of a SI model is the incorporation of gravity which requires the introduction of a dimensionful parameter, the Planck mass, $M_{\rm Pl}$. The presence of a Planck mass would explicitly break the classical symmetry of scale invariance and thereby reintroduce the issue of quadratic divergences. Addressing this problem lies beyond the scope of this work, but we note that attempts have been made in the literature [15, 16, 18, 19] to provide SI descriptions of quantum gravity.

It is remarkable that the removal of the one and only dimensionful parameter $-m^2$, which has been included for the sole purpose of generating EWSSB, would render the whole tree-level Lagrangian of the SM naturally SI. However, as first discussed by Coleman and E. Weinberg [20] and later by Gildener and S. Weinberg [21], the exclusion of the $-m^2$ term does not necessarily mean the removal of EWSSB. This is because quantum corrections generate logarithmic terms which explicitly break the scale invariance of the theory and can trigger EWSSB. In this case, the VEVs of any scalar fields would be determined by a balance between the scalar quartic term and the quantum corrections rather than between the quartic term and a scalar mass term, which is the case for the SM. The seemingly simple solution of imposing scale invariance on the SM is complicated and suffers from a number of issues. To overcome these problems, several authors have considered various SI extensions to the SM either with real or complex singlet scalar fields [15, 18, 22, 23, 24, 25, 26, 27, 28].

In this thesis, we present a detailed study of a SI extension of the SM which includes a new complex singlet scalar field, S, which transforms as a singlet

under SU(3)$_c\times$ SU(2)$_L\times$U(1)$_Y$. We call this model the Minimal Scale Invariant extension of the Standard Model (MSISM) [29]. Unlike the aforementioned scalar extended SI SM analyses, we impose no additional constraints on the theory, for example a U(1) symmetry or some other specific discrete symmetry acting on S. Hence, the MSISM potential contains all possible interactions allowed by gauge invariance:

$$\begin{aligned} V(\Phi,S) &= \frac{\lambda_1}{2}(\Phi^\dagger\Phi)^2 + \frac{\lambda_2}{2}(S^*S)^2 + \lambda_3\,\Phi^\dagger\Phi\,S^*S + \lambda_4\,\Phi^\dagger\Phi\,S^2 \\ &\quad + \lambda_4^*\,\Phi^\dagger\Phi\,S^{*2} + \lambda_5\,S^3S^* + \lambda_5^*\,SS^{*3} + \frac{\lambda_6}{2}\,S^4 + \frac{\lambda_6^*}{2}\,S^{*4}\,, \end{aligned}$$

where the quartic couplings $\lambda_{1,2,\ldots,6}$ are all dimensionless constants and Φ is the familiar SM Higgs doublet $\Phi = \begin{pmatrix} G^+ \\ \frac{1}{\sqrt{2}}(\phi + iG) \end{pmatrix}$, where G^+ and G are the Goldstone bosons and ϕ is the CP-even real scalar field which in the SM is equivalent to H_{SM}. Recall that the imposition of scale invariance forbids the appearance of dimensionful mass parameters or trilinear couplings in the potential[2].

In our analysis of the MSISM, we follow the perturbative approach introduced by Gildener and S. Weinberg (GW) [21]. With the aid of this approach, we can find expressions for the scalar boson mass spectrum and the scale at which the scale invariance is broken Λ. By determining the theoretically allowed region of parameter space from the following two criteria: firstly keeping the theory perturbative, i.e. the theory has perturbative couplings (similar to the SM triviality bound), and secondly keeping the effective potential BFB (the vacuum stability bound), we can provide numerical predictions for the scalar masses and Λ. Further experimental constraints on the MSISM are obtained from an analysis of the LEP2 data [9], the Tevatron results [10] and the electroweak oblique parameters, S, T and U [32, 33].

[2]For recent studies of non-SI models with dimensionful self-couplings and with real or complex scalar singlet extensions see [30, 31] and references therein.

The approach of GW [21] is based on minimising the full potential perturbatively along a flat direction of the scalar potential. The tree-level MSISM scalar potential can possess a large number of different phenomenologically viable flat directions, which can be classified into three major categories: Type I, Type II and Type III. Flat directions of Type I are characterised by a zero valued VEV for the complex singlet scalar S, whereas in flat directions of Type II both S and Φ possess non-zero VEVs. Finally, in flat directions of Type III the SM Φ has a zero VEV, this makes it difficult to naturally realise EWSSB without large differences in the scalar VEVs [27, 28] and therefore we do not study them.

The MSISM also provides some interesting phenomenology which the current SM can not address. A natural extension to the MSISM would be to include right-handed neutrinos which could couple to the complex singlet scalar S in a SI way [15, 25, 26, 27, 28]. If the VEV of S is non-zero then the low-scale seesaw mechanism [34] can be used, this would provide a natural explanation for the smallness in mass of the light neutrinos as seen in the low-energy neutrino data [6]. The Majorana mass scale generated has an expected size of the order of the EW scale which would generate a relatively light set of heavy neutrinos as well as the experimentally observed light neutrinos. Unlike the SM, in specific circumstances the scalar sector of the MSISM can contain either explicit or spontaneous CP violation, or both. The new CP-violating phase could act as a source for creating the observed baryon asymmetry in the Universe. Moreover, the MSISM has the ability to produce stable massive scalar particles that could qualify as dark matter (DM) candidates. One scenario of particular phenomenological interest, as it contains all the aforementioned phenomenology, is a new minimal model of maximal spontaneous CP violation with a Type II flat direction. This scenario also remains perturbative up to energy scales of the order of the Planck scale, which, following the discussion above, is a necessary criteria to remove the gauge hierarchy problem.

In this thesis we present a thorough investigation of the MSISM based on

our previous work in [29]. In Chapter 2 we review the basic properties of a SI classical action. We derive the Ward identity which is obeyed by SI tree-level scalar potentials and include a review of the GW [21] approach to EWSSB in multi-scalar SI models. In Chapter 3, we present the general Lagrangian that describes the MSISM and provide a general classification of the flat directions which occur in the tree-level scalar potential of the MSISM. We also present the one-loop effective potential for the MSISM, as calculated in Appendix C, which is used to determine the scalar mass spectrum and the scale at which scale invariance is broken. At this point we briefly discuss the short-comings of the SI SM. Furthermore, we discuss the possible phenomenology of the different flat directions. Chapter 4 investigates the MSISM with a Type I flat direction, specifically in a scenario invariant under a U(1) symmetry acting on the complex scalar S and also the general non-invariant scenario. Similarly, Chapter 5 investigates the MSISM with a Type II flat direction, in the U(1) invariant limit and a simplified non-invariant scenario. In Chapter 6, we discuss extending the MSISM with right-handed neutrinos, which can interact with the complex singlet field S and its complex conjugate S^*. Finally, our conclusions are contained in Chapter 7 and technical details of all our calculations are presented in a number of appendices.

Chapter 2

Scale Invariance

In this chapter we discuss some general aspects of SI theories which are pertinent to our analysis of the MSISM. We first impose a scale transformation on a simple scalar model and show why dimensionful parameters must be excluded in SI theories. We then proceed to derive the Ward identity (WI) that results from imposing scale invariance on a general theory. Finally, we shall review the perturbative GW approach to EWSSB in weakly coupled multi-scalar SI theories [21]. The analytic results presented in this chapter will be used throughout our study of the MSISM.

We start by considering a simple model consisting of only one real massive scalar field, $\phi(x)$, which is described by the Lagrangian

$$\mathcal{L} \;=\; \frac{1}{2}\partial_{x\mu}\phi(x)\partial_x^{\mu}\phi(x) \;-\; \frac{1}{2}m^2\phi^2(x) \;-\; \lambda\phi^4(x)\;, \tag{2.1}$$

with the notation $\partial_x^{\mu} \equiv \frac{\partial}{\partial x_\mu}$. A scale transformation is a space-time transformation such that $x \to x' = \sigma^{-1}x$, where $\sigma = e^{\epsilon} > 0$, which acts linearly on all the fields of the theory. Keeping space-time fixed, the general field $\Phi(x)$, which could be a scalar, fermion or gauge boson, transforms under the scale transformation as

$$\Phi(x) \to \Phi'(x) = \sigma^a \Phi(\sigma x)\;, \tag{2.2}$$

where a is the scaling dimension of $\Phi(x)$ and, at the classical level, a takes the values, $a = 1$ if $\Phi(x)$ is a scalar or gauge boson and $a = \frac{3}{2}$ if $\Phi(x)$ is a fermion.

The classical action $S[\phi(x)] = \int d^4x \mathcal{L}[\partial_\mu \phi(x), \phi(x)]$ transforms under a scale transformation as follows

$$S[\sigma\phi(\sigma x)] \;=\; \int_{-\infty}^{\infty} d^4x \left[\sigma^2 \frac{1}{2} \partial_{x\mu}\phi(\sigma x)\partial_x^\mu \phi(\sigma x) \;-\; \frac{1}{2} m^2 \sigma^2 \phi^2(\sigma x) \;-\; \lambda \sigma^4 \phi^4(\sigma x) \right]$$

$$= \int_{\sigma(-\infty)}^{\sigma(\infty)} d^4(\sigma x) \left[\frac{1}{2} \partial_{(\sigma x)\mu}\phi(\sigma x)\partial^\mu_{(\sigma x)} \phi(\sigma x) \;-\; \frac{1}{2} \sigma^{-2} m^2 \phi^2(\sigma x) \;-\; \lambda \phi^4(\sigma x) \right], \quad (2.3)$$

where in the last line the variable of integration and the partial derivative have been adjusted to act on σx instead of x through the simple relations

$$d^4x \;=\; \frac{1}{\sigma^4} d^4(\sigma x)\,, \qquad \partial_x^\mu \;=\; \frac{\partial}{\partial x_\mu} \;=\; \sigma \frac{\partial}{\partial(\sigma x_\mu)} \;=\; \sigma \partial^\mu_{(\sigma x)}\,. \quad (2.4)$$

If the classical action is SI we expect $S[\sigma\phi(\sigma x)] = S[\phi(x)]$, which would only occur in (2.3) if the dimensionful parameter m^2 vanishes. Concisely, the absence of the scalar mass term results in a SI theory.

We can further show that quantum corrections, which contain terms of the type $\phi^4(x) \ln \frac{\phi^2(x)}{\mu^2}$, are not SI. Under a scale transformation, the quantum corrections transform as

$$\begin{aligned} \phi^4(x) \ln \frac{\phi^2(x)}{\mu^2} \;&\rightarrow\; (\sigma\phi(\sigma x))^4 \ln \frac{(\sigma\phi(\sigma x))^2}{\mu^2} \\ &=\; \sigma^4 \phi^4(\sigma x) \ln \frac{\phi^2(\sigma x)}{\mu^2} \;+\; \sigma^4 \phi^4(\sigma x) \ln \sigma^2\,. \end{aligned} \quad (2.5)$$

Inserting the last line into (2.3) we can see that the first term is SI whilst the second is not. Thus, we have shown that classical scale invariance holds at tree-level in a theory with no dimensionful couplings, but it is broken by the quantum corrections' logarithmic terms.

2.1 The Ward Identity for Scale Invariance

Having gained some insight into scale invariance from the above simple scalar model, we now consider a general theory, where $\Phi(x)$ represents a generic field of the theory, which could be a scalar, fermion or vector boson. The variation of the classical action under a scale transformation is calculated via

$$\begin{aligned}\delta S[\Phi(x)] \;=\; & \int d^4y \left[\delta\big(\partial_\mu\Phi_i(y)\big)\, \frac{\delta}{\delta\big(\partial_\mu\Phi_i(y)\big)} \;+\; \delta\big(\partial_\mu\Phi_i^\dagger(y)\big)\, \frac{\delta}{\delta\big(\partial_\mu\Phi_i^\dagger(y)\big)} \right. \\ & \left. +\, \delta\Phi_i(y)\frac{\delta}{\delta\Phi_i(y)} \;+\; \delta\Phi_i^\dagger(y)\frac{\delta}{\delta\Phi_i^\dagger(y)} \right] \int d^4x\; \mathcal{L}[\Phi(x)] \end{aligned} \tag{2.6}$$

where summation over repeated indices is implied for all the fields in the theory. Under an infinitesimal scale transformation, the variation of the generic field $\Phi(x)$ takes the form

$$\delta\Phi(x) = \epsilon\big(a + x^\mu\partial_\mu\big)\Phi(x)\,. \tag{2.7}$$

Using (2.7) it can be shown (see Appendix A) that the variation of the classical action $\delta S[\Phi(x)]$ is

$$\begin{aligned}\delta S[\Phi(x)] \;=\; & \epsilon \int d^4x \left[a\frac{\partial\mathcal{L}[\Phi(x)]}{\partial\Phi_i(x)}\Phi_i(x) \;+\; (1+a)\frac{\partial\mathcal{L}[\Phi(x)]}{\partial\big(\partial_\mu\Phi_i(x)\big)}\big(\partial_\mu\Phi_i(x)\big) \right. \\ & +\, a\Phi_i^\dagger(x)\frac{\partial\mathcal{L}[\Phi(x)]}{\partial\Phi_i^\dagger(x)} \;+\; (1+a)\big(\partial_\mu\Phi_i^\dagger(x)\big)\frac{\partial\mathcal{L}[\Phi(x)]}{\partial\big(\partial_\mu\Phi_i^\dagger(x)\big)} \\ & \left. -\, 4\mathcal{L}[\Phi(x)] \right]. \end{aligned} \tag{2.8}$$

Assuming $S[\Phi(x)]$ describes a SI theory so that $\delta S[\Phi(x)] = 0$, we obtain the WI for scale invariance:

$$4\mathcal{L}[\Phi] = (a+1)\left[\frac{\partial\mathcal{L}[\Phi]}{\partial\big(\partial_\mu\Phi_i\big)}\big(\partial_\mu\Phi_i\big) + \big(\partial_\mu\Phi_i^\dagger\big)\frac{\partial\mathcal{L}[\Phi]}{\partial\big(\partial_\mu\Phi_i^\dagger\big)}\right] + a\left[\frac{\partial\mathcal{L}[\Phi]}{\partial\Phi_i}\Phi_i \;+\; \Phi_i^\dagger\frac{\partial\mathcal{L}[\Phi]}{\partial\Phi_i^\dagger}\right]. \tag{2.9}$$

For notational simplicity, we have suppressed the x-dependence of the generic field Φ, i.e. $\Phi = \Phi(x)$. If the WI for scale invariance (2.9) is applied to just the

SI tree-level scalar potential $V^{\rm tree}(\Phi)$, rather than to the whole Lagrangian, then we obtain the WI relation

$$4V^{\rm tree}(\Phi) \;=\; \frac{\partial V^{\rm tree}(\Phi)}{\partial \Phi_i}\Phi_i \;+\; \Phi_i^\dagger \frac{\partial V^{\rm tree}(\Phi)}{\partial \Phi_i^\dagger}\;. \tag{2.10}$$

In a multi-scalar model, the scalars of the theory can be rewritten in terms of a vector whose components represent all the scalar fields of the theory as real degrees of freedom, i.e.

$$\mathbf{\Phi} \;=\; (\phi_1, \phi_2, \ldots, \phi_n)\;. \tag{2.11}$$

Likewise, the WI (2.10) can be generalised to

$$4V^{\rm tree}(\mathbf{\Phi}) \;=\; \mathbf{\Phi}\cdot\nabla V^{\rm tree}(\mathbf{\Phi})\;, \tag{2.12}$$

where $\nabla \equiv \left(\frac{\partial}{\partial\phi_1}, \frac{\partial}{\partial\phi_2}, \cdots, \frac{\partial}{\partial\phi_n}\right)$, and the single dot in (2.12) indicates the usual scalar product of two vectors in an n-dimensional vector space.

It is possible to apply the WI (2.12) to a specific direction, or ray, in the n-dimensional real scalar field space. To do this, we parametrise the scalar field vector $\mathbf{\Phi}$ as

$$\mathbf{\Phi} \;=\; \varphi\mathbf{N}\;, \tag{2.13}$$

where $\mathbf{N}$ is an n-dimensional unit vector in the field space and φ is the radial distance from the origin of the field space. Using this parameterisation, we can rewrite (2.12) as

$$\begin{aligned} 4V^{\rm tree}(\varphi\mathbf{N}) &= \varphi\mathbf{N}\cdot\nabla V^{\rm tree}(\varphi\mathbf{N}) \\ &= \varphi\frac{d\mathbf{\Phi}}{d\varphi}\cdot\frac{d}{d\mathbf{\Phi}}V^{\rm tree}(\varphi\mathbf{N}) \\ &= \varphi\frac{dV^{\rm tree}(\varphi\mathbf{N})}{d\varphi}\;. \end{aligned} \tag{2.14}$$

The condition for $V^{\rm tree}(\varphi\mathbf{N})$ to have an extremal or stationary line, called a

flat direction, along a specific unit vector $\mathbf{N} = \mathbf{n}$ is

$$\nabla V^{\text{tree}}(\mathbf{\Phi})\Big|_{\mathbf{\Phi}=\mathbf{\Phi}^{\text{flat}}} = \mathbf{0}\,, \tag{2.15}$$

where $\mathbf{\Phi}^{\text{flat}} = \varphi\mathbf{n}$ is the flat direction. Applying (2.15) in the first line of (2.14) we find $V^{\text{tree}}(\varphi\mathbf{n}) = 0$, that is, the tree-level potential is both zero and an extremum when evaluated for the flat direction. From the last line of (2.14) we obtain an equivalent condition to (2.15):

$$\frac{dV^{\text{tree}}(\varphi\mathbf{N})}{d\varphi}\Big|_{\mathbf{N}\,=\,\mathbf{n}} = 0\,. \tag{2.16}$$

The flat direction is an extremum, but in order for it to also be a local minimum of the potential $\mathbf{\Phi}^{\text{flat}}$ also has to satisfy

$$(\mathbf{v}\cdot\nabla)^2 V^{\text{tree}}(\mathbf{\Phi})\Big|_{\mathbf{\Phi}\,=\,\mathbf{\Phi}^{\text{flat}}} \geq 0\,, \tag{2.17}$$

for any arbitrary vector $\mathbf{v}$ belonging to the n-dimensional field space. Finally, to ensure that the scalar potential is BFB, we require $V^{\text{tree}}(\varphi\mathbf{N}) \geq 0$, for all possible directions $\mathbf{N}$.

2.2 The Gildener and Weinberg Approach to EWSSB

In this section we review the GW [21] approach to EWSSB in SI multi-scalar renormalisable gauge field theories. According to this approach, the minimisation of the full potential V is performed perturbatively along a minimal flat direction $\mathbf{\Phi}^{\text{flat}}$, which was discussed in the previous section. The full potential V consists of the classical tree-level potential V^{tree} as well as a set of quantum corrections, $V_{\text{eff}}^{\text{k-loop}}$, generated at the k$^{\text{th}}$-loop level (k $= 1, 2, ...$). Each k-loop contribution is a k$^{\text{th}}$ order polynomial in $\ln\frac{\phi^2}{\mu^2}$, where μ is the renormalisation group (RG) scale.

The GW approach requires that the logarithms are not too large so that $V^{\rm tree} > V_{\rm eff}^{1-{\rm loop}} > V_{\rm eff}^{2-{\rm loop}} > ...$ and perturbation theory can be applied. The theory must also be weakly coupled for this approach to be valid, which constitutes the regime of validity for our investigations.

Assuming that the logarithmic terms of the quantum corrections are small then the full potential V is dominated by the tree-level (or zero-loop) term

$$V^{\rm tree}(\mathbf{\Phi}) \;=\; \frac{1}{4!}\, f_{ijkl}\, \phi_i \phi_j \phi_k \phi_l \;, \tag{2.18}$$

where repeated indices are summed over and $\mathbf{\Phi}$ (2.11) is an n-dimensional field multiplet composed of the real scalar fields of the theory, ϕ_i (with $i = 1, 2, \ldots, n$). In (2.18), the quartic couplings of the potential are represented by f_{ijkl} which is fully symmetric in all its indices. It can easily be verified that the tree-level potential $V^{\rm tree}(\mathbf{\Phi})$ (2.18) is a general solution to the WI for SI given in (2.12).

To ensure that perturbation theory stays valid, the idea of GW is to choose a value of the RG scale $\mu = \Lambda$ at which $V^{\rm tree}(\mathbf{\Phi})$ has a non-trivial continuous local minimum along a ray $\mathbf{\Phi}^{\rm flat}$. Using the parameterisation for $\mathbf{\Phi}$ in (2.13), the local minimum is found by adjusting the RG scale μ so that

$$\min_{N_i N_i = 1} V^{\rm tree}(\mathbf{N}) \;=\; \min_{N_i N_i = 1} f_{ijkl}(\mu) N_i N_j N_k N_l \;=\; 0 \;, \tag{2.19}$$

which it is assumed occurs for a particular unit vector $\mathbf{N} = \mathbf{n}$ and at a specific value of the RG scale, $\mu = \Lambda$. It should be noted that (2.19) imposes only one constraint on the parameters $f_{ijkl}(\Lambda)$, independent of the number of parameters f_{ijkl} contains and specifically only at the RG scale Λ. Since (2.19) is equivalent to applying (2.16) to (2.18), then according to Section 2.1, the tree-level potential is both zero and an extremum along the ray $\mathbf{\Phi}^{\rm flat} = \varphi \mathbf{n}$. Applying the extremum relation (2.15) to (2.18) leads to the constraint

$$\frac{\partial V^{\rm tree}(\mathbf{N})}{\partial N_i}\Big|_{\mathbf{N}=\mathbf{n}} \;=\; 0 \quad \Leftrightarrow \quad f_{ijkl}(\Lambda)\, n_j n_k n_l \;=\; 0 \;. \tag{2.20}$$

To ensure that the stationary flat direction is a local minimum requires satisfying the condition in (2.17). To achieve this the Hessian matrix $\mathbf{P}$, which is defined as

$$(\mathbf{P})_{ij} \equiv \frac{1}{\varphi^4}\frac{\partial^2 V^{\rm tree}(\mathbf{N})}{\partial N_i \partial N_j}\bigg|_{\mathbf{N}=\mathbf{n}} = \frac{1}{2} f_{ijkl} n_k n_l \,, \tag{2.21}$$

must be non-negative definite, i.e. the $n \times n$-dimensional matrix $\mathbf{P}$ has either vanishing or positive eigenvalues. To ensure $\mathbf{P}$ is non-negative definite requires $u_i(\mathbf{P})_{ij}u_j \geq 0$, for all non-zero vectors u in the n-dimensional real scalar field space.

Since $V^{\rm tree}(\mathbf{\Phi})$ vanishes along $\mathbf{\Phi}^{\rm flat}$, the full potential V will be dominated by higher-order loop contributions along the flat direction, specifically by the one-loop effective potential, $V_{\rm eff}^{1-{\rm loop}}(\mathbf{\Phi})$. Adding higher-order quantum corrections gives a small curvature in the radial direction of $\mathbf{\Phi}^{\rm flat}$, which picks out a specific value of φ, v_φ, along the ray as the minimum. In addition, a small shift may also be produced in a direction $\delta\mathbf{\Phi} = v_\varphi \delta\mathbf{n}$ which is perpendicular to the flat direction $\mathbf{n}$, i.e. $\mathbf{n}\cdot\delta\mathbf{n} = 0$.

The stationary condition (2.15) can be extended to find the minimum of the new one-loop corrected scalar potential

$$\nabla\left(V^{\rm tree}(\mathbf{\Phi}) + V_{\rm eff}^{1-{\rm loop}}(\mathbf{\Phi})\right)\Big|_{\mathbf{\Phi} \,=\, v_\varphi(\mathbf{n}+\delta\mathbf{n})} = \mathbf{0}\,. \tag{2.22}$$

According to the GW perturbative approach, one has to consistently expand this last expression to the first-loop order, where the perpendicular shift $\delta\mathbf{\Phi}$ is considered to be a first-loop order parameter. Thus, expanding to first order in small quantities gives

$$v_\varphi^2 \mathbf{P}\cdot\delta\mathbf{\Phi} + \nabla V_{\rm eff}^{1-{\rm loop}}(\mathbf{\Phi})\Big|_{\mathbf{\Phi}=v_\varphi\mathbf{n}} = \mathbf{0}\,, \tag{2.23}$$

where the dot indicates the matrix multiplication of the Hessian matrix $\mathbf{P}$ with the vector $\delta\mathbf{\Phi}$. The perturbative minimisation condition (2.23) uniquely determines

$\delta\mathbf{\Phi}$, except for directions along eigenvectors of $\mathbf{P}$ with zero eigenvalues. These zero eigenvectors include the flat direction $\mathbf{n}$ itself, since $\mathbf{n}\cdot\mathbf{P}=\mathbf{0}$ by virtue of (2.20) and (2.21). They also include any Goldstone boson directions which result from the spontaneous symmetry breaking (SSB) of any continuous symmetries. There is no reason to expect any more zero eigenvalues of $\mathbf{P}$, and it is assumed that this is the case.

Instead of using (2.23) to determine $\delta\mathbf{\Phi}$, it can be used to find a relation that defines the value of v_φ. Contracting (2.23) from the left with $\mathbf{n}$, leads to the minimisation condition along the radial direction:

$$\mathbf{n}\cdot\nabla V_{\rm eff}^{1-\rm loop}(\mathbf{\Phi})\Big|_{\mathbf{\Phi}=v_\varphi\mathbf{n}} \;=\; \frac{dV_{\rm eff}^{1-\rm loop}(\varphi\mathbf{n})}{d\varphi}\Big|_{\varphi=v_\varphi} \;=\; 0\,. \tag{2.24}$$

Along the flat direction the one-loop effective potential, $V_{\rm eff}^{1-\rm loop}(\varphi\,\mathbf{n})$, can be written in the general form:

$$V_{\rm eff}^{1-\rm loop}(\varphi\,\mathbf{n}) \;=\; A(\mathbf{n})\,\varphi^4 \;+\; B(\mathbf{n})\,\varphi^4\ln\frac{\varphi^2}{\Lambda^2}\,, \tag{2.25}$$

where the $\mathbf{n}$-dependent renormalised dimensionless constants A and B are given in the modified minimal subtraction ($\overline{\rm MS}$) renormalisation scheme[1] [35] by

$$\begin{aligned} A &= \frac{1}{64\pi^2 v_\varphi^4}\left\{ {\rm Tr}\left[m_S^4\left(-\frac{3}{2}+\ln\frac{m_S^2}{v_\varphi^2}\right)\right] + 3{\rm Tr}\left[m_V^4\left(-\frac{5}{6}+\ln\frac{m_V^2}{v_\varphi^2}\right)\right]\right. \\ &\quad \left. -4{\rm Tr}\left[m_F^4\left(-1+\ln\frac{m_F^2}{v_\varphi^2}\right)\right]\right\}, \\ B &= \frac{1}{64\pi^2 v_\varphi^4}\left({\rm Tr}m_S^4 + 3{\rm Tr}m_V^4 - 4{\rm Tr}m_F^4\right), \end{aligned} \tag{2.26}$$

where the trace is taken over the mass matrix and over all internal degrees of

[1] In the $\overline{\rm MS}$ renormalisation scheme one absorbs the divergent part of the Feynman diagram calculations plus a universal constant into the counterterms, see (D.16).

freedom[2]. The scalar, vector and fermion masses $m_{S,V,F}$ in (2.26) are the tree-level scalar, vector and fermion mass matrices evaluated at $v_\varphi\,\mathbf{n}$.

Minimising (2.25) according to (2.24) implies that the potential has a non-trivial stationary point at a value of the RG scale Λ, given by

$$\Lambda \;=\; v_\varphi\,\exp\left(\frac{A}{2B}\;+\;\frac{1}{4}\right)\,. \tag{2.27}$$

Note that since the effective potential coefficients A and B are of the same loop order, the RG scale Λ and the minimum v_φ are expected to be of comparable order as well. Thus, provided potentially large logarithms of the type $\ln\frac{v_\varphi^2}{\Lambda^2}$ can be kept under control, i.e. of the order of unity, then perturbation theory should be a valid approximation.

The relation in (2.27) can now be used to define the one-loop effective potential along the flat direction in terms of the one-loop VEV v_φ

$$V_{\rm eff}^{1-{\rm loop}}(\varphi\,\mathbf{n}) \;=\; B(\mathbf{n})\,\varphi^4\left(\ln\frac{\varphi^2}{v_\varphi^2}\;-\;\frac{1}{2}\right)\,. \tag{2.28}$$

Even though the explicit dependence of $V_{\rm eff}^{1-{\rm loop}}(\varphi\,\mathbf{n})$ on the RG scale Λ has disappeared, there still exists an indirect dependence on Λ through the kinematic parameters in $B(\mathbf{n})$. At the minimum $V_{\rm eff}^{1-{\rm loop}}(\varphi\,\mathbf{n})$ reduces to

$$V_{\rm eff}^{1-{\rm loop}}(v_\varphi\,\mathbf{n}) \;=\; -\frac{1}{2}\,B(\mathbf{n})\,v_\varphi^4\,. \tag{2.29}$$

For $v_\varphi\mathbf{n}$ to be a minimum, $V_{\rm eff}^{1-{\rm loop}}(v_\varphi\mathbf{n})$ must be less than the value of the potential at the origin $V(\mathbf{\Phi}=\mathbf{0})=0$, hence $V_{\rm eff}^{1-{\rm loop}}(v_\varphi\mathbf{n})$ must be negative. This can only happen if $B(\mathbf{n})>0$. This constraint also ensures that the potential is BFB, i.e. the one-loop effective potential (2.28) remains non-negative for infinitely large values of φ.

[2]Note that the internal degrees of freedom for Majorana fermions are half those of the Dirac fermions. Consequently, if the fermion F is Majorana, the pre-factor -4 in front of the trace should be replaced with -2.

At tree-level the squared masses of the scalar bosons are given by the eigenvalues of the matrix

$$(m_S^2)_{ij} \;=\; \left.\frac{\partial^2 V^{\rm tree}(\mathbf{\Phi})}{\partial\phi_i\,\partial\phi_j}\right|_{\mathbf{\Phi}\,=\,v_\varphi\,\mathbf{n}} \;=\; v_\varphi^2\,(\mathbf{P})_{ij}\;. \tag{2.30}$$

Previously, we demanded that the Hessian matrix $\mathbf{P}$ had positive definite eigenvalues, except for a set of zero eigenvalues due to the Goldstone bosons associated with the SSB of continuous symmetries of the theory and one zero eigenvalue due to the flat direction. Hence the model contains a set of massive scalars, a set of massless Goldstone bosons and a single massless scalar, which we denote as h, associated with the flat direction.

Beyond the tree approximation, h does not remain massless. By including the one-loop correction $V_{\rm eff}^{1-\rm loop}$, the mass matrix will shift to

$$(m_S^2+\delta m_S^2)_{ij} \;=\; \left.\frac{\partial^2\big(V^{\rm tree}(\mathbf{\Phi})\;+\;V_{\rm eff}^{1-\rm loop}(\mathbf{\Phi})\big)}{\partial\phi_i\partial\phi_j}\right|_{\mathbf{\Phi}=v_\varphi(\mathbf{n}+\delta\mathbf{n})}\;, \tag{2.31}$$

which to first order in small quantities becomes

$$(\delta m_S^2)_{ij} \;=\; \left.\frac{\partial^2 V_{\rm eff}^{1-\rm loop}(\mathbf{\Phi})}{\partial\phi_i\partial\phi_j}\right|_{\mathbf{\Phi}=v_\varphi\mathbf{n}} \;+\; v_\varphi\;f_{ijkl}n_k\delta\phi_l\;. \tag{2.32}$$

Using perturbation theory to first order, the mass of h can be calculated by taking the expectation value of δm_S^2 with respect to the unperturbed eigenvector $\mathbf{n}$:

$$\begin{aligned} m_h^2 \;&=\; n_i n_j(\delta m_S^2)_{ij} \\ &=\; n_i n_j\left.\frac{\partial^2 V_{\rm eff}^{1-\rm loop}(\mathbf{\Phi})}{\partial\phi_i\partial\phi_j}\right|_{\mathbf{\Phi}=v_\varphi\mathbf{n}} \\ &=\; \left.\frac{d^2 V_{\rm eff}^{1-\rm loop}(\varphi\mathbf{n})}{d\varphi^2}\right|_{\varphi=v_\varphi} \\ &=\; 8Bv_\varphi^2\;, \end{aligned} \tag{2.33}$$

where we have used (2.25) and (2.27) to arrive at the last line. The field h is the pseudo-Goldstone boson of the anomalously broken scale invariance, since it is massless at tree-level when scale invariance holds, but acquires a non-zero mass at the one-loop level (2.33) once scale invariance is broken by quantum corrections.

The other massive scalar states of the theory can be easily determined provided $(\delta m_S^2)_{ij}$ remains a small effect compared to the tree-level mass matrix $(m_S^2)_{ij}$. If this is the case, their masses are given by the relation:

$$m_H^2 \;=\; \tilde{n}_i \tilde{n}_j \frac{\partial^2 V^{\rm tree}(\mathbf{\Phi})}{\partial\phi_i \partial\phi_j}\bigg|_{\mathbf{\Phi}=v_\varphi \mathbf{n}} \;=\; \tilde{\mathbf{n}}\cdot\mathbf{P}\cdot\tilde{\mathbf{n}}\,, \tag{2.34}$$

where the massive scalar directions are defined similarly to $\mathbf{\Phi}^{\rm flat}$ as $\mathbf{\Phi}^{\rm H} = \varphi\tilde{\mathbf{n}}$, where $\tilde{\mathbf{n}}$ is a unit vector perpendicular to $\mathbf{n}$. The Goldstone bosons associated with the SSB of continuous symmetries of the theory remain massless provided $V_{\rm eff}^{1-{\rm loop}}(\mathbf{\Phi})$ respects the same global symmetries as $V^{\rm tree}(\mathbf{\Phi})$.

Chapter 3

The Minimal Scale Invariant Extension of the Standard Model

In this chapter we present the Minimal Scale Invariant extension of the Standard Model. We begin with a review of the general Lagrangian that describes the MSISM, we then determine several necessary conditions for the MSISM tree-level potential and consider the effects of applying the WI to it. We continue by discussing the flat directions of the MSISM, first considering an appropriate parameterisation and then presenting a general classification of the types of flat directions that can occur in the tree-level scalar potential. We also present the one-loop effective potential for the MSISM from which we derive the mass of the pseudo-Goldstone boson of the broken scale invariance h and the RG scale Λ. At this point, we also take the opportunity to discuss the short-comings of the SI SM. Finally, we briefly discuss the generic phenomenological features of the different types of flat directions in the MSISM. A detailed investigation of the physically viable flat directions of the MSISM in a number of different scenarios is continued in Chapters 4 and 5.

3.1 The MSISM Lagrangian

The Lagrangian that defines the MSISM can be written as a sum of five terms:

$$\mathcal{L}_{\text{MSISM}} \;=\; \mathcal{L}_{\text{inv}} \;+\; \mathcal{L}_{\text{GF}} \;+\; \mathcal{L}_{\text{FP}} \;+\; \mathcal{L}_{\nu} \;-\; V^{\text{tree}}(\Phi, S)\,. \tag{3.1}$$

Of these five terms, the gauge-invariant $\mathcal{L}_{\text{inv}}$, gauge-fixing $\mathcal{L}_{\text{GF}}$ and Faddeev–Popov $\mathcal{L}_{\text{FP}}$ Lagrangians are discussed in depth in Appendix B, whilst analysis of the right-handed neutrino Lagrangian $\mathcal{L}_{\nu}$ is postponed until Chapter 6. The last term $V^{\text{tree}}(\Phi, S)$ is the tree-level potential of the MSISM which is given by

$$\begin{aligned} V^{\text{tree}}(\Phi, S) \;=\; & \frac{\lambda_1}{2}(\Phi^\dagger\Phi)^2 \;+\; \frac{\lambda_2}{2}(S^*S)^2 \;+\; \lambda_3\Phi^\dagger\Phi S^*S \;+\; \lambda_4\Phi^\dagger\Phi\, S^2 \\ & + \lambda_4^*\Phi^\dagger\Phi S^{*2} \;+\; \lambda_5 S^3S^* \;+\; \lambda_5^* S S^{*3} \;+\; \frac{\lambda_6}{2}S^4 \;+\; \frac{\lambda_6^*}{2}S^{*4}\,. \end{aligned} \tag{3.2}$$

We can linearly decompose the $\text{SU}(2)_L$ scalar doublet Φ and the complex singlet field S as follows

$$\Phi \;=\; \begin{pmatrix} G^+ \\ \frac{1}{\sqrt{2}}(\phi + iG) \end{pmatrix}\,, \qquad S \;=\; \frac{1}{\sqrt{2}}(\sigma + iJ)\,, \tag{3.3}$$

where ϕ and σ are the CP-even real scalar fields, G and J the CP-odd real scalar fields and G^+ is the charged Goldstone boson.

To obtain a stable minimum for the scalar potential we must ensure that V^{tree} is BFB. This can be achieved by placing a set of constraining conditions on the quartic couplings $\lambda_{1,2,\ldots,6}$. These conditions are determined by analysing the potential in terms of two real and independent gauge-invariant field bilinears: $\Phi^\dagger\Phi$ and S^*S. To convert (3.2) into this representation, we re-express the field S as $S = |S|e^{i\theta_S}$, where θ_S is the phase of the complex field and $S^*S = |S|^2$. The

tree-level scalar potential can then be rewritten as

$$V^{\text{tree}} = \frac{1}{2}\left(\Phi^\dagger\Phi\,,\, S^*S\right)\begin{pmatrix}\Lambda_{11} & \Lambda_{12}\\ \Lambda_{21} & \Lambda_{22}\end{pmatrix}\begin{pmatrix}\Phi^\dagger\Phi\\ S^*S\end{pmatrix}\,, \tag{3.4}$$

where the elements of the matrix take the form:

$$\begin{aligned}
\Lambda_{11} &= \lambda_1\,,\\
\Lambda_{12} &= \Lambda_{21} = \lambda_3 + \lambda_4 e^{2i\theta_S} + \lambda_4^* e^{-2i\theta_S}\,,\\
\Lambda_{22} &= \lambda_2 + 2\lambda_5 e^{2i\theta_S} + 2\lambda_5^* e^{-2i\theta_S} + \lambda_6 e^{4i\theta_S} + \lambda_6^* e^{-4i\theta_S}\,.
\end{aligned} \tag{3.5}$$

Since, by definition, the two bilinears $\Phi^\dagger\Phi$ and S^*S are positive-definite, the requirement for V^{tree} to be BFB depends exclusively on the matrix elements. We find that the following two conditions are required to keep V^{tree} BFB:

$$\text{(i)}\quad \text{Tr}\mathbf{\Lambda} \geq 0\,, \qquad \text{(ii)}\quad \begin{cases} \Lambda_{12} \geq 0\,, & \text{if } \Lambda_{11} = 0 \text{ or } \Lambda_{22} = 0\\ \text{Det}\mathbf{\Lambda} \geq 0\,, & \text{if } \Lambda_{11} \neq 0 \text{ and } \Lambda_{22} \neq 0 \end{cases}\,. \tag{3.6}$$

Obviously, these conditions explicitly depend on the phase θ_S through the matrix elements given in (3.5). Since θ_S is the phase of the complex field S it determines the direction of a ray in the σ-J plane within the entire real scalar field space. It is therefore essential that the conditions (3.6) hold true for all values of θ_S thereby ensuring that V^{tree} remains BFB in all possible field directions, including along the flat direction.

The WI for scale invariance (2.10) can be applied to the MSISM. We first note that the derivatives of the tree-level potential V^{tree} (3.2) with respect to the different representations, real fields, complex fields and bilinears, are related

through

$$
\begin{aligned}
2\Phi^\dagger\Phi\frac{\partial V^{\rm tree}}{\partial(\Phi^\dagger\Phi)} &= \frac{\partial V^{\rm tree}}{\partial\Phi}\Phi+\Phi^\dagger\frac{\partial V^{\rm tree}}{\partial\Phi^\dagger} \\
&= \Re G^+\frac{\partial V^{\rm tree}}{\partial\Re G^+}+\Im G^+\frac{\partial V^{\rm tree}}{\partial\Im G^+}+G\frac{\partial V^{\rm tree}}{\partial G}+\phi\frac{\partial V^{\rm tree}}{\partial\phi}\ , \\
2S^*S\frac{\partial V^{\rm tree}}{\partial(S^*S)} &= S\frac{\partial V^{\rm tree}}{\partial S}+S^*\frac{\partial V^{\rm tree}}{\partial S^*} \\
&= \sigma\frac{\partial V^{\rm tree}}{\partial\sigma}+J\frac{\partial V^{\rm tree}}{\partial J}\ ,
\end{aligned}
\tag{3.7}
$$

where $\Re G^+=\frac{1}{\sqrt{2}}(G^++G^-)$ and $\Im G^+=\frac{i}{\sqrt{2}}(G^--G^+)$ with $G^-=(G^+)^*$. The second equation in (3.7) involving the complex singlet field S was derived by employing the relations:

$$
\begin{aligned}
S^*S\,\frac{\partial V^{\rm tree}}{\partial(S^*S)}\ +\ \frac{\partial V^{\rm tree}}{\partial(2i\theta_S)} &= S\frac{\partial V^{\rm tree}}{\partial S}\ , \\
S^*S\,\frac{\partial V^{\rm tree}}{\partial(S^*S)}\ -\ \frac{\partial V^{\rm tree}}{\partial(2i\theta_S)} &= S^*\frac{\partial V^{\rm tree}}{\partial S^*}\ .
\end{aligned}
\tag{3.8}
$$

Using these relations, we can re-express the WI (2.10) in terms of derivatives with respect to bilinears only, explicitly we find

$$
S^*S\,\frac{\partial V^{\rm tree}}{\partial(S^*S)}\ +\ \Phi^\dagger\Phi\,\frac{\partial V^{\rm tree}}{\partial(\Phi^\dagger\Phi)}\ =\ 2V^{\rm tree}\ . \tag{3.9}
$$

As expected the absence of a derivative term with respect to the phase θ_S implies that θ_S can not affect whether the MSISM is SI or not.

It is now an appropriate time to discuss the predictive power of the scalar sector of the MSISM. The MSISM potential contains nine real quartic couplings, implying that the MSISM is much less predictive than the SM, which contains only two real couplings, m^2 and λ. However, imposing the flat direction condition (2.15) and including possible additional symmetries, such as a U(1) symmetry acting on S, can reduce the number of independent parameters significantly. In

fact, most of the scenarios we study rely on only two or three essential independent quartic couplings, thereby making the MSISM a comparatively predictive theory.

3.2 Classification of the Flat Directions

Following the approach presented in Chapter 2, the flat direction is parameterised as an n-dimensional vector $\mathbf{\Phi}^{\text{flat}}$, whose components represent all the real degrees of freedom of the scalars fields in the theory. In the MSISM there are six real scalar fields, $\Re G^+$, $\Im G^+$, G, ϕ, σ and J, and the flat direction lies in the vector space spanned by all of them. However, by exploiting the SM gauge symmetry, the flat direction can be restricted to the vector space spanned by the fields ϕ, σ and J only. This does not result in a loss of generality since the VEVs of the Goldstone bosons $G^\pm$ and G can be chosen to be zero, and remain so even beyond tree-level, therefore they will always contribute zero components to the flat direction. Thus, the general flat direction $\mathbf{\Phi}^{\text{flat}}$ can be dimensionally reduced to[1]

$$\mathbf{\Phi}^{\text{flat}} \;=\; \varphi \begin{pmatrix} n_\phi \\ n_\sigma \\ n_J \end{pmatrix} \;=\; \begin{pmatrix} \varphi_\phi \\ \varphi_\sigma \\ \varphi_J \end{pmatrix} , \tag{3.10}$$

where the components $n_{\phi,\sigma,J}$ satisfy the unit vector constraint: $n_\phi^2 + n_\sigma^2 + n_J^2 = 1$. At the one-loop minimum of the flat direction we have

$$v_\varphi n_\phi \;\equiv\; v_\phi \,, \qquad v_\varphi n_\sigma \;\equiv\; v_\sigma \,, \qquad v_\varphi n_J \;\equiv\; v_J \,, \tag{3.11}$$

where v_φ is the specific value of φ picked out to be the minimum along the flat direction by the addition of the quantum corrections to the full potential V. The VEV of the real fields σ and J are v_σ and v_J respectively, whilst v_ϕ is the VEV of ϕ. Since σ and J do not interact with the gauge bosons or the fermions, the

[1] We introduce a new notation for the second vector which is different from that used in [29] so that we may explicitly differentiate between the scalar field and the flat direction component.

VEV of ϕ is equal to the SM VEV of the field H_{SM}, $v_{\rm SM} = 246$ GeV, whereas v_σ and v_J are dependent on the conditions of the specific scenario.

To minimise the potential and ensure that the flat direction represents an extremum of the tree-level potential, we need to satisfy relation (2.15), i.e. we require that all the derivatives of $V^{\rm tree}$ with respect to the real fields ϕ, σ and J vanish when evaluated along the flat direction. Using (3.7), it is much simpler to calculate these derivatives with respect to the fields Φ and S instead. We find that the following two complex tadpole conditions (and their complex conjugates) need to be satisfied

$$\left.\frac{\partial V^{\rm tree}}{\partial \Phi}\right|_{\mathbf{\Phi}^{\rm flat}} = \varphi_\Phi^\dagger\Big[\lambda_1(\Lambda)\varphi_\Phi^\dagger\varphi_\Phi + \lambda_3(\Lambda)\varphi_S^*\varphi_S + \lambda_4(\Lambda)\varphi_S^2 + \lambda_4^*(\Lambda)\varphi_S^{*2}\Big] = 0\,, \tag{3.12}$$

$$\begin{aligned}\left.\frac{\partial V^{\rm tree}}{\partial S}\right|_{\mathbf{\Phi}^{\rm flat}} &= \varphi_S^*\Big[\lambda_2(\Lambda)\varphi_S^*\varphi_S + \lambda_3(\Lambda)\varphi_\Phi^\dagger\varphi_\Phi + 3\lambda_5(\Lambda)\varphi_S^2 + \lambda_5^*(\Lambda)\varphi_S^{*2}\Big] \\ &\quad + \varphi_S\Big[2\lambda_4(\Lambda)\varphi_\Phi^\dagger\varphi_\Phi + 2\lambda_6(\Lambda)\varphi_S^2\Big] = 0\,,\end{aligned} \tag{3.13}$$

where $\mathbf{\Phi}^{\rm flat}$ is defined in (3.10). To clarify the notation, we assume along the dimensionally reduced flat direction Φ and S become respectively $\varphi_\Phi = \frac{1}{\sqrt{2}}\varphi_\phi$ and $\varphi_S = \frac{1}{\sqrt{2}}(\varphi_\sigma + i\varphi_J)$, this is analogous to the decomposition of the fields (3.3). There are three distinct approaches to simultaneously satisfying both of the above minimisation conditions, which generically lead to three different types of flat directions: Type I, Type II and Type III.

3.2.1 The Type I Flat Direction

The Type I flat direction is defined so that along the flat direction the scalar doublet Φ develops a VEV but the singlet S does not, i.e. $\varphi_\Phi \neq 0$ and $\varphi_S = 0$. Since $\varphi_S = 0$, the minimisation condition (3.13) is automatically satisfied, whilst the other condition (3.12) forces us to set $\lambda_1(\Lambda) = 0$. The values of the other quartic couplings in $V^{\rm tree}$ are constrained by the BFB conditions (3.6), such that

$\Lambda_{22} > 0$ and $\Lambda_{12} > 0$.

Since the flat direction components φ_σ and φ_J are both zero, the flat direction (3.10) can be further reduced to

$$\mathbf{\Phi}^{\text{flat}} \;=\; \varphi\, n_\phi \;=\; \varphi_\phi \;, \tag{3.14}$$

where $n_\phi = 1$. This implies that the flat direction lies directly along the ϕ axis in the real scalar field space. Therefore, since the field which is associated with the flat direction corresponds to the massless pseudo-Goldstone boson of the anomalously broken scale invariance h (see Section 2.2), we have that for the Type I flat direction $\phi \equiv h$.

3.2.2 The Type II Flat Direction

Along the Type II flat direction, both the doublet Φ and the singlet S develop non-zero VEVs. This implies (3.12) and (3.13) can only be satisfied if specific relations among the quartic couplings are met at some RG scale Λ. To examine what this means let us consider a U(1) invariant MSISM scalar potential which is invariant under U(1) rephasings of the field $S \to e^{i\alpha}S$, where α is an arbitrary phase. As a direct consequence of the U(1) invariance the quartic couplings $\lambda_{4,5,6}$ in (3.2) vanish. Moreover, the minimisation conditions (3.12) and (3.13) lead to the constraint:

$$\frac{\varphi_\Phi^\dagger \varphi_\Phi}{\varphi_S^* \varphi_S} \;=\; \frac{n_\phi^2}{n_\sigma^2 + n_J^2} \;=\; -\frac{\lambda_3(\Lambda)}{\lambda_1(\Lambda)} \;=\; -\frac{\lambda_2(\Lambda)}{\lambda_3(\Lambda)} \,. \tag{3.15}$$

In order to satisfy the above relation and the BFB condition (3.6), we must demand that $\lambda_1 > 0$, $\lambda_2 > 0$ and $\lambda_3 < 0$.

In a general Type II flat direction, both σ and J will develop VEVs, since S is a complex field. However, if a U(1) symmetry is acting on the scalar potential, any possible phase of S can be eliminated through a U(1) rephasing, such that φ_S is real and $\varphi_J = 0$. Consequently, for the U(1) invariant scenario, the flat

direction can be dimensionally reduced to a two component vector and applying the constraints (3.15) and $n_\phi^2 + n_\sigma^2 = 1$ yields

$$\mathbf{\Phi}^{\text{flat}} \;=\; \varphi \begin{pmatrix} \sqrt{\frac{-\lambda_3(\Lambda)}{\lambda_1(\Lambda)-\lambda_3(\Lambda)}} \\ \sqrt{\frac{\lambda_1(\Lambda)}{\lambda_1(\Lambda)-\lambda_3(\Lambda)}} \end{pmatrix} \;=\; \varphi_\phi \begin{pmatrix} 1 \\ \sqrt{\frac{\lambda_1(\Lambda)}{-\lambda_3(\Lambda)}} \end{pmatrix} . \tag{3.16}$$

Since the U(1) invariant Type II flat direction is composed of both the ϕ and σ fields, there will be mixing between the two CP even states in the mass basis. The mass basis is defined by the field associated with the flat direction h and those fields associated with directions perpendicular to the flat direction. Thus, for the U(1) invariant scenario, the mass eigenstates are the massless Goldstone boson J, associated with the spontaneous breaking of the U(1) symmetry, the massless pseudo-Goldstone boson associated with broken scale invariance h, and a single massive scalar H, where h and H are given by

$$h \;=\; \cos\theta\,\phi \;+\; \sin\theta\,\sigma\;, \qquad H \;=\; -\;\sin\theta\,\phi \;+\; \cos\theta\,\sigma\;, \tag{3.17}$$

where $\cos^2\theta = \frac{-\lambda_3(\Lambda)}{\lambda_1(\Lambda)-\lambda_3(\Lambda)}$.

The general U(1) non-invariant scenario is much more involved and will be discussed in more detail in Section 5.2. However, in general, the flat direction of the U(1) non-invariant scenario is a three component vector, which implies that the scalar boson mass eigenstates will be a mixture of all three quantum fields ϕ, σ and J.

3.2.3 The Type III Flat Direction

The Type III flat direction is characterised so that along the flat direction the doublet field Φ has a zero VEV. This poses a phenomenological problem because without a VEV for Φ, or consequently ϕ, the Higgs mechanism can not occur and the electroweak gauge bosons remain massless. However, beyond the tree approximation, there will be a small shift perpendicular to the direction of the

flat direction. If this shift is in a direction which gives the field ϕ a VEV, it will in general be too small to account for the $W^{\pm}$ and Z boson masses unless a large hierarchy between the VEVs of the Φ and S fields is introduced [27, 28]. For this reason we do not study the Type III flat direction.

The three types of flat direction described above provide a complete classification of the flat directions in the MSISM. However, we should note that each type of flat direction may contain several different variations. For example, consider the U(1) non-invariant Type II flat direction. It requires (3.12) and (3.13), but places no explicit constraints on how the quartic couplings of the scalar potential satisfy these relations. Each choice provides a unique and valid flat direction and this gives rise to a vast number of possible variants. We do not intend to go through each such variant, but rather concentrate on a few representative scenarios which appear to be physically interesting, in terms of new sources of CP violation, neutrino masses and DM candidates.

3.3 The One-Loop Effective Potential

The one-loop effective potential of the MSISM has been computed in terms of Φ and S in Appendix C, where the full one-loop renormalised effective potential $V_{\text{eff}}^{1-\text{loop}}$ is given in (D.17). Along the flat direction, the RG scale takes the specific value $\mu = \Lambda$ and the renormalised $V_{\text{eff}}^{1-\text{loop}}$ can be written in a form similar to the one in (2.25)

$$V_{\text{eff}}^{1-\text{loop}}(\varphi_\phi) \;=\; \alpha\,\varphi_\phi^4 \;+\; \beta\,\varphi_\phi^4\,\ln\frac{\varphi_\phi^2}{\Lambda^2}\,, \tag{3.18}$$

where the coefficients α and β are dimensionless renormalised parameters and are given in the $\overline{\rm MS}$ renormalisation scheme [35] by

$$\begin{aligned}
\alpha &= \frac{1}{64\pi^2 v_\phi^4}\Bigg[\sum_{i=1}^{2} m_{H_i}^4\left(-\frac{3}{2}+\ln\frac{m_{H_i}^2}{v_\phi^2}\right) + 6m_W^4\left(-\frac{5}{6}+\ln\frac{m_W^2}{v_\phi^2}\right) \\
&\quad + 3m_Z^4\left(-\frac{5}{6}+\ln\frac{m_Z^2}{v_\phi^2}\right) - 12m_t^4\left(-1+\ln\frac{m_t^2}{v_\phi^2}\right) \\
&\quad - 2\sum_{i=1}^{3} m_{Ni}^4\left(-1+\ln\frac{m_{Ni}^2}{v_\phi^2}\right)\Bigg], \\
\beta &= \frac{1}{64\pi^2 v_\phi^4}\left(\sum_{i=1}^{2} m_{H_i}^4 + 6m_W^4 + 3m_Z^4 - 12m_t^4 - 2\sum_{i=1}^{3} m_{Ni}^4\right). \qquad (3.19)
\end{aligned}$$

In the above, we have neglected all the light fermions and retained only the top quark and possible heavy Majorana neutrinos $N_{1,2,3}$ [cf. (D.17)]. The mass terms m_X, where $X = \{H_{1,2},\, W,\, Z,\, t,\, N_{1,2,3}\}$, are the particle masses, which are determined by evaluating the mass parameters M_X, defined in Appendix C, at the minimum of the flat direction.

In the MSISM it is possible to write the one-loop effective potential $V_{\rm eff}^{1-\rm loop}(\Lambda)$ in (3.18) entirely in terms of φ_ϕ and v_ϕ, without the need to involve the other flat direction components φ_σ or φ_J. This is possible because either, $\varphi_\sigma = \varphi_J = 0$ along the Type I flat direction, or φ_σ and φ_J are related to φ_ϕ along the Type II flat direction.

It is possible to rewrite the MSISM effective potential (3.18) in the general parameterisation of (2.25). Employing the fact that $\varphi_\phi = \varphi n_\phi$ in (3.18), we find the following relations between the parameters A, B, α and β:

$$A = \alpha\, n_\phi^4 + \beta\, n_\phi^4 \ln n_\phi^2\,, \qquad B = \beta\, n_\phi^4\,, \qquad (3.20)$$

which can be substituted into (3.18) to give (2.25). Futhermore, substituting the above expressions for A and B into (2.33) and (2.27), we obtain the explicit dependence of the mass of h and the RG scale Λ on the effective potential coefficients

α and β:

$$m_h^2 \;=\; 8\,\beta\, n_\phi^2 v_\phi^2\,, \tag{3.21}$$

$$\Lambda \;=\; v_\phi \exp\left(\frac{\alpha}{2\beta}+\frac{1}{4}\right)\,. \tag{3.22}$$

These two relations m_h (3.21) and Λ (3.22) will be used in our detailed investigation of the Type I and Type II flat directions in Chapters 4 and 5 respectively.

With the aid of (3.22), we can eliminate the explicit dependence of the one-loop effective potential in (3.18) on the RG scale Λ,

$$V_{\rm eff}^{1-{\rm loop}}(\varphi_\phi) \;=\; \beta\,\varphi_\phi^4\left(\ln\frac{\varphi_\phi^2}{v_\phi^2} \;-\; \frac{1}{2}\right)\,, \tag{3.23}$$

where all kinematic quantities on the right-hand side, such as β, φ_ϕ and v_ϕ, are evaluated at the RG scale Λ [cf. (2.28)]. Hence, the size of the radiative corrections along the minimum flat direction is determined by the effective potential coefficient β and is therefore highly model dependent.

Now we have presented the one-loop effective potential we can summarise the scalar mass spectrum of the MSISM. The scalar mass spectrum consists of two scalars $H_{1,2}$ which generally both have non-zero masses $m_{H_{1,2}}$, unless, for example, the $U(1)$ symmetry acts on S so that $m_{H_2} = m_J = 0$, and one other scalar h, which gains a mass at one-loop via (3.21). We note that the Goldstone bosons $G^\pm$ and G associated with the EWSSB of the SM gauge group receive gauge-dependent masses along the minimum flat direction e.g. see (B.9). However, the one-loop effective potential $V_{\rm eff}^{1-{\rm loop}}(\Lambda)$ remains gauge independent, since the gauge-dependent mass terms of the Goldstones cancel against the gauge-dependent parts of the gauge boson and ghost contributions. For more extensive details see Appendix C.

We also take this opportunity to consider the short-comings of the SI SM. Given the explicit form of the effective potential coefficient β for the MSISM in (3.19), we can see why a SI version of the SM using the one-loop perturbative

GW [21] approach is not phenomenologically viable. The SI extension of the SM is similar to the Type I flat direction except that the extra scalar S does not exist, but the flat direction still lies along the ϕ axis. This implies that the Higgs boson $H_{\rm SM}$ corresponds to $\phi \equiv h$ and is massless at the tree level, but acquires a one-loop radiatively generated mass given by (3.21). Consequently, the SM Higgs boson mass $m_{H_{\rm SM}} \equiv m_h$ is explicitly dependent on β, i.e.

$$\beta \;=\; \frac{1}{64\pi^2 v_\phi^4}\left(6m_W^4 \;+\; 3m_Z^4 \;-\; 12m_t^4\right). \tag{3.24}$$

Given the presently well-known experimental values of the top quark, $W^\pm$ and Z boson masses [6], the coefficient β is negative and hence so is $m^2_{H_{\rm SM}}$. This is in violation of the LEP2 limit [9]: $m_{H_{\rm SM}} > 114.4$ GeV. Additionally, considering our discussion in Section 2.2, since β and B are negative, the SI limit of the SM has a potential which is not BFB.

Other attempts have been made in the literature to discuss the SI SM without using the one-loop perturbative GW approach, for example see [36, 37]. However, it appears that these approaches require large values of the quartic coupling λ which would approach a Landau pole not far beyond the EW scale. Also, without the additional scalars, the SI SM would not be able to address any of the phenomenology that the SM currently can not incorporate.

3.4 Phenomenology of the MSISM

As previously mentioned in the introduction, the MSISM could provide a conceptually simple solution to the gauge hierarchy problem by including a minimal set of new fields and new couplings. It is interesting to see what effect these new fields and couplings have on the phenomenological features of the different variations of flat direction in the MSISM. In particular, we are interested in scenarios which include new sources of CP violation, provide massive DM candidates and can incorporate a natural mechanism for generating the small light-neutrino

Flat Direction Type	U(1) Invariant	CP Violation	Massive DM Candidate	Seesaw Neutrinos
Type I				
$\varphi_S = 0$	Yes	None	Yes	No
$\varphi_S = 0$	No	Explicit	Yes	No
Type II				
$\varphi_S =$ real	Yes	None	No	Yes
$\varphi_S =$ real	No	Explicit	Model Dependent	Yes
$\varphi_S =$ imaginary	No	Explicit	Model Dependent	Yes
$\varphi_S =$ complex	No	Explicit or Spontaneous	Model Dependent	Yes

Table 3.1: *The possible phenomenology that could occur in the Type I and Type II flat directions of the MSISM for different variations of the complex singlet scalar S VEV. This includes their potential to realise explicit or spontaneous CP violation, massive DM candidates and possible implementation of the seesaw mechanism for naturally explaining the small light-neutrino masses.*

masses. We should note here that any U(1) symmetry imposed on the MSISM is not gauged, unlike [22, 27], and so there will be no additional gauge bosons in any of these considered scenarios.

A natural extension of MSISM is to include right-handed neutrinos, which would couple to the complex singlet scalar S in a SI way [15, 25, 26, 27, 28]. If the VEV of S is non-zero, such as in the Type II flat direction, then the naturally small Majorana masses for the light neutrinos can be generated via the seesaw mechanism [34]. In the Type I flat directions, where $\varphi_S = 0$, Dirac-type neutrino masses can still be generated from the SM Higgs VEV, however, just like the SM, the neutrino Yukawa couplings would need to be many orders of magnitude lower than the electron Yukawa coupling, of which there would be no explanation.

Hence, as we have listed in Table 3.1, only Type II flat directions have the ability to realise the seesaw mechanism.

The Sakharov Criteria [38] requires CP violation as one of its conditions for the Universe to dynamically evolve a baryon asymmetry. However, the level of CP violation in the SM from the Kobayashi-Maskawa phase [39] is not enough to generate the large matter-antimatter asymmetry in the Universe today and additional CP violation is required. We have presented in Table 3.1 the scenarios of the MSISM which can contain either explicit CP violation, through the complex quartic couplings $\lambda_{4,5,6}$, or spontaneous CP violation, from the complex VEV of S, in the newly extended scalar sector. Notice that the Type II flat direction with an imaginary φ_S does not violate CP spontaneously, since one may redefine S as $S' \equiv iS$ to render this flat direction real without introducing any new phase in the quartic couplings of the scalar potential[2].

Finally, Table 3.1 also shows the scenarios which could contain a massive stable scalar particle that could qualify as a DM candidate. As was pointed out in [41], a natural way of including a massive stable scalar boson is to impose a parity symmetry on the scalar potential. Such parity symmetries could be: $\sigma \to -\sigma$, $J \to -J$, or $\sigma \leftrightarrow \pm J$. Therefore, as we comment in Table 3.1, the existence of a DM candidate is model dependent and requires more specific details about the scenario.

In the next two chapters we discuss the phenomenology of a few representative scenarios of the MSISM in more detail, without the inclusion of right-handed neutrinos. A detailed analysis of the MSISM extended by right-handed neutrinos is given in Section 6.

[2]An analogous approach is discussed in [40].

Chapter 4

The Type I Flat Direction

In this chapter we investigate the Type I flat direction of the MSISM. We consider two different scenarios: the U(1) invariant and the general U(1) non-invariant, and for both scenarios make predictions on the size of their scalar mass spectrum and the RG scale Λ. These predictions are achieved by first determining the allowed region of quartic coupling parameter space permitted by both theoretical and experimental constraints, and then applying these limits to the scalar masses and Λ. The theoretical constraints are determined by keeping the quartic couplings perturbative and keeping the potential BFB, whilst the experimental constraints come from the electroweak oblique parameters S, T and U [32], the LEP2 Higgs mass limit: $m_{H_{\rm SM}} > 114.4$ GeV [9] and the recently determined Tevatron excluded range: 158 GeV $< m_{H_{SM}} <$ 175 GeV [10]. Having determined the scalar mass spectrum we can discuss the possible phenomenology for each scenario in detail.

Before we begin this investigation, we shall briefly review some general aspects that occur in all Type I MSISM flat directions. The Type I flat direction is defined so that along the flat direction the complex singlet scalar S does not develop a VEV at tree level. This implies that the flat direction lies along the ϕ axis in the real scalar field space and as a direct consequence, the quantum field ϕ is the pseudo-Goldstone boson associated with the anomalously broken scale invariance h. As discussed in Section 3.2.1, in addition to $\varphi_S = 0$, the Type I flat direction

also requires $\lambda_1(\Lambda) = 0$ to satisfy the tree-level minimisation condition (3.12).

4.1 The U(1) Invariant Scenario

In the U(1) invariant limit, which assumes the MSISM is symmetric under U(1) rephasings of the field $S \to e^{i\alpha}S$, where α is an arbitrary phase, the tree-level potential (3.2) for a Type I flat direction reduces to

$$V^{\text{tree}}(\Lambda) \;=\; \frac{\lambda_2(\Lambda)}{2}\,(S^*S)^2 \;+\; \lambda_3(\Lambda)\,\Phi^\dagger\Phi\,S^*S\,. \tag{4.1}$$

The two quartic couplings $\lambda_2(\Lambda)$ and $\lambda_3(\Lambda)$ are both positive due to the BFB conditions (3.6). Although the scalar potential (4.1) depends on two independent couplings $\lambda_2(\Lambda)$ and $\lambda_3(\Lambda)$, it is not difficult to show that the scalar masses and the RG scale Λ are completely dependent on only one, namely $\lambda_3(\Lambda)$. By setting $S = \varphi_S = 0$, $\phi = v_\phi$ and $\lambda_1(\Lambda) = 0$ in the general squared scalar mass matrix $\mathcal{M}_S^2$ (C.9), we find that the masses of σ and J are given by

$$m_\sigma^2 \;=\; m_J^2 \;=\; \frac{1}{2}\,\lambda_3(\Lambda)\,v_\phi^2\,. \tag{4.2}$$

Since these are the only two non-zero elements of $\mathcal{M}_S^2$, i.e. $m_\phi = 0$ and there is no mixing between the scalars, the scalar spectrum consists of the mass eigenstates

$$\phi \;\equiv\; h\,, \qquad \sigma \;\equiv\; H_1\,, \qquad J \;\equiv\; H_2\,, \tag{4.3}$$

where σ and J have degenerate masses proportional to $\sqrt{\lambda_3(\Lambda)}$ (4.2). The other scalar h, the pseudo-Goldstone boson associated with the anomalously broken scale invariance, receives its mass m_h at the one-loop level, by means of (3.21), or more explicitly

$$m_h \;=\; \frac{1}{\sqrt{8}\pi v_\phi}\,\sqrt{m_\sigma^4 + m_J^4 + 6m_W^4 + 3m_Z^4 - 12m_t^4} \tag{4.4}$$

where $n_\phi = 1$, see Section 3.2.1, and the $V_{\text{eff}}^{1-\text{loop}}$ coefficient β is given in (3.19). From (4.4) we can see m_h is dependent on only one unknown, the quartic coupling $\lambda_3(\Lambda)$, through the scalar masses $m_{\sigma,J}$. Likewise, the RG scale Λ, also depends on $m_{H_{1,2}}^2 = m_{\sigma,J}^2$ through the $V_{\text{eff}}^{1-\text{loop}}$ coefficients α and β, and hence its value is also fixed by $\lambda_3(\Lambda)$.

Considering the above discussion it is now clear that any theoretical constraints on $\lambda_3(\Lambda)$ will directly translate into constraints on the scalar mass spectrum and the RG scale Λ. An upper theoretical constraint on the value of $\lambda_3(\Lambda)$ can be derived by requiring that all the couplings of the MSISM remain perturbative at the scale Λ. We enforce this constraint by requiring that the one-loop RG beta functions for all the generic couplings of the MSISM are less than one when evaluated at the scale Λ:

$$\beta_\lambda(\Lambda) \;\leq\; 1 \,, \tag{4.5}$$

where λ denotes the generic couplings of the MSISM, i.e.

$$\lambda = \{\lambda_{1,2,\ldots,6},\; g',\; g,\; g_s,\; \mathbf{h}^{e,u,d},\; \mathbf{h}^N,\; \tilde{\mathbf{h}}^N\} \,. \tag{4.6}$$

We have calculated the one-loop beta functions β_λ for all the significant couplings in the MSISM and present them in Appendix D along side their one-loop anomalous dimensions. The perturbative coupling constraint (4.5) is equivalent to the triviality bound on the SM Higgs mass discussed in Chapter 1. Setting $\lambda_1(\Lambda) = 0$, we find that the most stringent upper limit on $\lambda_3(\Lambda)$ comes from $\beta_{\lambda_3}(\Lambda) \leq 1$, which implies

$$2\lambda_3^2(\Lambda) \;+\; \big[1.86 \;+\; 2\lambda_2(\Lambda)\big]\lambda_3(\Lambda) \;\leq\; 8\pi^2 \,, \tag{4.7}$$

for $m_W = 80.40$ GeV, $m_Z = 91.19$ GeV and $m_t = 171.3$ GeV [6]. Assuming $\lambda_2(\Lambda)$ is negligible we obtain a maximum upper limit of $\lambda_3(\Lambda) \leq 5.84$, however

this value decreases if $\lambda_2(\Lambda)$ increases. To clarify, by calling $\beta_{\lambda_3}(\Lambda) \leq 1$ the most stringent limit we mean that the other two constraints on the quartic couplings $\beta_{\lambda_{1,2}}(\Lambda) \leq 1$ allow larger values of $\lambda_3(\Lambda)$ than $\beta_{\lambda_3}(\Lambda) \leq 1$ does. A lower theoretical constraint can be obtained by requiring that the potential remains BFB, which is analogous to the vacuum stability bound of the SM, see Chapter 1. This is assured at one-loop if the $V_{\rm eff}^{1-\rm loop}$ coefficient β is positive, thus giving rise to a lower theoretical bound of $\lambda_3(\Lambda) > 2.32$. In summary, the theoretical constraints require that $\lambda_3(\Lambda)$ lies in the range,

$$2.32 \ < \lambda_3(\Lambda) \ \leq 5.84 \, . \tag{4.8}$$

Further constraints on $\lambda_3(\Lambda)$ can be derived from the experimental data of direct Higgs searches and the electroweak oblique parameters S, T and U. The oblique parameters are used to parameterise the effect of new physics on the gauge boson self-energies. We discuss the oblique parameters and present the analytic results of the electroweak oblique parameter shifts δS, δT and δU evaluated in the MSISM with respect to the SM in Appendix E. In the U(1) invariant Type I MSISM, the only scalar which interacts with the $W^\pm$ and Z bosons at one-loop is h, since σ and J are decoupled from the SM particles. As a consequence, the shifts δS, δT and δU are obtained from the h interactions only. Since these interactions are identical to those of the SM Higgs boson $H_{\rm SM}$, the shift parameters δS, δT and δU only depend on the difference between the two masses, m_h and $m_{H_{\rm SM}}$. For a fixed SM Higgs boson mass reference value, e.g. $m_{H_{\rm SM}}^{\rm ref} = 117$ GeV [6], and assuming that δS, δT and δU fall within their 95% CL intervals, given in (E.10), we obtain the results presented in Table 4.1. For values of $\lambda_3(\Lambda) < 100$ the result for δU lies within the range set by $\delta U_{\rm exp}$ and provides no constraint, whilst the combined limit from δS and δT yields the constraint: $\lambda_3(\Lambda) < 49.12$. There are two direct Higgs boson searches that are of interest to us, the LEP2 limit: $m_{H_{\rm SM}} = m_h > 114.4$ GeV [9] and region excluded by the Tevatron results: $158\,\text{GeV} < m_{H_{\rm SM}} < 175$ GeV [10]. Applying the LEP2 Higgs mass limit on the

Oblique parameter	δS	δT	δU
Limit on $\lambda_3(\Lambda)$	$\lambda_3(\Lambda) < 49.12$	$\lambda_3(\Lambda) < 74.28$	All values of $\lambda_3(\Lambda) < 100$ are within the range of $\delta U_{\rm exp}$

Table 4.1: *Upper limits on $\lambda_3(\Lambda)$ from the S, T and U oblique parameters in the U(1) invariant MSISM with a Type I flat direction, assuming they fall within their respective 95% CL intervals given in (E.10).*

mass of the SM-like h boson we obtain the constraint $\lambda_3(\Lambda) > 6.29$, whilst the Tevatron results exclude the parameter space region $8.40 < \lambda_3(\Lambda) < 9.24$. Thus, the experimental constraints require $\lambda_3(\Lambda)$ lies in the ranges

$$6.29 \ < \lambda_3(\Lambda) \ < 8.40 \qquad \text{or} \qquad 9.24 \ < \lambda_3(\Lambda) \ < 49.12 \ , \tag{4.9}$$

where the lower of the two ranges is slightly outside the theoretical range given in (4.8).

In Figure 4.1, we apply the above theoretical and experimental constraints, (4.8) and (4.9) respectively, on the h (upper panel) and σ, J (lower panel) scalar boson masses where we display the dependence of m_h (4.4) and $m_{\sigma,J}$ (4.2) on the quartic coupling $\lambda_3(\Lambda)$. The solid black $\beta_{\lambda_3} < 1$ lines represent the theoretically permitted values of the scalar boson masses determined from (4.8), whereas the continuation of these lines into the dashed grey $\beta_{\lambda_3} > 1$ lines correspond to the non-perturbative regime, in which $\lambda_3(\Lambda) > 5.84$. The region of the scalar mass line between the horizontal blue LEP line and the horizontal red δS line, except the green TEV region which is excluded by the Tevatron results, indicates the region permitted by the combined experimental limits on $\lambda_3(\Lambda)$ summarised in (4.9). Similarly, the region above the horizontal red δT line is excluded by the weaker δT limit (see Table 4.1). It is interesting to remark that Figure 4.1 shows

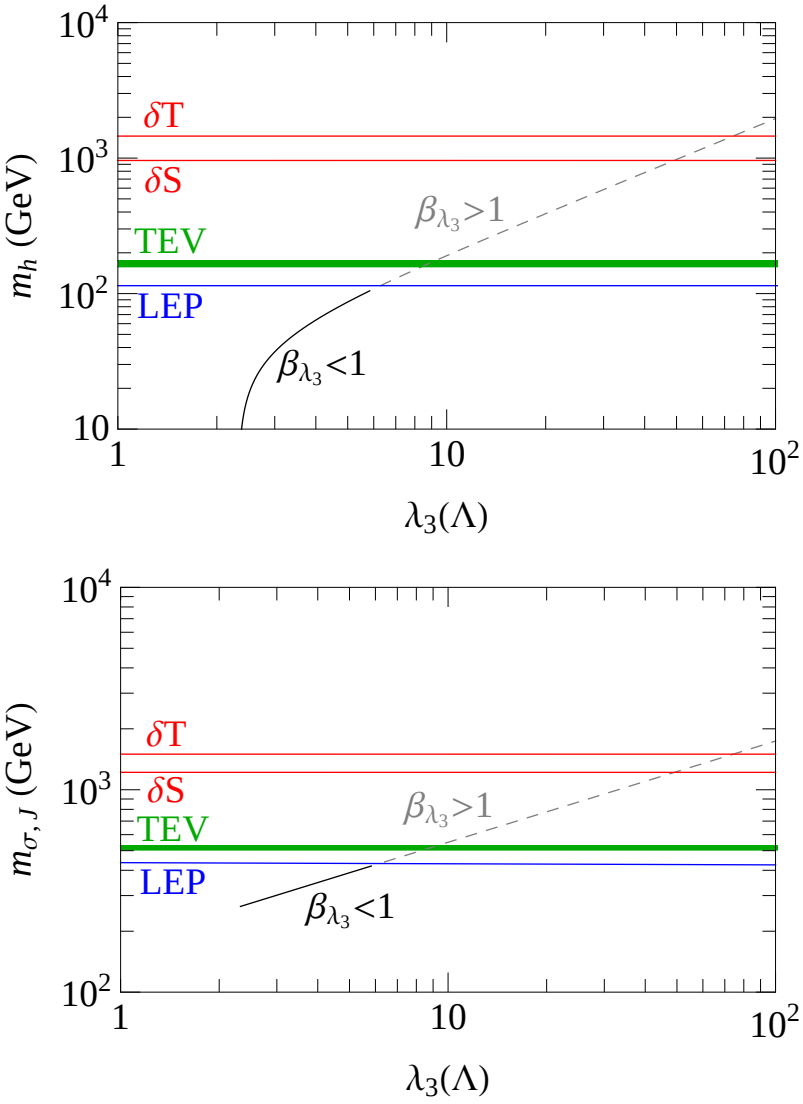

Figure 4.1: *The scalar masses m_h (upper plot) and $m_{\sigma,J}$ (lower plot) as functions of $\lambda_3(\Lambda)$ in the U(1) invariant MSISM with a Type I flat direction. The solid/black $\beta_{\lambda_3} < 1$ lines represent the scalar masses for theoretically permitted values of $\lambda_3(\Lambda)$, whilst the dashed/grey $\beta_{\lambda_3} > 1$ extensions show the non-perturbative values with $\lambda_3(\Lambda) > 5.84$. The region of the mass line between the horizontal blue LEP line and the horizontal red δS line is allowed by experimental considerations of the LEP2 Higgs mass limit on the SM-like h boson and the δS oblique parameter respectively, except for the green TEV region which is excluded by the Tevatron results. The area above the horizontal red δT line is excluded by the δT parameter constraint.*

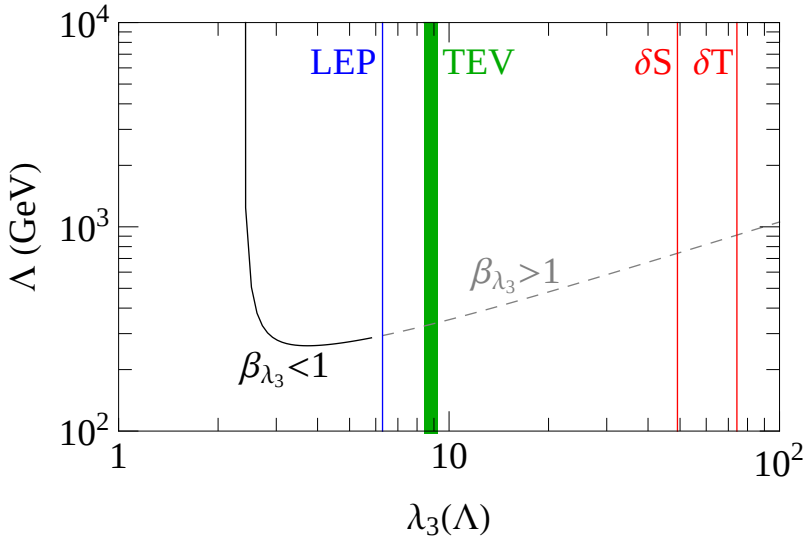

Figure 4.2: *The RG scale Λ plotted as a function of the quartic coupling $\lambda_3(\Lambda)$ in the U(1) invariant MSISM with a Type I flat direction. The same line colour convention as Figure 4.1 is applied. The only difference is the horizontal blue LEP line, green TEV region and red δS and δT lines are now vertical, where the area between the LEP and δS lines, excluding the green TEV region, is allowed by the experimental conditions (4.9) and to the right of the δT line is excluded.*

an exact value (the solid black and dashed grey line) for the physical scalar masses $m_{h,\sigma,J}$ against the quartic coupling $\lambda_3(\Lambda)$. This implies that if the Type I U(1) invariant flat direction of the MSISM was physically true, then a measurement of m_h would automatically give $\lambda_3(\Lambda)$ which in turn gives the RG scale Λ and the other scalar masses $m_{\sigma,J}$.

The effect of the constraints (4.8) and (4.9) on the RG scale Λ is shown in Figure 4.2 as a dependence on the quartic coupling $\lambda_3(\Lambda)$. We have used the same line colour convention as Figure 4.1, only now the horizontal LEP, TEV, δS and δT lines are vertical, such that the green TEV region and the regions to the right of the red δS and δT lines and to the left of the blue LEP line are experimentally excluded. We observe that as $\lambda_3(\Lambda)$ approaches its minimum value, the coefficient β gets closer to zero, and so the RG scale Λ tends to infinity. However, this is not an issue since the area is not physically viable as it is excluded by the LEP2 Higgs mass limit. For the majority of the line, except when $\lambda_3(\Lambda) \to 2.32$, Λ is of the

order of the EW scale. This is important for a reason we have not yet addressed; the running of the coupling constants. Given the circular nature of the following argument; the value of the RG scale Λ is unknown until a value of $\lambda_3(\Lambda)$ which depends on Λ is given, we have, for simplicity, evaluated all the quartic couplings at the EW scale 246 GeV. This assumes that the quartic couplings do not vary much between the EW scale and the RG scale Λ, which we have verified, and we acknowledge that there could be an error on the values of the scalar masses and RG scale Λ present here, but of no more than about 5%.

If we assume the LEP2 limit $\lambda_3(\Lambda) \approx 6.3$ as the most experimentally and theoretically favourable value of $\lambda_3(\Lambda)$ then we obtain a value for the RG scale of $\Lambda \approx 294$ GeV. We find that although $\lambda_3(\Lambda) \approx 6.3$ is non-perturbative at Λ, i.e. $\beta_{\lambda_3}(\Lambda) > 1$, the theory does not develop a Landau pole until 10^4 GeV. By virtue of (4.2), we are also able to predict the masses of the heavier degenerate scalar bosons σ and J, specifically, $m_{\sigma,J} \approx 437$ GeV. Since the fields σ and J are both stable, massive and have zero VEVs, they can qualify as DM candidates in the so-called "Higgs-portal" scenario (also known as scalar phantoms) [41].

Phenomenological distinction between the MSISM with a Type I U(1) invariant flat direction and the SM would be very difficult as the two theories so closely resemble each other. Since all the non-scalar couplings in the MSISM are the same as the SM and the h-boson couplings to fermions and electroweak gauge bosons are exactly the same as those for the SM Higgs boson, they can not be used as a distinguishing factor. However, one subtle difference is the lack of tree-level trilinear and quadrilinear h self-couplings in the MSISM with a Type I flat direction, which are present in the SM. Thus, any experiment in search of the trilinear Higgs boson coupling λ_{HHH}, for example see [42], will see a dramatically reduced value for the trilinear coupling than that expected for the SM. Since these are precision Higgs experiments they will not be performed at the Large Hadron Collider (LHC), but could be tested at a collider like the International e^+e^- Linear Collider (ILC). Since the two scalars σ and J only interact with h,

they could be inferred through missing energy or because of the large $h\sigma^2$ and hJ^2 couplings which would give sizable contributions at the one-loop quantum level. Therefore, to distinguish between the MSISM with a Type I U(1) invariant flat direction and the SM, precision Higgs experiments at an ILC-type collider would be required.

Considering the analysis above, it is clear that in spite of being very predictive by predominantly relying on only one unknown parameter $\lambda_3(\Lambda)$, the U(1) invariant MSISM with a Type I flat direction has a number of weaknesses. This scenario satisfies all experimental limits for a large quartic coupling $\lambda_3(\Lambda) \approx 6.3$, but it lies above the boundary of non-perturbative dynamics given in (4.8). Another problematic feature is that it exhibits a Landau pole at energy scales of order 10^4 GeV, which is many orders of magnitude below the standard GUT ($M_{\rm GUT} \approx 10^{16}$ GeV) and Planck ($M_{\rm Planck} \approx 10^{19}$ GeV) mass scales. Therefore, in the next section, we relax the constraint of U(1) invariance and investigate whether a general MSISM with a Type I flat direction can remain perturbative up to the GUT or Planck scales.

4.2 The U(1) Non-Invariant Scenario

If the U(1) symmetry on the scalar field S is removed then the MSISM with a Type I flat direction permits an extensive general tree level potential:

$$\begin{aligned} V^{\rm tree}(\Lambda) \;=\; & \frac{\lambda_2(\Lambda)}{2}\,(S^*S)^2 \;+\; \lambda_3(\Lambda)\,\Phi^\dagger\Phi\,S^*S \;+\; \lambda_4(\Lambda)\,\Phi^\dagger\Phi\,S^2 \;+\; \lambda_4^*(\Lambda)\,\Phi^\dagger\Phi\,S^{*2} \\ & + \lambda_5(\Lambda)\,S^3S^* \;+\; \lambda_5^*(\Lambda)\,SS^{*3} \;+\; \frac{\lambda_6(\Lambda)}{2}\,S^4 \;+\; \frac{\lambda_6^*(\Lambda)}{2}\,S^{*4}\,. \end{aligned} \tag{4.10}$$

Similar to the U(1) invariant scenario we can show that the scalar boson masses and the RG scale Λ do not depend on all the quartic couplings in $V^{\rm tree}(\Lambda)$ (4.10) but only rely on two; $\lambda_3(\Lambda)$ and the modulus $|\lambda_4(\Lambda)| = \sqrt{\lambda_4(\Lambda)\lambda_4^*(\Lambda)}$ of the generally complex coupling $\lambda_4(\Lambda)$. By substituting $S = \varphi_S = 0$, $\phi = v_\phi$ and

$\lambda_1(\Lambda) = 0$ into the general squared scalar boson mass matrix $\mathcal{M}_S^2$ given in (C.9), we obtain three non-zero matrix elements

$$\begin{aligned} m_\sigma^2 &= \frac{1}{2}\Big(\lambda_3(\Lambda) + \lambda_4(\Lambda) + \lambda_4^*(\Lambda)\Big) v_\phi^2 \,, \\ m_J^2 &= \frac{1}{2}\Big(\lambda_3(\Lambda) - \lambda_4(\Lambda) - \lambda_4^*(\Lambda)\Big) v_\phi^2 \,, \\ m_{\sigma J} &= \frac{i}{2}\Big(\lambda_4(\Lambda) - \lambda_4^*(\Lambda)\Big) v_\phi^2 \,. \end{aligned} \tag{4.11}$$

Determining the eigenvalues of $\mathcal{M}_S^2$ provides the tree-level scalar boson masses

$$m_{H_1}^2 = \frac{1}{2}\Big(\lambda_3(\Lambda) + 2|\lambda_4(\Lambda)|\Big) v_\phi^2 \,, \qquad m_{H_2}^2 = \frac{1}{2}\Big(\lambda_3(\Lambda) - 2|\lambda_4(\Lambda)|\Big) v_\phi^2 \,, \tag{4.12}$$

thus, in the most general case, the scalar spectrum consists of the mass eigenstates,

$$h \equiv \phi \,, \qquad H_1 = \cos\theta\, \sigma + \sin\theta\, J \,, \qquad H_2 = -\sin\theta\, \sigma + \cos\theta\, J \,, \tag{4.13}$$

where $\cos^2\theta = \frac{m_\sigma^2 - m_{H_2}^2}{m_{H_1}^2 - m_{H_2}^2}$. From (4.12) we can see that the scalar masses depend on only two coupling parameters, $\lambda_3(\Lambda)$ and $|\lambda_4(\Lambda)|$. Consequently, the two effective potential coefficients α and β also depend on $\lambda_3(\Lambda)$ and $|\lambda_4(\Lambda)|$ through the scalar boson masses $m_{H_{1,2}}$. It is therefore not difficult to see that the one-loop induced h boson mass and the RG scale Λ also only depend on $\lambda_3(\Lambda)$ and $|\lambda_4(\Lambda)|$ through (3.21) and (3.22) respectively.

We can see that if $\lambda_4(\Lambda)$ is complex then the two particle scalar-pseudoscalar mixing term $m_{\sigma J}$ (4.11) explicitly violates CP and so the mass eigenstates $H_{1,2}$ have indefinite CP parities. If, however, $\lambda_4(\Lambda)$ is real then the CP violating term $m_{\sigma J} = 0$ and under this condition the scalar fields reduce to $H_1 = \sigma$ and $H_2 = J$ and CP is preserved. Throughout this analysis we use $|\lambda_4(\Lambda)|$ and are not required to specify the complexity of $\lambda_4(\Lambda)$.

The quartic couplings are constrained at tree-level by the BFB conditions given in (3.6). The allowed parameter spaces of the couplings λ_2, λ_5 and λ_6 are

restricted by the first condition in (3.6) which is only fulfilled if $\Lambda_{22}(\Lambda) \geq 0$. In order for the first BFB condition to hold for any possible value of the phase θ_S, we require that

$$\lambda_2(\Lambda) \;\geq\; 4\,|\lambda_5(\Lambda)| \;+\; 2\,|\lambda_6(\Lambda)| \;>\; 0\,. \tag{4.14}$$

For the second $V^{\rm tree}$ BFB condition in (3.6), i.e $\Lambda_{12}(\Lambda) \geq 0$, for $\Lambda_{11}(\Lambda) = 0$, to hold for any value of θ_S requires

$$\lambda_3(\Lambda) \;\geq\; 2|\lambda_4(\Lambda)| \;>\; 0\,. \tag{4.15}$$

Comparing this latter condition to the scalar boson masses given in (4.12), then (4.15) ensures that $m_{H_{1,2}}$ are positive and consequently is an important condition for the quartic couplings to respect.

As in the U(1) invariant scenario, we can derive more specific theoretical constraints on the values of $\lambda_3(\Lambda)$ and $|\lambda_4(\Lambda)|$, by demanding that the couplings remain perturbative at Λ and that the one-loop effective potential $V_{\rm eff}^{1-\rm loop}$ is BFB. The most stringent theoretical upper limit on $\lambda_3(\Lambda)$ and $|\lambda_4(\Lambda)|$ is obtained by requiring that $\beta_{\lambda_3} \leq 1$ at Λ and assuming $\lambda_2(\Lambda)$, $\lambda_5(\Lambda)$ and $\lambda_6(\Lambda)$ are negligible, which gives the constraint

$$2\,\lambda_3^2(\Lambda) \;+\; 8\,|\lambda_4(\Lambda)|^2 \;+\; 1.86\,\lambda_3(\Lambda) \;\leq\; 8\pi^2\,. \tag{4.16}$$

This upper limit decreases if $\lambda_2(\Lambda)$, $\lambda_5(\Lambda)$ and $\lambda_6(\Lambda)$ increase. The lower theoretical limit is obtained by requiring that $\beta > 0$, which translates into the constraint

$$\lambda_3^2(\Lambda) \;+\; 4\,|\lambda_4(\Lambda)|^2 \;>\; 5.39\,. \tag{4.17}$$

Complementary experimental constraints on the quartic couplings $\lambda_3(\Lambda)$ and $|\lambda_4(\Lambda)|$ arise from the electroweak oblique parameters S, T and U and the direct Higgs boson searches at LEP2 and Tevatron. Once again only h interacts with the SM particles and useful experimental constraints on $\lambda_3(\Lambda)$ and $|\lambda_4(\Lambda)|$ are derived

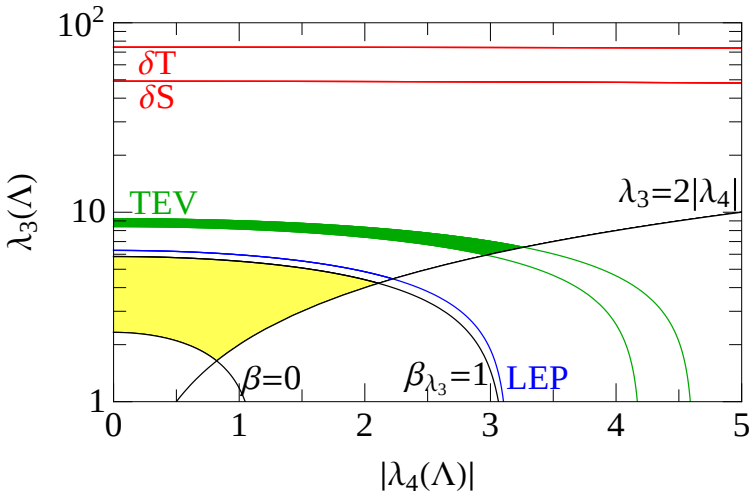

Figure 4.3: *Theoretical and experimental exclusion contours in the* $\lambda_3(\Lambda)$-$|\lambda_4(\Lambda)|$ *parameter space of the general MSISM with a Type I flat direction. The theoretically permitted region is shaded yellow and is enclosed by the black lines which correspond to keeping* $\lambda_3(\Lambda) \geq 2|\lambda_4(\Lambda)| > 0$, $\beta_{\lambda_3}(\Lambda) \leq 1$ *and* $\beta > 0$. *Above the blue LEP line is experimentally allowed by the LEP2 Higgs mass limit and below the red* δS *and* δT *lines is allowed by their respective 95% CL interval limits. The green TEV region is excluded by the direct Higgs searches at the Tevatron.*

from the 95% CL interval of the electroweak oblique parameters δS and δT using the fixed SM Higgs boson mass reference value $m_{H_{\rm SM}}^{\rm ref} = 117$ GeV. The shift δU does not provide a constraint since all values of $\lambda_3(\Lambda)$ and $|\lambda_4(\Lambda)|$ evaluate a value of δU within its experimental 95% CL interval. Applying the LEP2 Higgs mass limit to h, $m_{H_{\rm SM}} = m_h > 114.4$ GeV, gives rise to the constraint:

$$\lambda_3^2(\Lambda) \; + \; 4\,|\lambda_4(\Lambda)|^2 \; > \; 39.54\,. \tag{4.18}$$

Similarly, the Tevatron exclusion range $158\,\text{GeV} < m_{H_{\rm SM}} < 175$ GeV [10], excludes the region

$$70.54 \; < \; \lambda_3^2(\Lambda) \; + \; 4\,|\lambda_4(\Lambda)|^2 \; < \; 85.31\,. \tag{4.19}$$

Combining all the aforementioned theoretical and experimental constraints, we present the pertinent region of the $\lambda_3(\Lambda)$-$|\lambda_4(\Lambda)|$ parameter space in Figure 4.3.

The theoretically permitted region is shaded yellow and is enclosed by the black $\lambda_3 = 2|\lambda_4|$, $|\lambda_4| = 0$, $\beta_{\lambda_3} = 1$ and $\beta = 0$ lines, which respectively represent keeping the scalar masses positive (4.15), keeping the quartic couplings perturbative at Λ (4.16) and keeping $V_{\text{eff}}^{1-\text{loop}}(\Lambda)$ BFB (4.17). The regions below both the $\lambda_3 = 2|\lambda_4|$ and $\beta = 0$ lines are theoretically excluded, and above the $\beta_{\lambda_3} = 1$ line corresponds to the non-perturbative regime where $\beta_{\lambda_3}(\Lambda) > 1$. The region above the blue LEP line is permitted by the LEP2 Higgs mass limit (4.18), implying that the experimentally permitted region once again lies just outside the region of perturbative dynamics. The regions above the red δS and δT lines are excluded by their respective 95% CL intervals, δS_{exp} and δT_{exp}, and the green shaded TEV region is excluded by the Tevatron excluded range (4.19).

We present the effect of all the theoretical and experimental constraints, displayed in Figure 4.3, on the scalar boson masses m_h (upper panel), m_{H_1} (middle panel) and m_{H_2} (lower panel) as functions of the quartic coupling $\lambda_3(\Lambda)$ in Figure 4.4. In each plot the white areas between the black lines represent the perturbative regions ($\beta_{\lambda_3} < 1$) which also contain positive scalar masses (4.15) and keep the one-loop effective potential coefficient $\beta > 0$, which corresponds to the shaded yellow region in Figure 4.3. Whereas, the non-perturbative extrapolations ($\beta_{\lambda_3} > 1$) are shaded grey with black dashed border lines. The areas above or to the right of the red δS and δT lines are excluded by their respective 95% CL limits on δS_{exp} and δT_{exp} (E.10). Likewise, the areas below or to the left of the blue LEP lines are also excluded by the LEP2 Higgs mass limit applied to m_h. For clarity, the Tevatron excluded range has been neglected from the figures, but from Figure 4.3 we can see it clearly lies in the non-pertubative region.

In Figure 4.5 we display the dependence of the RG scale Λ on the quartic coupling $\lambda_3(\Lambda)$ after incorporating all the theoretical and experimental limits and using the same line colour convention as Figure 4.4. Similar to the U(1) invariant scenario, as $\lambda_3(\Lambda)$ approaches values which set $\beta = 0$, the RG scale Λ tends to infinity, however, once again these values are all excluded by the LEP2

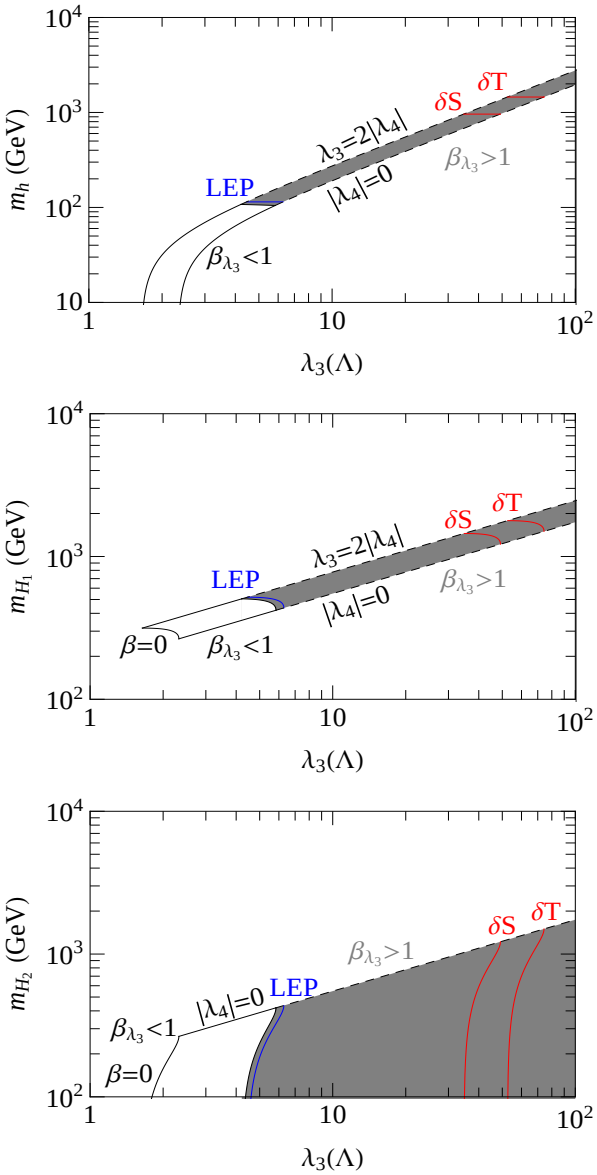

Figure 4.4: *The scalar masses m_h (upper panel), m_{H_1} (middle panel) and m_{H_2} (lower panel) as functions of $\lambda_3(\Lambda)$ in the general MSISM with a Type I flat direction. The white areas between the black lines show the regions which respect the theoretical constraints; $\beta_{\lambda_3}(\Lambda) \leq 1$, $\lambda_3(\Lambda) \geq 2|\lambda_4(\Lambda)| > 0$ and $\beta > 0$, whilst the grey-shaded areas show their non-perturbative extensions, i.e. $\beta_{\lambda_3}(\Lambda) > 1$. The areas lying to the right or above the red lines for δS and δT are excluded. Likewise, the areas to the left or below the blue LEP line are ruled out by the LEP2 Higgs mass limit.*

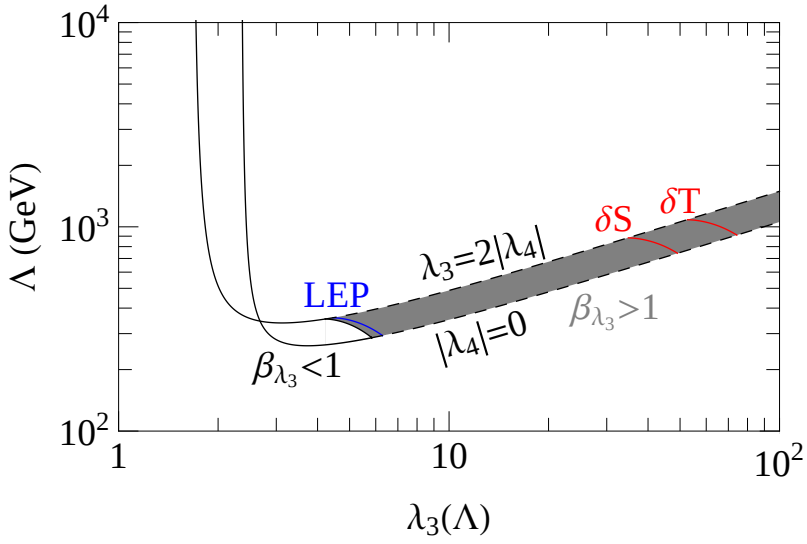

Figure 4.5: *The RG scale Λ as a function of $\lambda_3(\Lambda)$ in the general MSISM with a Type I flat direction. The white area between the black lines shows the region that corresponds to perturbative values of $\lambda_3(\Lambda)$ and $|\lambda_4(\Lambda)|$, whilst the grey-shaded area shows the non-perturbative region, both of which respect the constraint (4.15). The area lying to the left of the blue LEP line is ruled out by the LEP2 Higgs mass limit. Likewise, the areas to the right of the red lines for δS and δT are also excluded.*

Higgs mass limit.

Since the experimentally permitted regions lie just outside the boundary for perturbative dynamics, we again take $m_h \sim 115$ GeV as the most favourable value from which we can predict the range of the RG scale Λ and the mass ranges for the other scalars $H_{1,2}$. From Figure 4.5, we see that the RG scale Λ lies in the range $293\,\text{GeV} \lesssim \Lambda \lesssim 359$ GeV and is of the order of the EW scale. We note that the change from a specific value in the U(1) invariant scenario to a range of values is entirely due to the addition of the quartic coupling $\lambda_4(\Lambda)$. Similarly, from the middle and lower panels of Figure 4.4, we find that the preferred values of the H_1 and H_2 masses are constrained to lie in the intervals:

$$436\ \text{GeV} \lesssim m_{H_1} \lesssim 519\ \text{GeV}\,, \qquad 0\ \text{GeV} \leq m_{H_2} \lesssim 436\ \text{GeV}\,. \tag{4.20}$$

The general Type I MSISM can provide two types of stable DM candidates,

H_1 and H_2, however specific criteria must be met by both scalars. For H_1, it could only become a viable DM candidate provided its decay via the quartic interaction $H_1 H_2^3$ is kinematically forbidden, i.e. as long as $3m_{H_2} > m_{H_1}$. The other scalar H_2 has similar mass problems, however this time the scalar must not have a small mass, otherwise it would form hot or warm DM which is undesirable for galaxy formation. Determining exact limits on the minimum value of m_{H_2} is beyond the scope of this work. However, we note that if m_{H_2} is small, then it opens a new decay channel for the SM-like Higgs boson h via $h \to 2H_2$ which could compete with $h \to b\overline{b}$ to be the dominant decay mode when $m_h \sim 115$ GeV. This decay is not present in the SM and could be used as an indication of the general MSISM with a Type I flat direction. If however, $2m_{H_2} > m_h$, then as in the U(1) invariant scenario, the distinction of the Higgs sector of the general MSISM with a Type I flat direction from that of the SM would require precision Higgs experiments at an ILC-type collider and would again be based on the fact that the tree-level trilinear h self-coupling is zero at tree level [42] .

The general CP-violating MSISM with a Type I flat direction shares the same weakness as the U(1) invariant scenario. Assuming $m_h \sim 115$ GeV and $\lambda_4(\Lambda)$ is negligible, the theory generates a Landau pole at 10^4 GeV, which decreases as $\lambda_4(\Lambda)$ increases. As we can see the Landau pole is again far below the GUT and Planck scales. However, unlike the U(1) invariant scenario, the general model contains new sources of CP violation, provided $\lambda_4(\Lambda)$ is complex, which might be of particular importance for realising electroweak baryogenesis. One serious drawback of all scenarios of the MSISM with Type I flat directions is the inability to provide a natural implementation of the seesaw mechanism, since the VEV of the complex singlet scalar vanishes, i.e. $\varphi_S = 0$, and so no Majorana mass terms can be generated in this scenario. Therefore, in the next chapter, we turn our attention to the Type II flat direction, where $\varphi_S \neq 0$.

Chapter 5

The Type II Flat Direction

In this chapter we study the Type II flat direction of the MSISM. We investigate two distinct scenarios: (i) the U(1) invariant limit and (ii) a minimal U(1) non-invariant scenario where CP is maximally and spontaneously broken along the flat direction. In both these scenarios we determine the permitted quartic coupling parameter space, using both theoretical and experimental constraints, and apply these limits to make predictions on the scalar mass spectrum. We also discuss the possible phenomenology of the two scenarios.

The Type II flat direction of the MSISM is more scenario dependent than the Type I flat direction, however, the different scenarios do share some generic traits that we shall briefly discuss here. The Type II flat direction requires that both the Higgs doublet Φ and the complex singlet S develop non-zero VEVs along the flat direction. Thus, unlike the Type I flat direction, the flat direction in the Type II case is a 2 or 3 component vector and the pseudo-Goldstone boson h, which is the field associated with the flat direction, is in general a linear composition of all the neutral fields ϕ, σ and J. This has interesting phenomenological implications as it could be possible for all the Higgs mass eigenstates h, H_1 and H_2 to couple to the SM particles, but with reduced strengths compared to the respective SM Higgs boson coupling.

5.1 The U(1) Invariant Scenario

In the U(1) invariant limit, the tree-level MSISM with a Type II flat direction takes the simple form

$$V^{\text{tree}}(\Lambda) \;=\; \frac{\lambda_1(\Lambda)}{2}\,(\Phi^\dagger\Phi)^2 \;+\; \frac{\lambda_2(\Lambda)}{2}\,(S^*S)^2 \;+\; \lambda_3(\Lambda)\,\Phi^\dagger\Phi\,S^*S\,. \tag{5.1}$$

We have already discussed this case in some detail in Section 3.2.2, however, we shall review its main features here. The U(1) symmetry of the field $S \to e^{i\alpha}S$, where α is an arbitrary phase, allows us to set the VEV of the S field real, i.e. $\varphi_\sigma \neq 0$ and $\varphi_J = 0$. Hence, the flat direction $\mathbf{\Phi}^{\text{flat}}$ can be dimensionally reduced to a two-dimensional vector with components φ_ϕ and φ_σ, explicitly given in (3.16). Imposing the minimisation conditions (3.12) and (3.13) on the tree-level potential (5.1) generates the following relations between the flat direction components and the quartic couplings at the RG scale Λ:

$$\frac{\varphi_\phi^2}{\varphi_{\sigma^2}} \;=\; \frac{n_\phi^2}{n_\sigma^2} \;=\; -\frac{\lambda_2(\Lambda)}{\lambda_3(\Lambda)} \;=\; -\frac{\lambda_3(\Lambda)}{\lambda_1(\Lambda)}\,. \tag{5.2}$$

As stated after (3.15), the quartic couplings should lie in the ranges: $\lambda_1(\Lambda) > 0$, $\lambda_2(\Lambda) > 0$ and $\lambda_3(\Lambda) < 0$ to satisfy the BFB conditions (3.6) taking into account the form of (5.2).

The flat direction relation (5.2) may be used to reduce the number of independent quartic couplings at Λ to two, $\lambda_1(\Lambda)$ and $\lambda_3(\Lambda)$, by eliminating $\lambda_2(\Lambda)$ via the relation $\lambda_2(\Lambda) = \frac{\lambda_3^2(\Lambda)}{\lambda_1(\Lambda)}$. Consequently, it is possible to express the scalar masses and the RG scale Λ entirely in terms of the two quartic couplings $\lambda_1(\Lambda)$ and $\lambda_3(\Lambda)$. Taking the relations in (5.2) into account, the scalar mass matrix given in (C.9) contains the following non-zero elements:

$$m_\phi^2 \;=\; \lambda_1(\Lambda)\,v_\phi^2\,, \qquad m_\sigma^2 \;=\; -\lambda_3(\Lambda)\,v_\phi^2\,, \qquad m_{\phi\sigma} = -\sqrt{-\lambda_1(\Lambda)\lambda_3(\Lambda)}\,v_\phi^2\,. \tag{5.3}$$

Due to the scalar mixing term $m_{\phi\sigma}$, the scalar mass spectrum consists of the mass

eigenstates

$$h \;=\; \cos\theta\,\phi + \sin\theta\,\sigma\;, \qquad H_1 \;\equiv\; H \;=\; -\sin\theta\,\phi + \cos\theta\,\sigma\;, \qquad H_2 \;\equiv\; J\;, \tag{5.4}$$

where $\cos^2\theta = \frac{-\lambda_3(\Lambda)}{\lambda_1(\Lambda)-\lambda_3(\Lambda)}$. At tree-level, there is only one massive scalar, the H boson, whose mass squared is given by

$$m_{H_1}^2 \;=\; m_H^2 \;=\; \left[\lambda_1(\Lambda) - \lambda_3(\Lambda)\right] v_\phi^2\;, \tag{5.5}$$

the other two scalars h and J are massless since J is the massless Goldstone boson associated with the spontaneous breaking of the U(1) symmetry and h is the pseudo-Goldstone boson associated with the anomalously broken scale invariance. We note that although there is a non-zero two particle mixing term $m_{\phi\sigma}$ (5.3), there is no CP violation as the mixing is between two CP-even states, this means all the mass eigenstates have definite CP parity: h and H are CP-even and J is CP-odd.

From (5.5) we can see that m_H^2 depends on the combination $\lambda_1(\Lambda) - \lambda_3(\Lambda)$, and therefore, so too do the two effective potential coefficients α and β (3.19). Likewise, the RG scale Λ also depends on the combination $\lambda_1(\Lambda) - \lambda_3(\Lambda)$, through α and β, see (3.22). However, the one-loop contribution to m_h, given in (3.21), or explicitly

$$m_h \;=\; \frac{1}{\sqrt{8}\pi v_\phi}\sqrt{\frac{-\lambda_3(\Lambda)}{\lambda_1(\Lambda)-\lambda_3(\Lambda)}}\,\sqrt{m_H^4 + 6m_W^4 + 3m_Z^4 - 12m_t^4}\,, \tag{5.6}$$

shows m_h depends on $\lambda_3(\Lambda)$ independently as well, through the flat direction component $n_\phi = \cos\theta$, given in (3.16). Thus, the Higgs sector of the U(1) invariant MSISM with a Type II flat direction depends on $\lambda_1(\Lambda) - \lambda_3(\Lambda)$ and $\lambda_3(\Lambda)$, or equivalently on $\lambda_1(\Lambda)$ and $\lambda_3(\Lambda)$.

We display the theoretical and experimental limits on the two quartic couplings $\lambda_1(\Lambda)$ and $\lambda_3(\Lambda)$ in Figure 5.1. The top panel displays the full perturbative

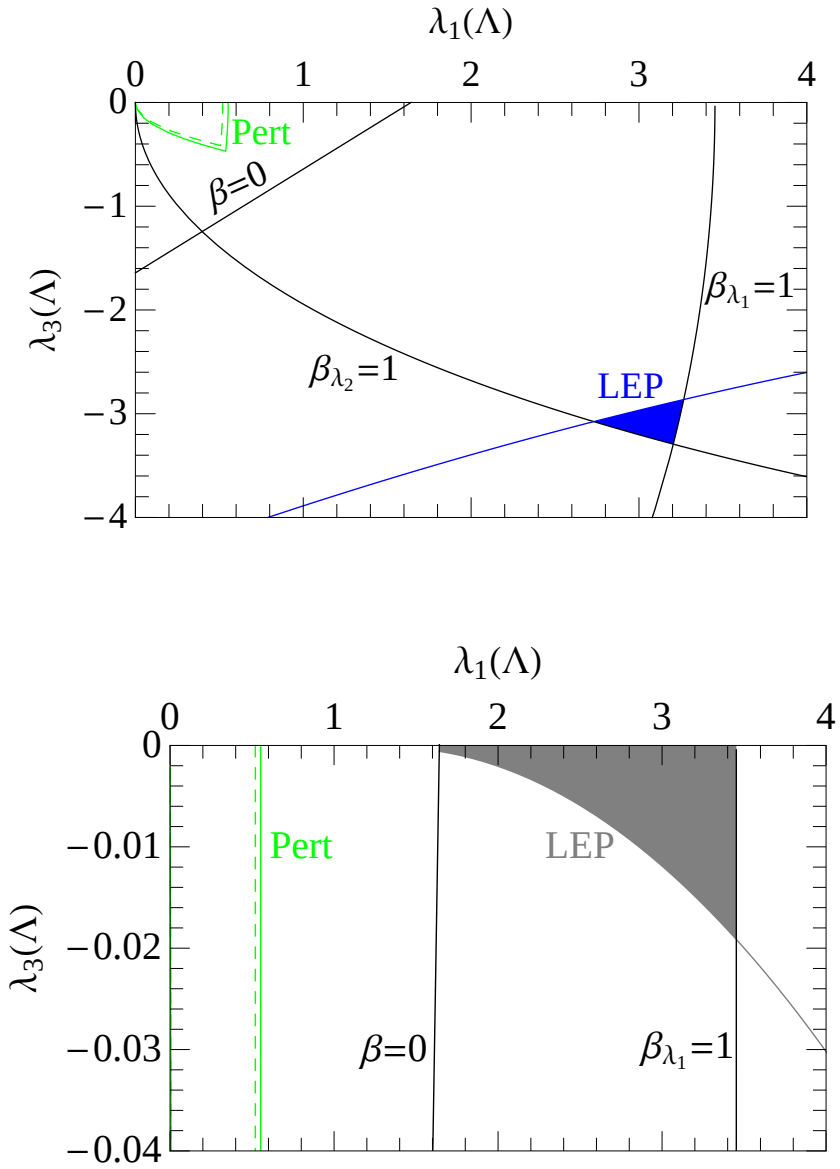

Figure 5.1: *Theoretical and experimental exclusion contours in the* $\lambda_1(\Lambda)$-$\lambda_3(\Lambda)$ *parameter space of the U(1) invariant MSISM with a Type II flat direction. The upper panel shows the full perturbative parameter space, whilst the lower panel focuses on the region with small values of* $\lambda_3(\Lambda)$*. The theoretically permitted areas are the regions enclosed by the black lines which correspond to keeping* $\beta_{\lambda_{1,2}}(\Lambda) \leq 1$*,* $\beta > 0$ *and* $\lambda_3(\Lambda) \leq 0$*. The LEP2 constraint is given by the blue (grey) LEP line and above (below) is excluded for the upper (lower) panel so that the blue and grey shaded areas are allowed by the theoretical constraints, the LEP2 constraint and the oblique parameters. The region of parameter space which remains perturbative to GUT (Planck) scale is enclosed by the solid (dashed) green Pert lines.*

range, whilst the lower panel focuses on a very narrow region which is viable for very small values of $\lambda_3(\Lambda)$, this region would not be clear if it were included in the top panel. The theoretical constraints we impose are that the quartic couplings remain perturbative at the RG scale Λ and that the one-loop effective potential $V_{\text{eff}}^{1-\text{loop}}$ is BFB. There are two limits that come into play to keep the quartic couplings perturbative at Λ; $\beta_{\lambda_1}(\Lambda) \leq 1$ and $\beta_{\lambda_2}(\Lambda) \leq 1$, which are represented by the black $\beta_{\lambda_{1,2}} = 1$ lines in Figure 5.1. The other one-loop β function, $\beta_{\lambda_3}(\Lambda)$, is much less constraining and is not included in the figure. From the above considerations, we find the upper limits $\lambda_1(\Lambda) \leq 3.45$ and $\lambda_3(\Lambda) \geq -3.29$. Requiring that the one-loop effective potential remains BFB or $\beta > 0$, generates the constraint

$$\lambda_1(\Lambda) - \lambda_3(\Lambda) \ > \ 1.64 \, , \tag{5.7}$$

which is represented by the black $\beta = 0$ lines in Figure 5.1. In summary, the theoretically relevant regions are the areas enclosed by the $\beta_{\lambda_{1,2}} = 1$, $\beta = 0$ and $\lambda_3(\Lambda) = 0$ lines in the upper panel and between the $\beta = 0$, $\beta_{\lambda_1} = 1$ and $\lambda_3(\Lambda) = 0$ lines in the lower panel.

The $\lambda_1(\Lambda)$-$\lambda_3(\Lambda)$ parameter space may be further constrained by experimental data of direct Higgs searches and the electroweak oblique parameters S, T and U. We find that all values of $\lambda_1(\Lambda)$ and $\lambda_3(\Lambda)$ which respect the theoretical limits give values of δS, δT and δU within the 95% CL limits of δS_{exp}, δT_{exp} and δU_{exp} respectively. This means that the oblique parameters provide no constraints within the theoretically admissible region and so have not been included in the figures.

The LEP2 Higgs boson mass limit, however, significantly restricts the $\lambda_1(\Lambda)$-$\lambda_3(\Lambda)$ parameter space. To apply the experimental results correctly, we first observe that h and H interact with reduced couplings, g_{hVV} and g_{HVV}, to a pair of vector bosons $V = W^{\pm}, Z$, compared to the SM coupling of H_{SM} to two vector bosons, $g_{H_{\text{SM}}VV}$. This is because h and H are linear compositions of ϕ and σ (5.4), but only ϕ interacts with the SM particles. The squared reduced couplings g_{hVV}^2

and g^2_{HVV} are given by the amount of h or H the scalar ϕ contains, multiplied by the SM coupling squared of $H_{\rm SM}$ to a pair of vector bosons $g^2_{H_{\rm SM}VV}$, explicitly

$$\begin{aligned} g^2_{hVV} &= \cos^2\theta\; g^2_{H_{\rm SM}VV} = \frac{-\lambda_3(\Lambda)}{\lambda_1(\Lambda)-\lambda_3(\Lambda)}\; g^2_{H_{\rm SM}VV}\;, \\ g^2_{HVV} &= \sin^2\theta\; g^2_{H_{\rm SM}VV} = \frac{\lambda_1(\Lambda)}{\lambda_1(\Lambda)-\lambda_3(\Lambda)}\; g^2_{H_{\rm SM}VV}\;, \end{aligned} \tag{5.8}$$

which satisfies the identity: $g^2_{hVV}+g^2_{HVV}=g^2_{H_{\rm SM}VV}$. Since the reduced hZZ and HZZ couplings are smaller than the $H_{\rm SM}$ coupling, the LEP2 Higgs boson mass limit $m_h > 114.4$ GeV no longer applies. Instead, we have to use the combined constraints on $\xi^2_{h,H}$ and the scalar masses $m_{h,H}$ which are presented in Figure 10(a) of Ref. [9] where we define

$$\xi^2_h = \frac{g^2_{hZZ}}{g^2_{H_{\rm SM}ZZ}}\;, \qquad\qquad \xi^2_H = \frac{g^2_{HZZ}}{g^2_{H_{\rm SM}ZZ}}\;. \tag{5.9}$$

In short, Figure 10(a) of Ref. [9] shows that as the coupling of a scalar to ZZ reduces compared to the $H_{\rm SM}ZZ$ coupling, the LEP2 Higgs mass limit also drops, i.e. if $\xi^2_h = 0.5$ then the LEP2 Higgs mass limit falls from $m_h > 114.4$ GeV to $m_h \gtrsim 86$ GeV. We note that the minimum value of $\lambda_1(\Lambda)-\lambda_3(\Lambda)$ given by the BFB constraint (5.7) gives a lower limit of $m_H = 315.0$ GeV, which is comfortably above the LEP2 Higgs mass limit for any value of ξ^2_H. Therefore, the LEP2 Higgs mass limit is applied only to the lighter scalar h. We perform a polynomial fit up to order 10 on the LEP2 Higgs mass data to obtain a reliable constraint on ξ^2_h as a function of m_h, which in turn restricts the $\lambda_1(\Lambda)$-$\lambda_3(\Lambda)$ parameter space. This constraint is represented by the blue (grey) LEP line in the upper (lower) panel of Figure 5.1, where the blue (grey) shaded region respects the theoretical constraints, the LEP2 Higgs mass limit and also falls within the 95% CL limits of oblique parameters. For clarity, the results of applying the LEP2 Higgs mass limit to m_h will hereafter be referred to as the LEP2 constraint. Consequently, we can apply the LEP2 constraint restriction on the values of $\lambda_1(\Lambda)$ and $\lambda_3(\Lambda)$

to obtain a limit on the mass of the other scalar H and the RG scale Λ.

In Figure 5.1, we note that the region of parameter space that remains perturbative to GUT or Planck scales (enclosed by the dashed and solid green lines respectively) lies firmly in the region excluded by the requirement that $\beta > 0$ and so neither of the two regions permitted by the LEP2 constraint will remain perturbative up to GUT or Planck scales. Finally, to date, the Tevatron Higgs mass exclusion range [10] has only been applied to SM-like Higgs bosons and so can not be applied in a general manner in this scenario.

We apply the aforementioned theoretical and LEP2 constraints, presented in Figure 5.1, to the scalar masses m_h (5.6) and m_H (5.5) and display the results, m_h in the upper panel and m_H in the lower panel, as a dependence on $\lambda_1(\Lambda)$ in Figure 5.2. The areas enclosed by the black lines are the regions which respect the theoretical constraints, $\beta_{\lambda_{1,2}}(\Lambda) \leq 1$, $\beta > 0$ and $\lambda_3(\Lambda) \leq 0$. The blue and grey shaded regions correspond to the two regions permitted by the LEP2 constraint. The grey shaded area is not clearly visible in the lower panel of Figure 5.2, as it closely follows the $\lambda_3 = 0$ line.

In Figure 5.3, we have similarly applied these constraints to the RG scale Λ as a function of $\lambda_1(\Lambda)$, where we have used the same line colour convention as Figure 5.2. Again the theoretically permitted region corresponds to the region enclosed by the black lines and the blue and grey (not clearly visible as it follows the $\lambda_3 = 0$ line) shaded regions correspond to the two regions permitted by the LEP2 constraint.

As we can see there are two distinct regions permitted by the LEP2 constraint, shaded blue and grey on the various figures. These two regions correspond respectively to higher and lower values of m_h and to different values of the quartic couplings $\lambda_1(\Lambda)$ and $\lambda_3(\Lambda)$. Therefore, we shall consider the scalar mass spectrum and phenomenology of each region separately.

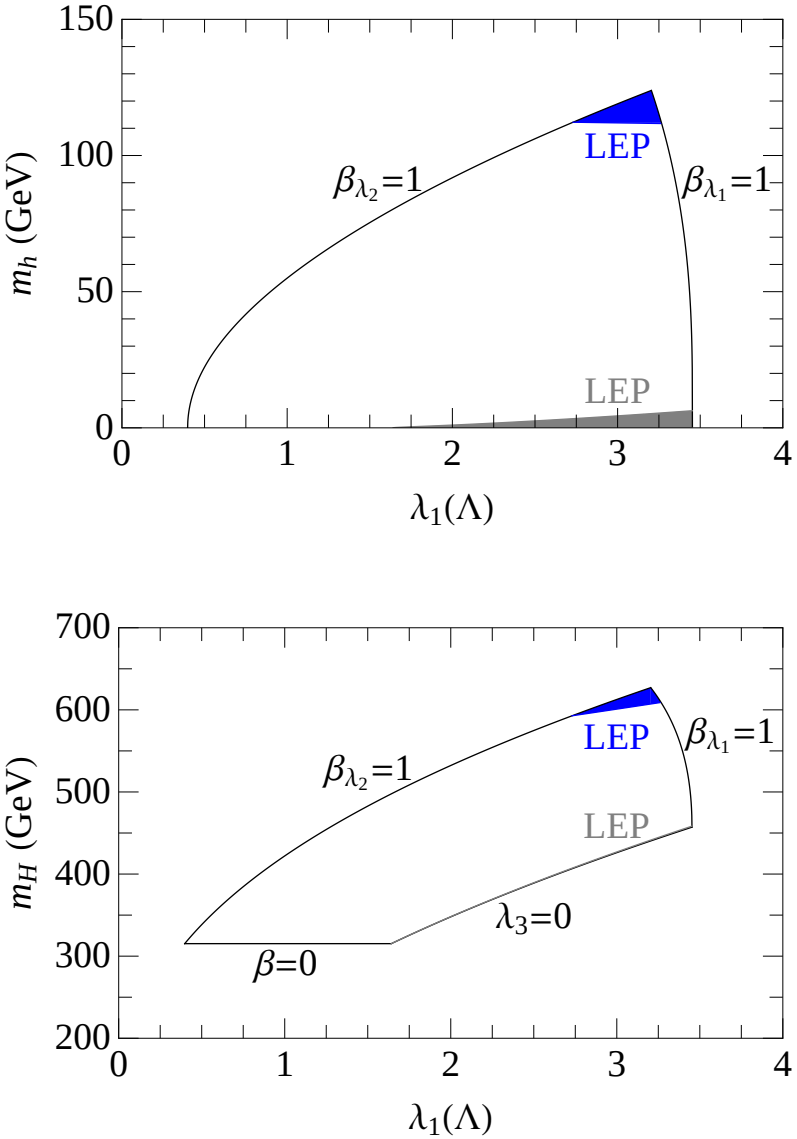

Figure 5.2: *The scalar masses m_h (upper panel) and m_H (lower panel) as functions of $\lambda_1(\Lambda)$ in the U(1) invariant MSISM with a Type II flat direction. The areas within the black lines show the regions which respect the theoretical constraints i.e. keeping $\beta_{\lambda_{1,2}}(\Lambda) \leq 1$, the potential BFB and $\lambda_3(\Lambda) \leq 0$. The blue (heavier m_h) and grey (ultra-light m_h) shaded regions (denoted LEP) are permitted by the LEP2 constraint, the oblique parameters and the theoretical constraints.*

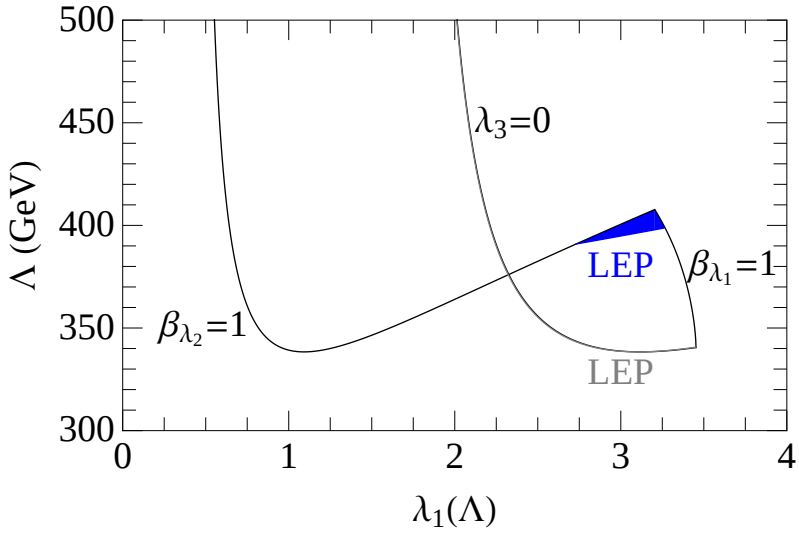

Figure 5.3: *The RG scale* Λ *as a function of* $\lambda_1(\Lambda)$ *in the U(1) invariant MSISM with a Type II flat direction. The theoretically permitted regions, which keep* $\beta_{\lambda_{1,2}}(\Lambda) \leq 1$*, the potential BFB and* $\lambda_3(\Lambda) \leq 0$*, are enclosed by the black lines. The blue (heavier* m_h*) and grey (ultra-light* m_h*) shaded regions (denoted LEP) are permitted by the LEP2 constraint, the oblique parameters and the theoretical constraints.*

5.1.1 The Heavier h Boson Region

In this section we consider the heavier h boson region which is dominated by large values of $\lambda_1(\Lambda)$ and $\lambda_3(\Lambda)$ and corresponds to the blue shaded area in Figures 5.1, 5.2 and 5.3.

The two scalar masses m_h (5.6) and m_H (5.5) are shown in Figure 5.2 and have the following allowed ranges

$$111.7 \text{ GeV} < m_h \leq 123.9 \text{ GeV} , \qquad 592.7 \text{ GeV} < m_H \leq 627.1 \text{ GeV} , \tag{5.10}$$

assuming they respect the theoretical constraints and the upper LEP2 constraint (shaded blue). The h boson could be observed at the LHC, through the decay channel $h \to \gamma\gamma$, whilst the heavier H boson may be detected via the so-called "golden channel", $H \to ZZ \to 4l$. However, in this region of parameter space $\lambda_1(\Lambda) \approx -\lambda_3(\Lambda)$ which implies that $g^2_{hVV} \approx g^2_{HVV} \approx 0.5\, g^2_{H_{\rm SM}VV}$, see (5.8), and

means both decays will have reduced signals compared to the SM Higgs signals. Moreover, the heavier H boson may predominantly decay invisibly into a pair of J bosons, thanks to the relatively large quartic couplings. This new decay could be detected at the LHC along the lines of [43]. This last characteristic and the fact that two scalar bosons would be detected with very specific masses and reduced couplings makes this region of the U(1) invariant MSISM with a Type II flat direction distinguishable from the Type I flat direction and the SM.

The RG scale Λ as a function of $\lambda_1(\Lambda)$ is presented in Figure 5.3. Assuming $\lambda_1(\Lambda)$ and $\lambda_3(\Lambda)$ are within the blue shaded region, so that the theoretical and experiment constraints are met, then the RG scale Λ is of the order of the EW scale and lies in the range 390.9 GeV $\leq \Lambda <$ 407.7 GeV.

Since we are only just within the constraints $\beta_{\lambda_{1,2}}(\Lambda) \leq 1$, this region of the parameter space does not remain perturbative up to either the GUT or Planck scales and develops a Landau pole at around 2×10^4 GeV.

5.1.2 The Ultra-Light h Boson Region

The other experimentally and theoretically viable region of the $\lambda_1(\Lambda)$-$\lambda_3(\Lambda)$ parameter space corresponds to a very small quartic coupling $\lambda_3(\Lambda)$ which gives rise to an ultra-light h boson. The relevant regions are shaded grey in the lower panel of Figure 5.1 and also Figures 5.2 and 5.3. Since this region is based on an extrapolation of the LEP2 Higgs mass limit to low masses we will not present a detailed phenomenological analysis of this scenario, but rather highlight its key features.

In Figure 5.1 it can be seen that the LEP2 constraint places an upper bound on $\lambda_3(\Lambda)$ of $-\lambda_3(\Lambda) \lesssim 0.019$. As a direct consequence of this very low upper bound, the h boson mass is ultra-light, $m_h \lesssim 6.3$ GeV, as illustrated by the grey shaded region in the upper panel of Figure 5.2. In this ultra-light h boson region, the reduced hZZ-coupling is strongly suppressed with $g^2_{hVV} \leq 0.0055\, g^2_{H_{\rm SM}VV}$, as can be determined from (5.8), which will make h almost impossible to directly

detect at the LHC.

The other CP-even H boson has an almost SM-like coupling to the vector bosons, with $g^2_{hVV} \approx g^2_{H_{\rm SM}VV}$. The grey shaded region representing the H boson mass is unclear in the lower plot of Figure 5.2 as it closely follows the $\lambda_3 = 0$ line, nevertheless its mass lies in the range 315.2 GeV $< m_H <$ 458.4 GeV. Since $H \approx H_{\rm SM}$ the Tevatron exclusion range [10] can be approximately applied, however, m_H is large and avoids the excluded region. For this region the $H \to JJ$ decay is suppressed since the HJJ-coupling is proportional to the small $\lambda_3(\Lambda)$ quartic coupling, therefore the SM-like H boson would most likely be detected via the "golden channel" $H \to ZZ \to 4l$.

In Figure 5.3, the grey shaded area representing Λ for this ultra-light h boson region is not clear as it closely follows the $\lambda_3 = 0$ line. Furthermore, we notice that unlike the previous cases there appears to be nothing to stop Λ from taking very large non-EW scale values. This is clear in Figure 5.1 since the grey shaded LEP2 constraint permitted region touches the $\beta = 0$ line implying $\Lambda \to \infty$. However, in Section 2.2, we required that for the perturbative GW approach to work $V^{\rm tree} > V^{1-{\rm loop}}_{\rm eff} > V^{2-{\rm loop}}_{\rm eff} > ...$, i.e. we can require that the coefficients α and β of the one-loop effective $V^{1-{\rm loop}}_{\rm eff}$ in (3.18) are small, e.g. $\alpha,\ \beta \leq 1$. Requiring $\alpha \leq 1$ places an upper constraint on Λ of $\Lambda \lesssim 680$ GeV, whilst $\beta \leq 1$ requires Λ of $\Lambda \lesssim 750$ GeV.

An interesting feature of the ultra-light h boson region is that it remains perturbative to higher scales than the previously considered models, indicated by the proximity to the area enclosed by the solid and dashed green lines in Figure 5.1. Specifically, within the allowed region, the model does not develop a Landau pole until energies of the order 10^6 GeV, which is higher than the heavier mass h boson scenario, but is still far below the GUT and Planck scales.

In conclusion, it is worth reiterating (cf. Table 3.1) that the U(1) invariant MSISM with a Type II flat direction has no new source of CP violation and

predicts no massive DM candidate, since J is massless and both h and H decay to SM particles. However, the model does have the ability to generate Majorana neutrino masses through the seesaw mechanism, which we have not included here but will discuss in more detail in Chapter 6. In the following section, we consider a minimal U(1) non-invariant MSISM with a Type II flat direction which realises maximal spontaneous CP violation (SCPV).

5.2 Minimal U(1) Non-Invariant Scenario with Maximal SCPV

The general MSISM tree-level potential with a Type II flat direction, without the restriction of U(1) invariance, contains a total of nine real quartic couplings, see (3.2), where the couplings are evaluated at Λ along the flat direction. Due to the large number of couplings there is a multitude of valid solutions that all satisfy the minimisation requirements (3.12) and (3.13). Not all of these possible solutions are phenomenologically interesting, therefore we have focused our investigation on one scenario: the U(1) non-invariant MSISM with a Type II flat direction that minimally realises maximal SCPV.

The tree-level scalar potential of this scenario is given by

$$V^{\text{tree}} \;=\; \frac{\lambda_1}{2}\,(\Phi^\dagger\Phi)^2 \;+\; \frac{\lambda_2}{2}\,(S^*S)^2 \;+\; \lambda_3\,\Phi^\dagger\Phi\,S^*S \;+\; \frac{\lambda_6}{2}\,(S^4 + S^{*4})\,, \qquad (5.11)$$

where λ_6 is real due to CP invariance and $\lambda_4 = \lambda_5 = 0$ to make the model minimal. In addition to CP invariance, the tree-level scalar potential (5.11) also possesses an accidental $\mathbf{Z}_4$ discrete symmetry: $S \to S' = \omega S$ and $\Phi \to \Phi' = \Phi$, where $\omega^4 = 1$. The CP symmetry and the $\mathbf{Z}_4$ discrete symmetry are sufficient to uniquely define the form of the tree-level scalar potential V^{tree} (5.11).

Minimising the tree-level potential at the RG scale Λ, by means of (3.12) and

(3.13), generates the following two conditions for the flat direction:

$$\begin{aligned} &\text{i)} \quad \frac{\varphi_\phi^2}{\varphi_\sigma^2} \;=\; \frac{n_\phi^2}{n_\sigma^2} \;=\; -\frac{2\lambda_3(\Lambda)}{\lambda_1(\Lambda)} \;=\; -\frac{2\big[\lambda_2(\Lambda)-2\lambda_6(\Lambda)\big]}{\lambda_3(\Lambda)}\,, \\ &\text{ii)} \quad \varphi_\sigma^2 \;=\; \varphi_J^2 \quad\Leftrightarrow\quad n_\sigma^2 \;=\; n_J^2\,. \end{aligned} \tag{5.12}$$

Note that the second condition implies a flat direction that triggers maximal spontaneous CP violation. Any choice of angle $\theta_S = (2n-1)\frac{\pi}{4}$ where $n = 1, 2, ...$ will minimise the flat direction and give maximal CP-violation. Arbitrarily we set $\theta_S = \pi/4$ so that $\varphi_\sigma \;=\; \varphi_J$. Even values of n will give $\varphi_\sigma = -\varphi_J$, but this does not affect the scalar masses or the phenomenology of the model in an essential manner. Combining (5.12) with the BFB condition (3.6) requires that

$$\lambda_1(\Lambda) > 0\,, \qquad \lambda_3(\Lambda) < 0\,, \qquad \lambda_2(\Lambda) - 2\lambda_6(\Lambda) > 0\,, \tag{5.13}$$

where the signs of $\lambda_2(\Lambda)$ and $\lambda_6(\Lambda)$ individually remain undetermined.

Other solutions to the minimisation conditions, (3.12) and (3.13), are possible for V^{tree} (5.11), but they either modify it to a Type I flat direction ($\varphi_\sigma = \varphi_J = 0$) or reduce the potential to the U(1) invariant scenario ($\lambda_6(\Lambda) = 0$), both of which have been previously investigated in Chapter 4 and Section 5.1, respectively.

The flat direction for this scenario can not be dimensionally reduced further than the 3-dimensional vector, i.e. the ϕ, σ and J components are all non-zero,

$$\mathbf{\Phi}^{\text{flat}} \;=\; \frac{\varphi}{\sqrt{2\big[\lambda_1(\Lambda)-\lambda_3(\Lambda)\big]}} \begin{pmatrix} \sqrt{-2\lambda_3(\Lambda)} \\ \sqrt{\lambda_1(\Lambda)} \\ \sqrt{\lambda_1(\Lambda)} \end{pmatrix} \;=\; \frac{\varphi_\phi}{\sqrt{-2\lambda_3(\Lambda)}} \begin{pmatrix} \sqrt{-2\lambda_3(\Lambda)} \\ \sqrt{\lambda_1(\Lambda)} \\ \sqrt{\lambda_1(\Lambda)} \end{pmatrix}. \tag{5.14}$$

Considering the flat direction conditions in (5.12), the scalar mass matrix (C.9) contains no non-zero components, and evaluating at the minimum, the scalar

mass matrix elements in (C.10) become

$$\begin{aligned} m_\phi^2 &= \lambda_1(\Lambda)\, v_\phi^2 \,, \qquad & m_\sigma^2 &= m_J^2 = \left[\lambda_2(\Lambda) + 2\lambda_6(\Lambda)\right] v_\sigma^2 \,, \\ m_{\sigma J} &= \left[\lambda_2(\Lambda) - 6\lambda_6(\Lambda)\right] v_\sigma^2 \,, \qquad & m_{\phi\sigma} &= m_{\phi J} = \lambda_3(\Lambda)\, v_\phi v_\sigma \,, \end{aligned} \tag{5.15}$$

where the elements $m_{\phi J}$ and $m_{\sigma J}$ are CP-violating. Diagonalising the matrix (C.9) gives the eigenvalues

$$m_h^2 = 0 \,, \qquad m_{H_1}^2 = \left[\lambda_1(\Lambda) - \lambda_3(\Lambda)\right] v_\phi^2 \,, \qquad m_{H_2}^2 = 4\frac{\lambda_1(\Lambda)\lambda_6(\Lambda)}{-\lambda_3(\Lambda)}\, v_\phi^2 \,, \tag{5.16}$$

with the corresponding mass eigenstates

$$\begin{aligned} h &= \sqrt{\frac{-\lambda_3(\Lambda)}{\lambda_1(\Lambda) - \lambda_3(\Lambda)}}\, \phi \;+\; \sqrt{\frac{\lambda_1(\Lambda)}{2(\lambda_1(\Lambda) - \lambda_3(\Lambda))}}\, (\sigma + J) \,, \\ H_1 &= \sqrt{\frac{\lambda_1(\Lambda)}{\lambda_1(\Lambda) - \lambda_3(\Lambda)}}\, \phi \;-\; \sqrt{\frac{-\lambda_3(\Lambda)}{2(\lambda_1(\Lambda) - \lambda_3(\Lambda))}}\, (\sigma + J) \,, \\ H_2 &= \frac{1}{\sqrt{2}}\, (-\sigma + J) \,. \end{aligned} \tag{5.17}$$

where have we employed the relation $\lambda_2(\Lambda) = \frac{\lambda_3^2(\Lambda)}{\lambda_1(\Lambda)} + 2\lambda_6(\Lambda)$, which can easily be derived from (5.12). In order for the H_2 boson mass squared $m_{H_2}^2$ to be positive, we require that $\lambda_6(\Lambda) > 0$, implying from (5.13), $\lambda_2(\Lambda) > 2\lambda_6(\Lambda) > 0$.

We can show through the first condition in (5.12) that the scalar sector of the U(1) non-invariant scenario with maximal SCPV can be written entirely in terms of only three quartic couplings, which we choose to be $\lambda_1(\Lambda)$, $\lambda_2(\Lambda)$ and $\lambda_3(\Lambda)$ with $\lambda_6(\Lambda) = \frac{1}{2}\left(\lambda_2(\Lambda) - \frac{\lambda_3^2(\Lambda)}{\lambda_1(\Lambda)}\right)$. Explicitly, the scalar masses m_{H_1} and m_{H_2} depend on the three quartic couplings $\lambda_{1,2,3}(\Lambda)$, as can be seen from (5.16). Likewise, the RG scale Λ determined in (3.22) depends on the effective potential coefficients α and β that are both functions of m_{H_1} and m_{H_2}. Finally, the one-loop induced h boson mass depends on β and $n_\phi = \sqrt{\frac{-\lambda_3(\Lambda)}{\lambda_1(\Lambda) - \lambda_3(\Lambda)}}$ which is given

in (5.14), see (3.21), or explicitly

$$m_h \;=\; \frac{1}{\sqrt{8}\pi v_\phi}\sqrt{\frac{-\lambda_3(\Lambda)}{\lambda_1(\Lambda)-\lambda_3(\Lambda)}}\,\sqrt{m_{H_1}^4+m_{H_2}^4+6m_W^4+3m_Z^4-12m_t^4}\,. \quad (5.18)$$

Consequently, the entire scalar boson mass spectrum and the RG scale Λ of the model depend on only three quartic couplings: $\lambda_{1,2,3}(\Lambda)$.

The extra freedom which comes from having three independent quartic couplings can be exploited to place tighter constraints on the values of the quartic coupling constants. To be precise, instead of requiring that the couplings are perturbative at Λ, we now require them to remain perturbative to the Planck scale. Explicitly, we require that $\beta_{\lambda_{1,2,3,6}}(M_{\rm Planck}) \leq 1$ to keep the quartic couplings perturbative to the Planck scales, and $\lambda_1(M_{\rm Planck}) > 0$, $\lambda_2(M_{\rm Planck}) - 2\lambda_6(M_{\rm Planck}) > 0$ and $\lambda_3(M_{\rm Planck}) < 0$ to keep the potential BFB up to the Planck scale. Moreover, we find that the tightest constraints are given by $\beta_{\lambda_1}(M_{\rm Planck}) \leq 1$ and $\lambda_1(M_{\rm Planck}) > 0$, which restricts $\lambda_1(\Lambda)$ to the range

$$0.39 \;\lesssim\; \lambda_1(\Lambda) \;\lesssim\; 0.52\,. \quad (5.19)$$

If we assume $\lambda_6(\Lambda) \approx \frac{1}{2}\lambda_2(\Lambda)$ with negligible values of $\lambda_1(\Lambda)$ and $\lambda_3(\Lambda)$, then $\beta_{\lambda_2}(M_{\rm Planck}) \leq 1$ can be used to find the maximum perturbative value of the $\lambda_2(\Lambda)$ quartic coupling, explicitly

$$0 \;<\; \lambda_2(\Lambda) \;\lesssim\; 0.20\,. \quad (5.20)$$

A further theoretical constraint is required to prevent $\lambda_3(\Lambda) \to 0$, since from (5.16) we observe that in the limit $\lambda_3(\Lambda) \to 0$ the H_2 boson mass m_{H_2} becomes infinite, which leads to undesirable infinite values for m_h and Λ. To obtain a lower limit on $\lambda_3(\Lambda)$, we can require that the coefficients α and β of the one-loop effective $V_{\rm eff}^{1-\rm loop}$ in (3.18) are small, e.g. $\alpha,\ \beta \leq 1$, so that the perturbative GW approach is valid. We apply the constraint $\alpha \leq 1$, which is slightly less

constraining than $\beta \leq 1$.

The parameter space can be further restricted by applying the LEP2 Higgs mass limit in a similar fashion to the U(1) invariant scenario, i.e. we have to use the combined constraints on ξ^2_{h,H_1} and the scalar masses m_{h,H_1} which are presented in Figure 10(a) of Ref. [9], since the scalars h and H_1 have reduced couplings compared to the $H_{\rm SM}$ coupling to the SM particles. In spite of the additional quartic coupling $\lambda_6(\Lambda)$, the interactions of the h and H_1 scalars to a pair of $V = W^{\pm}, Z$ bosons are very similar to the U(1) invariant scenario and their reduced hVV and H_1VV couplings are given by

$$g^2_{hVV} \;=\; \frac{-\lambda_3(\Lambda)}{\lambda_1(\Lambda)-\lambda_3(\Lambda)}\, g^2_{H_{SM}VV}\,, \qquad g^2_{H_1VV} \;=\; \frac{\lambda_1(\Lambda)}{\lambda_1(\Lambda)-\lambda_3(\Lambda)}\, g^2_{H_{SM}VV}\,. \tag{5.21}$$

The LEP2 Higgs mass limit is again only applied to the scalar h since m_{H_1} is greater than the LEP2 Higgs mass limit. Thus, we call the restriction on the quartic couplings which arises from applying the LEP2 Higgs mass limit to m_h the LEP2 constraint, which can subsequently be applied to m_{H_1}, m_{H_2} and Λ. We find that for values of the quartic couplings which respect the theoretical constraints the oblique parameters give values of δS, δT and δU within their respective 95% CL limits $\delta S_{\rm exp}$, $\delta T_{\rm exp}$ and $\delta U_{\rm exp}$ and so do not provide any constraints within the theoretically permitted region.

In summary, our numerical analysis uses the following theoretical constraints as the most stringent limits on the parameter space

$$\beta_{\lambda_1}(M_{\rm Planck}) \leq 1\,, \qquad \lambda_1(M_{\rm Planck}) > 0\,, \qquad \beta > 0\,, \qquad \alpha \leq 1\,, \tag{5.22}$$

whilst the only experimental constraint comes from the LEP2 constraint. Also due to the logistics of representing the effects of three independent parameters, we choose two representative values of $\lambda_2(\Lambda)$: $\lambda_2(\Lambda) = 0.02$ and $\lambda_2(\Lambda) = 0.2$.

In Figure 5.4, we apply the theoretical constraints (5.22) and the LEP2 constraint on the scalar boson masses, m_h (top panel) and m_{H_2} (middle panel) and

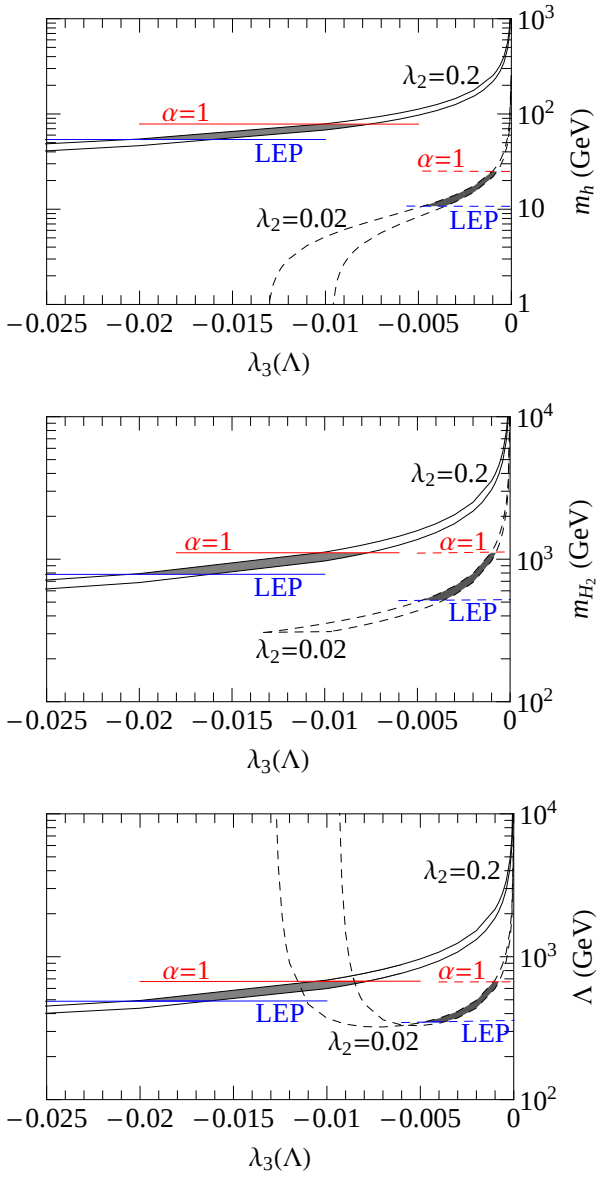

Figure 5.4: *The scalar masses m_h (top panel) and m_{H_2} (middle panel) and the RG scale Λ (bottom panel) as functions of $\lambda_3(\Lambda)$ in the U(1) non-invariant MSISM with a Type II flat direction that minimally realises maximal SCPV. The areas between the two solid (dashed) black lines correspond to the masses for which $\beta_{\lambda_1}(M_{\text{Planck}}) \leq 1$, $\lambda_1(M_{\text{Planck}}) > 0$ and $\beta > 0$ for $\lambda_2(\Lambda) = 0.02$ (0.2). The solid and dashed blue lines represent the LEP2 constraint, below which are excluded. The solid and dashed red lines represent the constraint $\alpha \leq 1$ and above each of the lines is excluded. The grey regions correspond to areas that respect the theoretical and LEP2 constraints. The solid lines correspond to $\lambda_2(\Lambda) = 0.2$ whilst the dashed lines correspond to $\lambda_2(\Lambda) = 0.02$.*

$\lambda_2(\Lambda)$	m_h		m_{H_1}		m_{H_2}		Λ	
	min	max	min	max	min	max	min	max
0.2	54	78	155	181	783	1110	490	675
0.1	34	56	155	180	703	1110	444	674
0.05	21	39	154	179	607	1110	395	674
0.02	11	25	154	178	515	1110	350	675

Table 5.1: *Minimum and maximum values of* m_h, m_{H_1}, m_{H_2} *and* Λ *as determined by the LEP2 constraint and the theoretical constraint* $\alpha \leq 1$ *for a range of* $\lambda_2(\Lambda)$.

the RG scale Λ (bottom panel), as functions of the quartic coupling $\lambda_3(\Lambda)$. The solid (dashed) black lines enclose the regions which respect the first three theoretical constraints in (5.22) with $\lambda_2(\Lambda) = 0.2$ (0.02). The solid and dashed red lines represent the theoretical limit $\alpha \leq 1$ for $\lambda_2(\Lambda) = 0.2$ and 0.02 respectively, where the area above the $\alpha = 1$ lines is excluded. The solid and dashed blue lines represent the LEP2 constraint for $\lambda_2(\Lambda) = 0.2$ and 0.02 respectively and the regions below the blue LEP lines are excluded for the specific values of $\lambda_2(\Lambda)$ considered. As a result, the $\lambda_3(\Lambda)$ coupling has to take small absolute values, with $\lambda_3(\Lambda) \gtrsim -0.02$. The grey shaded regions are the areas which respect all the theoretical constraints, the LEP2 constraint and lie within the 95% CL limits of the oblique parameters $\delta S_{\rm exp}$, $\delta T_{\rm exp}$ and $\delta U_{\rm exp}$. In Table 5.1, we present the upper and lower limits on the masses of the h and H_2 bosons and on the RG scale Λ for different values of $\lambda_2(\Lambda)$. The lower bounds are determined from the LEP2 constraint, whilst the upper bounds come from the theoretical constraint $\alpha \leq 1$.

We display the results of applying the theoretical constraints (5.22) and the LEP2 constraint to the H_1 boson mass m_{H_1} as a function of the $\lambda_3(\Lambda)$ in Figure 5.5. The black lines correspond to values of the quartic couplings which respect the limits $\lambda_1(M_{\rm Planck}) > 0$, $\beta_{\lambda_1}(M_{\rm Planck}) \leq 1$ and $\beta > 0$. Even though m_{H_1} does not explicitly depend on $\lambda_2(\Lambda)$ itself, see (5.16), the LEP2 constraint and the theoretical constraint $\alpha \leq 1$ do. The grey shaded areas between the solid (dashed) blue LEP and red $\alpha = 1$ lines are allowed by the respective constraints

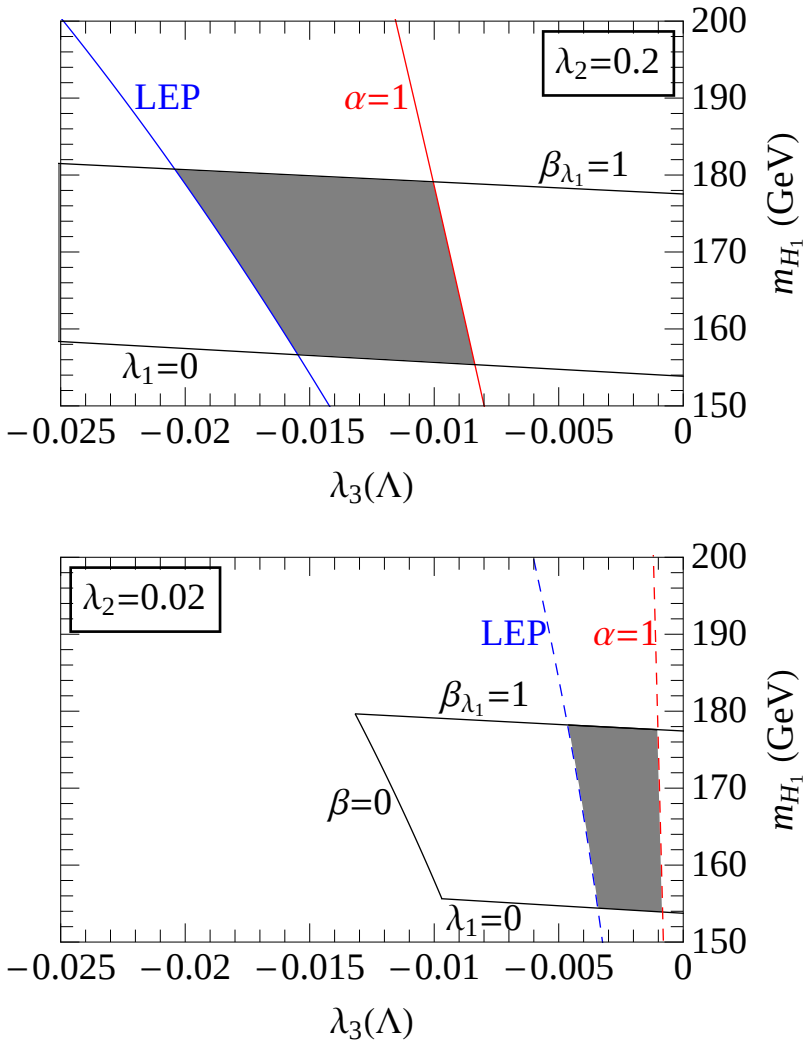

Figure 5.5: *The scalar mass m_{H_1} as a function of $\lambda_3(\Lambda)$ in the U(1) non-invariant MSISM with a Type II flat direction that minimally realises maximal SCPV. The upper panel shows $\lambda_2(\Lambda) = 0.2$ whilst the lower panel displays $\lambda_2(\Lambda) = 0.02$. The area enclosed by the black lines corresponds to masses restricted by the conditions: $\beta_{\lambda_1}(M_{\text{Planck}}) \leq 1$, $\lambda_1(M_{\text{Planck}}) > 0$ and $\beta > 0$ ($\lambda_2(\Lambda) = 0.02$ only). The grey shaded regions correspond to the areas permitted by the LEP2 constraint (solid and dashed blue lines) and the $\alpha \leq 1$ limit (solid and dashed red lines).*

for $\lambda_2(\Lambda) = 0.2$ (0.02). The LEP2 constraint provides an upper limit on the value of m_{H_1}, whilst the $\alpha \leq 1$ constraint gives a lower limit. These upper and lower limits on the H_1 boson mass are exhibited in Table 5.1, for various values of the $\lambda_2(\Lambda)$ coupling.

The U(1) non-invariant scenario with maximal SCPV gives rise to a plethora of phenomenology. As emphasized throughout this section, the model spontaneously and maximally violates the CP symmetry, which might open up the possibility for successful electroweak baryogenesis in this scenario. The model can also generate naturally small neutrino masses through the seesaw mechanism since the complex singlet S has a non-zero VEV. Moreover, the presence of a permutation parity symmetry, $\sigma \leftrightarrow J$, which remains intact after EWSSB, renders the massive H_2 boson stable with vanishing VEV. Hence, the H_2 boson could act as a cold DM candidate, according to the Higgs-portal scenario [41]. In general, there are two parity symmetries that could be imposed on the tree-level potential (5.11), they are: $\sigma \leftrightarrow J$ and $\sigma \leftrightarrow -J$, but since both symmetries lead to identical mass spectra we do not discuss them separately.

Experimental verification of the U(1) non-invariant scenario with maximal SCPV would be difficult. The scalar h has a very small coupling to the SM particles, $g^2_{hVV} \lesssim 0.05\, g^2_{H_{\rm SM}VV}$ where we have used (5.21), (5.19) and $\lambda_3(\Lambda) \gtrsim -0.02$ as determined by the LEP2 constraint. The small value of g^2_{hVV} makes it very difficult to directly detect h despite it having a reasonable sized mass, see Table 5.1. On the other hand, the H_1 boson has a SM-like coupling to the electroweak vector bosons $g^2_{H_1VV} \gtrsim 0.95\, g^2_{H_{\rm SM}VV}$ and would again most likely be detected through the discovery channel $H_1 \to ZZ \to 4l$. Distinguishing H_1 from $H_{\rm SM}$ could be performed by determining the trilinear and quadrilinear self-couplings since the trilinear and quadrilinear self-couplings of the SM Higgs are based on the same quartic coupling, whereas those for H_1 are based on different combinations of quartic couplings which are not easily related. Considering how similar H_1 and $H_{\rm SM}$ are, the Tevatron Higgs mass exclusion range for a SM-like

Higgs boson 158 GeV $< m_{H_{SM}} <$ 175 GeV [10], should approximately apply to m_{H_1}. Considering the range of values m_{H_1} can take, see Table 5.1, the Tevatron excludes most of this region, however the effect of the reduced coupling has not been applied. In any case, if the Tevatron continues to run there is a large possibility that it would either detect H_1 or exclude this scenario with quartic couplings which remain perturbative to the Planck scale.

In summary, the U(1) non-invariant MSISM with a Type II flat direction that minimally realises maximal SCPV is a theoretically and experimentally viable scenario. The quartic couplings of the model can remain perturbative up to Planck energy scales and its scalar boson mass spectrum is compatible with limits from the LEP2 and Tevatron Higgs searches and the S, T and U oblique parameters. Most importantly, the model does not require additional theory to stay perturbatively renormalisable up to the standard quantum gravity scale, M_{Planck}. Since the addition of right-handed neutrinos can have a significant impact on the one-loop effective potential $V_{\text{eff}}^{1-\text{loop}}$ and on the phenomenology of the model in general, we analyse the addition of right-handed neutrinos to the MSISM in detail in the next chapter.

Chapter 6

Neutrinos in the MSISM

In this chapter we consider the effect of including three right-handed neutrinos $\nu^0_{1,2,3R}$ in the MSISM. The motivation for this addition is to try to naturally generate the observed small neutrino masses [6] which are currently unexplained in the SM. The neutrino Lagrangian $\mathcal{L}_\nu$ in (3.1), contains the following SI terms

$$\begin{aligned}\mathcal{L}_\nu \;=\; & \bar{\nu}^0_{iR} i\gamma^\mu \partial_\mu \nu^0_{iR} \;-\; \mathbf{h}^\nu_{ij} \bar{L}_{iL} \tilde{\Phi} \nu^0_{jR} \;-\; \mathbf{h}^{\nu\dagger}_{ij} \bar{\nu}^0_{iR} \tilde{\Phi}^\dagger L_{jL} \;-\; \frac{1}{2}\, \mathbf{h}^N_{ij} \bar{\nu}^{0C}_{iR} S \nu^0_{jR} \\ & - \frac{1}{2}\, \mathbf{h}^{N\dagger}_{ij} \bar{\nu}^0_{iR} S^* \nu^{0C}_{jR} \;-\; \frac{1}{2}\, \tilde{\mathbf{h}}^N_{ij} \bar{\nu}^0_{iR} S \nu^{0C}_{jR} \;-\; \frac{1}{2}\, \tilde{\mathbf{h}}^{N\dagger}_{ij} \bar{\nu}^{0C}_{iR} S^* \nu^0_{jR} \,. \end{aligned} \tag{6.1}$$

where the summation convention for repeated indices is implied, and $i, j = 1, 2, 3$ denotes the three generations, e, μ and τ, respectively. In (6.1), $\mathbf{h}^\nu$ is a matrix containing the Dirac neutrino Yukawa couplings of the SM Higgs doublet Φ to the lepton doublets L_{iL}, which are defined in Appendix A. In addition, since we have not assumed any symmetries on $\mathcal{L}_\nu$, for example lepton number conservation, there are two Majorana neutrino Yukawa coupling matrices $\mathbf{h}^N$ and $\tilde{\mathbf{h}}^N$ that couple the singlet field S to the right-handed neutrinos $\nu^0_{1,2,3R}$. Due to the Majorana nature of the neutrinos, $\mathbf{h}^N$ and $\tilde{\mathbf{h}}^N$ are symmetric 3×3 matrices, i.e. $\mathbf{h}^N = \mathbf{h}^{N\,T}$, $\tilde{\mathbf{h}}^N = \tilde{\mathbf{h}}^{N\,T}$.

As previously mentioned in Section 3.4, the MSISM with a Type I flat direction cannot generate neutrino masses via the seesaw mechanism since the VEV

of the S field is zero along the minimal flat direction. Moreover, including Majorana neutrino masses by hand i.e. $-\frac{1}{2}\mathbf{m}^M_{ij}\bar{\nu}^0_{iR}\nu^{0C}_{jR}$, is not permitted in a SI theory because of the dimensional coupling $\mathbf{m}^M$. However, Dirac-type neutrino masses can still be obtained through the coupling with the SM Higgs doublet Φ. Unfortunately, this requires hugely suppressed Dirac neutrino Yukawa couplings of order 10^{-12}, about 6 orders of magnitude smaller than the electron Yukawa coupling. Just like the SM, such a scenario would have difficulty naturally explaining the smallness of the light neutrino masses. Moreover, if the Dirac-type neutrino masses existed then the MSISM with a Type I flat direction would not be greatly affected by the inclusion of right-handed neutrinos as the actual effect of the very small neutrino Yukawa couplings on the scalar mass spectrum, the RG scale Λ and the one-loop effective potential would be negligible. Thus, the results presented in Chapter 4 would not change.

We therefore turn our attention to the MSISM with a Type II flat direction. Since $\varphi_S \neq 0$ along the Type II flat direction, the following neutrino mass terms are generated:

$$\mathcal{L}^{\text{Mass}}_{\nu} \;=\; -\,\frac{1}{2}(\bar{\nu}^0_{iL}, \bar{\nu}^{0C}_{iR}) \begin{pmatrix} \mathbf{0} & \mathbf{m}_{Dij} \\ \mathbf{m}^T_{Dij} & \mathbf{m}_{Mij} \end{pmatrix} \begin{pmatrix} \nu^{0C}_{jL} \\ \nu^0_{jR} \end{pmatrix} \;+\; \text{h.c.} \tag{6.2}$$

where

$$\mathbf{m}_D \;=\; \frac{\varphi_\phi}{\sqrt{2}}\,\mathbf{h}^\nu\,, \qquad \mathbf{m}_M \;=\; \frac{1}{\sqrt{2}}\Big[\,\varphi_\sigma(\mathbf{h}^N + \tilde{\mathbf{h}}^{N\dagger}) + i\varphi_J(\mathbf{h}^N - \tilde{\mathbf{h}}^{N\dagger})\,\Big]\,, \tag{6.3}$$

and h.c. is the hermitian conjugate. Without loss of generality, we can work in the basis where $\mathbf{m}_M$ is diagonal, real and positive, whilst $\mathbf{h}^N$, $\tilde{\mathbf{h}}^N$ and $\mathbf{m}_D$ are in general 3×3 non-diagonal complex matrices.

The 6×6 mass matrix in $\mathcal{L}^{\text{Mass}}_{\nu}$ can be block-diagonalised via a unitary matrix U as follows:

$$U^T \begin{pmatrix} \mathbf{0} & \mathbf{m}_D \\ \mathbf{m}^T_D & \mathbf{m}_M \end{pmatrix} U \;=\; \begin{pmatrix} \mathbf{m}_\nu & \mathbf{0} \\ \mathbf{0} & \mathbf{m}_N \end{pmatrix}\,. \tag{6.4}$$

Assuming $\mathbf{m}_M \gg \mathbf{m}_D$ we can perform an expansion of the unitary matrix U in powers of $\mathbf{m}_D\mathbf{m}_M^{-1}$ and at leading order we obtain the standard seesaw formulas [34]:

$$\mathbf{m}_\nu \;=\; -\,\mathbf{m}_D\mathbf{m}_M^{-1}\mathbf{m}_D^T\,, \qquad \mathbf{m}_N \;=\; \mathbf{m}_M\,, \tag{6.5}$$

where $\mathbf{m}_\nu$ is the 3×3 light neutrino mass matrix of the observed light neutrinos $\nu_{1,2,3}$ whilst $\mathbf{m}_N$ is the heavy neutrino mass matrix of the new heavy Majorana neutrinos, which we denote as $N_{1,2,3}$, i.e.

$$\mathcal{L}_\nu^{\rm Mass} \;=\; -\,\frac{1}{2}\,(\,\bar{\nu}\mathbf{m}_\nu\nu \;+\; \bar{\mathbf{N}}\mathbf{m}_N\mathbf{N}\,)\,. \tag{6.6}$$

As we will see in this chapter, the heavy Majorana neutrinos $N_{1,2,3}$ in the MSISM with a Type II flat direction are typically not much heavier than the EW scale. However, these new heavy neutrino masses could have a large effect on the one-loop effective potential and the one-loop β functions, technical details are given in Appendices C and D, and consequently will have a knock-on effect on the scalar mass spectrum and the RG scale Λ. Assuming no large cancellations between the matrices we require that all the Dirac neutrino Yukawa couplings in $\mathbf{h}^\nu$ are about 10^{-6}, e.g. of order the electron Yukawa coupling, to generate the light neutrino masses $\mathbf{m}_\nu \sim$ few eV. Thus, even though we keep the analytical dependence of $\mathbf{h}^\nu$ in the main formulas, we assume that all $\mathbf{h}^\nu_{ij} \sim 10^{-6}$, such that their numerical impact on the one-loop effective potential and the one-loop β functions can be safely ignored.

In the following sections we study several representative scenarios within the framework of the MSISM with a Type II flat direction and right-handed neutrinos. First, we consider the U(1) invariant scenario that preserves lepton number. We then consider the inclusion of neutrinos in the U(1) non-invariant scenario that minimally realises maximal SCPV through two different symmetries on the neutrino sectors. The first scenario assumes a CP-symmetric neutrino sector, where the CP invariance is only violated spontaneously by the ground state of

the theory. The second scenario promotes the parity symmetry present in the scalar potential of the model to the neutrino Yukawa sector, thus giving rise to a massive stable scalar particle which could act as a potential candidate to solve the cold DM problem.

6.1 Neutrinos in the U(1) Invariant Type II Flat Direction

In its most general form the U(1) invariant MSISM with a Type II flat direction and right-handed neutrinos contains an impractically large number of new neutrino Yukawa couplings. This large number of new couplings becomes apparent when we consider the matrix $\mathbf{m}_M$ (6.3), which due to the U(1) symmetry reduces to the φ_σ term only, since $\varphi_J = 0$. Although we can work in a basis where $\mathbf{m}_M$ is diagonal, real and positive, this does not imply that the Majorana Yukawa coupling matrices $\mathbf{h}^N$ and $\tilde{\mathbf{h}}^{N\dagger}$ are also diagonal, real or positive, we only require that their off diagonal terms cancel when the two matrices are added. This leads to the possibility of up to 21 new real parameters, which must all be taken into account in calculations. However, if the U(1) symmetry acting on S is extended to include the neutrino sector then the number of real Majorana Yukawa couplings can be reduced to a maximum of three. Applying the U(1) symmetry to the Yukawa sector is equivalent to imposing lepton number conservation, where the right-handed neutrinos $\nu^0_{1,2,3R}$ carry the lepton number $+1$ and the singlet field S the lepton number -2. As a consequence of the lepton number conservation, the Majorana Yukawa coupling matrix $\tilde{\mathbf{h}}^N$ vanishes and $\mathbf{m}_M$ reduces to

$$\mathbf{m}_M \;=\; \frac{\varphi_\sigma}{\sqrt{2}}\,\mathbf{h}^N\;, \tag{6.7}$$

which implies that if $\mathbf{m}_M$ is diagonal, real and positive then $\mathbf{h}^N$ is too. Thus, the only new Majorana neutrino Yukawa couplings are the three diagonal elements

of $\mathbf{h}^N$.

In the lepton number conserving U(1) invariant Type II flat direction the light and heavy neutrino mass matrices $\mathbf{m}_\nu$ and $\mathbf{m}_N$ can be written as

$$\mathbf{m}_\nu \;=\; -\sqrt{\frac{-\lambda_3(\Lambda)}{2\lambda_1(\Lambda)}}\, v_\phi\, \mathbf{h}^\nu (\mathbf{h}^N)^{-1} \mathbf{h}^{\nu T}\,, \qquad \mathbf{m}_N \;=\; \sqrt{\frac{\lambda_1(\Lambda)}{-2\lambda_3(\Lambda)}}\, v_\phi\, \mathbf{h}^N\,. \quad (6.8)$$

were we have used (5.2) to write the masses in terms of the SM VEV v_ϕ. For simplicity, we assume that the three heavy Majorana neutrinos $N_{1,2,3}$ are degenerate, specifically, by assuming that $\mathbf{h}^N = h^N \mathbf{1}_{3\times 3}$. The maximum value of h^N can be determined by assuming the Majorana Yukawa coupling β function given in (D.15) remains perturbative at Λ, i.e. $\boldsymbol{\beta}_{\mathbf{h}^N}(\Lambda) \leq \mathbf{1}_{3\times 3}$. This constraint leads to the upper bound, $h^N(\Lambda) < 4.0$. If we insist on the tighter constraint, that the Majorana Yukawa coupling h^N stays perturbative up to the GUT (Planck) scale, we find the upper limit: $h^N(\Lambda) \leq 0.97$ (0.89). Finally, the condition that the one-loop effective potential is BFB, i.e. $\beta > 0$, within the parameter space permitted by the perturbation conditions $\beta_{\lambda_{1,2,3}}(\Lambda) \leq 1$, gives the upper limit on h^N of $h^N(\Lambda) < 2.5$. For clarity, if $h^N(\Lambda) > 2.5$ then the BFB condition excludes the whole region of parameter space permitted by $\beta_{\lambda_{1,2,3}}(\Lambda) \leq 1$, i.e. no region of parameter space is allowed by all the theoretical constraints.

Including heavy neutrinos has a dramatic impact on the mass of the scalar h, explicitly

$$m_h \;=\; \frac{1}{\sqrt{8}\pi v_\phi} \sqrt{\frac{-\lambda_3(\Lambda)}{\lambda_1(\Lambda) - \lambda_3(\Lambda)}} \sqrt{m_H^4 + 6m_W^4 + 3m_Z^4 - 12m_t^4 - 4\sum_{i=1}^{3} m_{Ni}^4}\,, \quad (6.9)$$

where m_{Ni} are the three degenerate heavy neutrino masses given in (6.8). Figure 6.1 shows the dependence of the h boson mass on the Majorana neutrino Yukawa coupling $h^N(\Lambda)$. The maximum value of m_h is represented by the black $m_h^{\max}$ line, such that the area between the black line and the $m_h = 0$ line is permitted by the constraints $\beta_{\lambda_{1,2}}(\Lambda) \leq 1$ and $\beta > 0$. The value of $m_h^{\max}$ is determined from

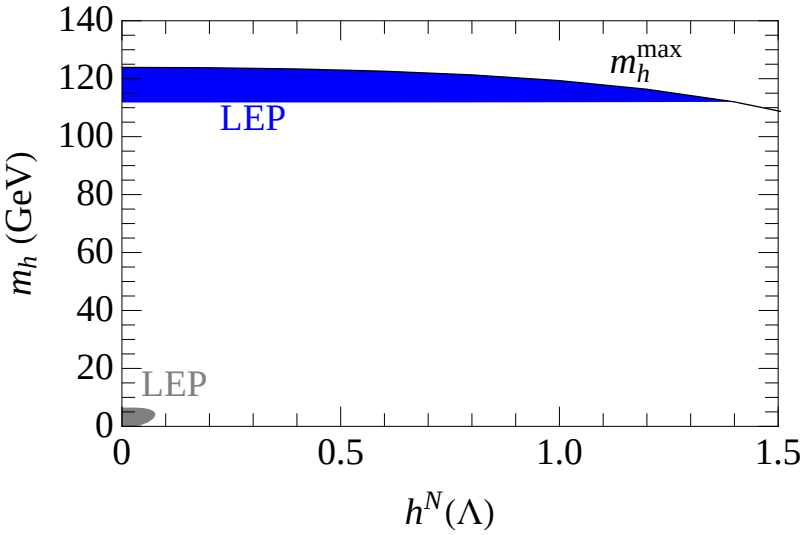

Figure 6.1: *The scalar mass m_h as a function of $h^N(\Lambda)$ in the U(1) invariant MSISM with a Type II flat direction and right-handed neutrinos. The blue and grey shaded areas correspond to the regions allowed by the LEP2 constraint for the heavier and ultra-light h boson regions respectively. The black $m_h^{\max}$ line represents the maximum perturbatively attainable values of m_h.*

the point at which $\beta_{\lambda_1}(\Lambda) = 1$ and $\beta_{\lambda_2}(\Lambda) = 1$ are simultaneously satisfied, as can be seen in the non-neutrino case in Section 5.1, specifically Figure 5.2, this is the point that gives the largest value of m_h. Since the right-handed neutrinos induce a negative contribution to m_h (6.9), $m_h^{\max}$ decreases as the right-handed neutrino Yukawa coupling h^N, correspondingly m_N, increases. In Figure 6.1, the areas which are permitted by the LEP2 constraint (the result of applying the LEP2 Higgs mass limit to m_h (6.9)) are shaded blue and grey for the heavier and ultra-light h boson regions, discussed in Sections 5.1.1 and 5.1.2, respectively. In the heavier h boson scenario, where $\lambda_3(\Lambda) \approx -3$, the LEP2 constraint restricts the Majorana neutrino Yukawa coupling h^N to be: $h^N < 1.40$. Conversely, for the ultra-light h boson scenario (with $\lambda_3(\Lambda) \approx -0.02$), we get the upper limit: $h^N < 0.074$. We have also verified that all values of $\lambda_1(\Lambda)$ and $\lambda_3(\Lambda)$ which respect the theoretical constraints $\beta_{\lambda_{1,2}}(\Lambda) \leq 1$ and $\beta > 0$ for all perturbative values of h^N, lie within the 95% CL interval of δS_{exp}, δT_{exp} and δU_{exp} (E.10).

The effect of the Majorana Yukawa coupling h^N on the heavy neutrino mass

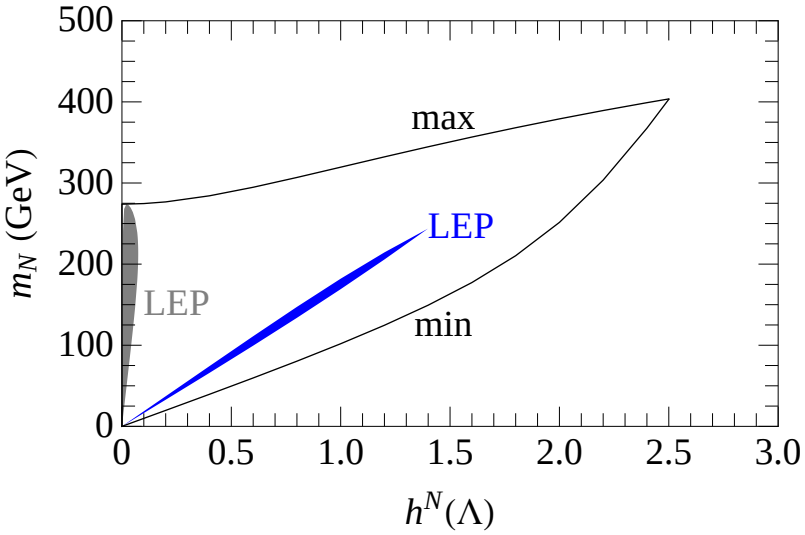

Figure 6.2: *The heavy neutrino mass m_N as a function of $h^N(\Lambda)$ in the U(1) invariant MSISM with a Type II flat direction and right-handed neutrinos. The perturbatively allowed region is given by the area between the black min and max lines. The internal blue and grey shaded areas represent the regions allowed by the LEP2 constraint, for the heavier and ultra-light h boson scenarios respectively.*

m_N is displayed in Figure 6.2. The area between the black min and max lines represents the values of m_N which are allowed by the theoretical constraints $\beta_{\lambda_{1,2}}(\Lambda) = 1$ and $\beta > 0$. The min line represents the minimum value of m_N and is given by the simultaneous satisfaction of the two relations $\beta_{\lambda_1}(\Lambda) = 1$ and $\beta > 0$, whilst the max line represents the maximum value of m_N given by the point satisfying the two relations $\beta_{\lambda_2}(\Lambda) = 1$ and $\beta > 0$. The blue and grey shaded areas indicate the regions which are allowed by the LEP2 constraint for the heavier and ultra-light h boson scenarios respectively. As can be seen from Figure 6.2, the resulting LEP2 constraint allowed areas set upper limits on the heavy Majorana neutrino masses, $m_N < 244$ GeV and $m_N < 274$ GeV, for the heavier and ultra-light h boson regions respectively. The values of m_N must be relatively light, compared to the normal seesaw mechanism, since m_h, given in (6.9) automatically places a limit on how large the heavy neutrinos can be. This is because m_h has to be positive, whilst m_H (5.5) is independent of the inclusion of neutrinos in the model and remains less than a TeV, see the lower panel of

Figure 5.2.

The masses of the other scalars, H and J and the RG scale Λ are not greatly affected by the inclusion of neutrinos. As expected J remains massless, whilst as we have just mentioned m_H does not explicitly rely on the neutrino masses masses, see (5.5). However, the inclusion of h^N in the β functions and the one-loop effective potential coefficient β, will decrease the allowed range of quartic coupling parameter space as h^N increases and consequently the allowed range of m_H will decrease, but its overall value will not be affected. The influence of the Majorana neutrino Yukawa coupling h^N on the RG scale Λ is not significant for the heavier h case as we find the maximum value of Λ which respects the LEP2 constraint for this case is $\Lambda^{\max} \approx 464$ GeV. In the ultra-light case, Λ is constrained to take values less than about a TeV by applying the constraint $\alpha \leq 1$.

The experimental significance of the inclusion of right-handed neutrinos is strongly $\lambda_{1,2,3}(\Lambda)$ and $h^N(\Lambda)$ coupling dependent. For example if $m_h > 2m_N$ then the scalars h and H develop new decay channels such as $h \to (\nu_i N_j,\ N_i N_j)$ and $H \to (\nu_i N_j,\ N_i N_j)$ [44]. However if $m_N > m_h$ the heavy neutrinos can decay via $N \to h\nu$. Due to the strong $\lambda_{1,2,3}(\Lambda)$ and $h^N(\Lambda)$ coupling dependence, a complete analysis of the effects of the heavy neutrinos is beyond the scope of this work.

The phenomenology of the U(1) invariant MSISM with a Type II flat direction and right-handed neutrinos does not change from that of the no-neutrino case in Section 5.1. There is still no massive stable scalar particle that could play the role of the cold DM and the inclusion of right-handed neutrinos does not change the UV behaviour of the model which still develops a Landau pole far below $M_{\rm GUT}$ and $M_{\rm Planck}$. For this reason, we turn our attention to the U(1) non-invariant MSISM with a Type II flat direction that minimally realises maximal SCPV which does not contain these weaknesses.

6.2 Neutrinos in the Minimal U(1) Non-Invariant Type II Flat Direction with Maximal SCPV

In this section we consider the effect of including right-handed neutrinos in the U(1) non-invariant Type II flat direction that minimally realises maximal SCPV which was presented and discussed for the no-neutrino scenario in Section 5.2. The minimisation of the flat direction leads to the requirement that $\varphi_\sigma = \varphi_J$ for maximal SCPV. Applying this to the heavy Majorana neutrino mass matrix $\mathbf{m}_M$ (6.3, 6.5) gives

$$\mathbf{m}_M \;=\; \frac{\varphi_\sigma}{\sqrt{2}} \left[(1+i)\, \mathbf{h}^N \;+\; (1-i)\, \tilde{\mathbf{h}}^{N\dagger} \right] . \tag{6.10}$$

Since the Majorana Yukawa couplings, $\mathbf{h}^N$ and $\tilde{\mathbf{h}}^N$, can contain a large number of independent parameters, we will not consider the complete neutrino Lagrangian (6.1) but will extend the symmetries already present in the tree-level potential to the neutrino sector. The tree-level potential for this scenario contains two symmetries of importance: CP invariance and the parity symmetry $\sigma \leftrightarrow J$, however, it is not possible for the neutrino sector to respect both these symmetries simultaneously without requiring $\mathbf{h}^N = \tilde{\mathbf{h}}^N = 0$. Therefore, we shall apply each symmetry separately and investigate two different variations of the model. In the first variant, we assume that both $\mathbf{h}^N$ and $\tilde{\mathbf{h}}^N$ are real, i.e. there are no sources of explicit CP violation in neutrino Yukawa sector. The second variant applies the parity symmetry $\sigma \leftrightarrow J$.

6.2.1 The CP Symmetric Scenario

Under CP invariance all the couplings of the theory must be real, including the new Majorana Yukawa couplings $\mathbf{h}^N_{ij}$ and $\tilde{\mathbf{h}}^N_{ij}$. Working in the basis where $\mathbf{m}_M$ is real and diagonal, we obtain the constraint: $\mathbf{h}^N = \tilde{\mathbf{h}}^N$. Implementing these

constraints on the neutrino mass matrices (6.3, 6.5) gives,

$$\mathbf{m}_\nu \;=\; -\,\frac{1}{2}\sqrt{\frac{-\lambda_3(\Lambda)}{\lambda_1(\Lambda)}}\;v_\phi\;\mathbf{h}^\nu\,(\mathbf{h}^N)^{-1}\,\mathbf{h}^{\nu T}\;, \qquad \mathbf{m}_N \;=\; \sqrt{\frac{\lambda_1(\Lambda)}{-\lambda_3(\Lambda)}}\;v_\phi\,\mathbf{h}^N\;, \tag{6.11}$$

where we have used (5.12) to write them in terms of the SM VEV v_ϕ. For simplicity we assume three degenerate heavy neutrinos, implying $\mathbf{h}^N = h^N\mathbf{1}_{3\times3}$, where the coupling parameter h^N has to be $h^N < 2.60$ to be perturbative at the RG scale Λ, i.e. $\boldsymbol{\beta}_{\mathbf{h}^N}(\Lambda) \leq \mathbf{1}_{3\times3}$. Requiring that the coupling remains perturbative to the GUT or Planck scales gives the upper limits $h^N \leq 0.52$ and $h^N \leq 0.47$, respectively.

We have previously shown in the no-neutrino case presented in Section 5.2, that the scalar sector can be expressed in terms of three independent theoretical parameters, namely $\lambda_1(\Lambda)$, $\lambda_2(\Lambda)$ and $\lambda_3(\Lambda)$, with $\lambda_6(\Lambda) = \frac{1}{2}\left(\lambda_2(\Lambda) - \frac{\lambda_3^2(\Lambda)}{\lambda_1(\Lambda)}\right)$ using (5.12). Including right-handed neutrinos in a CP invariant way provides a fourth independent theoretical parameter; h^N. Due to the large number of parameters we have decided to investigate three viable benchmark cases where we have fixed the values of $\lambda_2(\Lambda)$ and $\lambda_3(\Lambda)$. We consider the following three cases:

$$\begin{aligned}
&\text{Case A}: \qquad \lambda_2(\Lambda) \;=\; 0.1\,, \qquad \lambda_3(\Lambda) \;=\; -0.01\,,\\
&\text{Case B}: \qquad \lambda_2(\Lambda) \;=\; 0.1\,, \qquad \lambda_3(\Lambda) \;=\; -0.005\,,\\
&\text{Case C}: \qquad \lambda_2(\Lambda) \;=\; 0.05\,, \qquad \lambda_3(\Lambda) \;=\; -0.005\,.
\end{aligned} \tag{6.12}$$

These values have been chosen so that they respect the tight theoretical constraints,

- That all four independent couplings remain perturbative up to the Planck scale, i.e. $\beta_{\lambda_{1,2,3,6}}(M_{\text{Planck}}) \leq 1$ and $\boldsymbol{\beta}_{\mathbf{h}^N}(M_{\text{Planck}}) \leq \mathbf{1}_{3\times3}$;

- The tree-level potential and one-loop effective potential are BFB up to the Planck scale which requires $\lambda_1(M_{\text{Planck}}) > 0$, $\lambda_2(M_{\text{Planck}}) - 2\lambda_6(M_{\text{Planck}}) > 0$,

$\lambda_3(M_{\rm Planck}) < 0$ and $\beta > 0$;

- The $V_{\rm eff}^{1-{\rm loop}}$ coefficient $\alpha \leq 1$ so that the perturbative GW approach can be applied.

The tightest constraints are found to come from;

$$\beta_{\lambda_1}(M_{\rm Planck}) \leq 1\,, \qquad \lambda_1(M_{\rm Planck}) > 0\,,$$
$$\lambda_2(M_{\rm Planck}) - 2\lambda_6(M_{\rm Planck}) > 0\,, \qquad \beta > 0\,, \tag{6.13}$$

and $\alpha \leq 0$. In our numerical analysis we also apply the experimental LEP2 constraint i.e. we apply the LEP2 Higgs mass limit to m_h given in (6.14). We have verified that even with the addition of the heavy neutrinos the oblique parameters continue to lie within their respective 95% CL limits $\delta S_{\rm exp}$, $\delta T_{\rm exp}$ and $\delta U_{\rm exp}$ and provide no constraints on the theoretically permitted region.

Once again the influence of including the heavy neutrinos has a observable effect on the mass of the scalar h, explicitly

$$m_h \;=\; \frac{1}{\sqrt{8}\pi v_\phi}\sqrt{\frac{-\lambda_3(\Lambda)}{\lambda_1(\Lambda)-\lambda_3(\Lambda)}}\sqrt{m_{H_1}^4 + m_{H_2}^4 + 6m_W^4 + 3m_Z^4 - 12m_t^4 - 4\sum_{i=1}^{3} m_{Ni}^4}\,, \tag{6.14}$$

where $m_{H_{1,2}}$ are given in (5.16) and m_{Ni} are the three degenerate heavy neutrino masses given in (6.11). In Figure 6.3, we present the dependence of the h boson mass on the Majorana neutrino Yukawa coupling $h^N(\Lambda)$, for the three cases A, B and C given in (6.12). The area between the black lines is allowed by the considerations given in (6.13) where $\beta > 0$ forms the tighter constraint in cases A and C whilst $\lambda_2(M_{\rm Planck}) - 2\lambda_6(M_{\rm Planck}) > 0$ is tighter in case B. The constraint $\alpha \leq 1$ only occurs within the theoretically permitted region in case B and is represented by the red $\alpha = 1$ line and above which is excluded. For case A and C, the $\alpha = 1$ line is above the allowed region and has not been displayed. The region below the grey dashed LEP line is excluded by the LEP2 constraint.

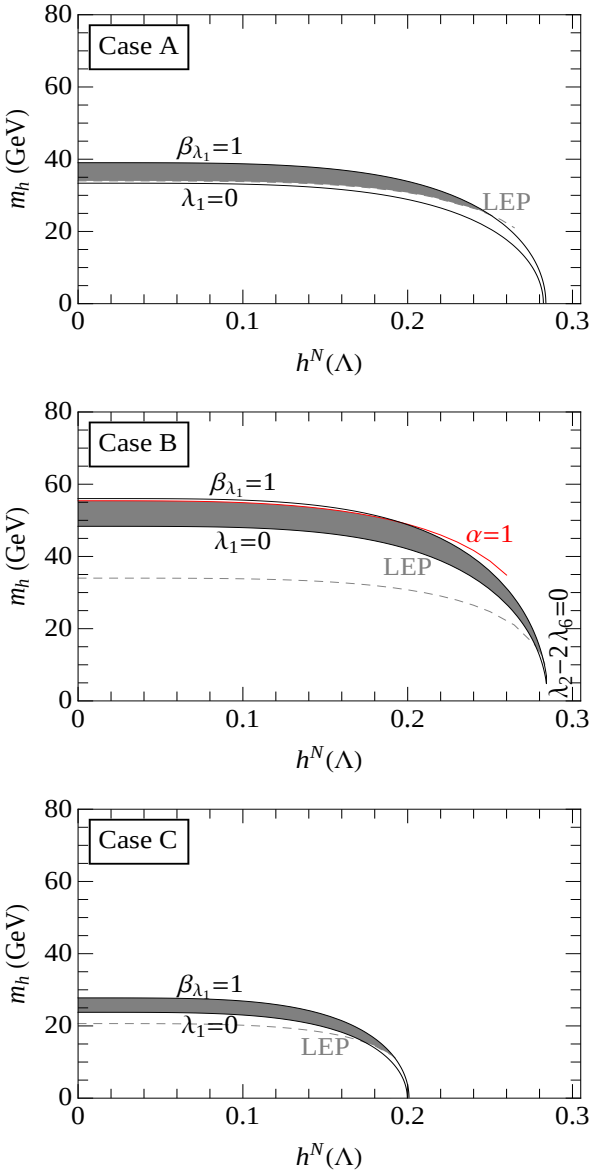

Figure 6.3: *The scalar mass m_h as a function of $h^N(\Lambda)$ in the U(1) non-invariant MSISM with a Type II flat direction that minimally realises maximal SCPV and includes CP symmetric right-handed neutrinos. The three panels represent the three different cases A (top panel), B (middle panel) and C (lower panel), as defined in (6.12). The area between the black lines show the regions which correspond to imposing the theoretical constraints given in (6.13) where $\beta > 0$ forms the tighter constraint in cases A and C whilst $\lambda_2(M_{\text{Planck}}) - 2\lambda_6(M_{\text{Planck}}) > 0$ is tighter in case B. The area above the red $\alpha = 1$ line in case B is excluded. The area below the grey dashed LEP line is excluded by LEP2 constraint. The grey shaded areas correspond to the regions allowed by theory and experiment.*

As a consequence, the grey shaded areas correspond to the regions which are allowed by the theoretical considerations, the LEP2 constraint and the oblique parameters. The presence of the right-handed neutrinos does not greatly affect m_h, except when h^N approaches its maximum allowed value which reduces the prediction for m_h, as shown in Figure 6.3. The other scalar masses, $m_{H_{1,2}}$, are not greatly affected by the inclusion of neutrinos, since they are independent of h^N at the tree level. However, the inclusion of h^N in the β functions will reduce the permitted parameter space and in-turn reduce the range the masses can take.

In Figure 6.4 we display the dependence of the heavy neutrino masses m_N on the Majorana neutrino Yukawa coupling $h^N(\Lambda)$ for the three benchmark scenarios listed in (6.12). Once again the areas between the black lines are permitted by the theoretical considerations given in (6.13) and the area above the red $\alpha = 1$ line in case B is excluded. The area below the grey dashed LEP line is excluded by LEP2 constraint, leaving the grey shaded area as the region permitted by theoretical and experimental constraints. Comparing the three cases A, B and C, we observe that if $\lambda_3(\Lambda)$ decreases or $\lambda_2(\Lambda)$ increases, both the upper limits on m_N and h^N increase. From Figure 5.4, we see that if $\lambda_2(\Lambda)$ increases then $\lambda_3(\Lambda)$ also needs to increase to remain within the theoretical and LEP2 constraint. This means we can not simultaneously decrease $\lambda_3(\Lambda)$ and increase $\lambda_2(\Lambda)$ whilst remaining within the theoretical constraints of (6.13) and $\alpha \leq 1$. We assume the maximal values of m_N and h^N do not vary significantly from the values given in case B and from this benchmark scenario we can then derive approximate upper limits on the values of m_N and h^N. Thus, from the middle panel of Figure 6.4, we observe that the heavy Majorana neutrinos can generically have masses up to TeV scale, i.e. $m_N \lesssim 1$ TeV, and h^N must remain relatively small in order for the one-loop effective potential to be BFB, i.e. $h^N \lesssim 0.3$.

The only weakness of the CP invariant scenario is that the would-be DM candidate, the H_2 boson, is no longer stable, since it can decay to neutrinos. The rate of decay is strongly coupling size dependent and so no further investigation

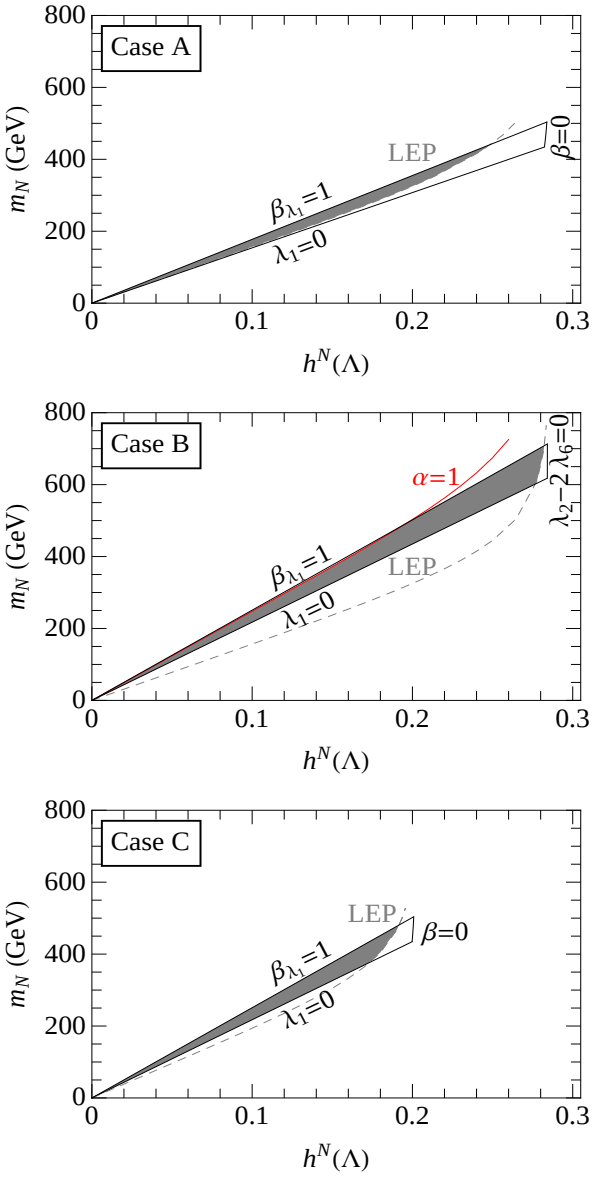

Figure 6.4: *The heavy neutrino mass m_N as a function of $h^N(\Lambda)$ in the U(1) non-invariant MSISM with a Type II flat direction that minimally realises maximal SCPV and includes CP symmetric right-handed neutrinos for the three cases A, B and C defined in (6.12). The area between the black lines show the regions corresponding to the constraints: $\beta_{\lambda_1}(M_{\text{Planck}}) < 1$, $\lambda_1(M_{\text{Planck}}) > 0$ and $\lambda_2(M_{\text{Planck}}) - 2\lambda_6(M_{\text{Planck}}) > 0$ in case B or $\beta > 0$ in cases A and C. The region above the red $\alpha = 1$ line is excluded and below the grey dashed LEP line is excluded by LEP2 constraint. This leaves the grey shaded areas which are permitted by both theoretical and experimental constraints.*

has been performed. The decay of the H_2 boson is a consequence of the violation of the parity symmetry, $\sigma \leftrightarrow J$, in the Majorana neutrino Yukawa sector. In the following section we consider extending the parity symmetry to the neutrino sector so that it would then act on the complete Lagrangian of the MSISM.

6.2.2 The $\sigma \leftrightarrow J$ Symmetric Scenario

Of the two symmetries that the U(1) non-invariant MSISM with a Type II flat direction which minimally realises maximal SCPV possesses, CP and $\sigma \leftrightarrow J$, the latter could be said to be the more phenomenologically important. This is because under the action of this symmetry, the scalar field H_2 as given in (5.17) is odd: $H_2 \to -H_2$, whilst h and H_1 are even. This implies that H_2 must always appear as H_2^2 to preserve the parity and so is a stable particle. This parity symmetry remains unbroken after the EWSSB and additionally since $\varphi_\sigma = \varphi_J$ to realise maximal SCPV, H_2 has no VEV. Thus H_2 is a massive stable scalar particle which could play the role of cold DM in the Universe.

Extending the parity symmetry $\sigma \leftrightarrow J$ to the neutrino sector requires that $\mathbf{h}^N = -i\tilde{\mathbf{h}}^{\mathbf{N}\dagger}$. Since the H_2 boson is odd under the parity, it can not interact with the neutrinos without the parity breaking and so will remain a massive stable particle even after the inclusion of neutrinos. Given the relation $\mathbf{h}^N = -i\tilde{\mathbf{h}}^{N\dagger}$, the light and heavy neutrino mass matrices (6.3, 6.5) become

$$\mathbf{m}_\nu \;=\; -\frac{1}{4}\sqrt{\frac{-\lambda_3(\Lambda)}{\lambda_1(\Lambda)}}\, v_\phi\, \mathbf{h}^\nu (\mathrm{Re}\,\mathbf{h}^N)^{-1}\, \mathbf{h}^{\nu T}\,, \qquad \mathbf{m}_N \;=\; 2\sqrt{\frac{\lambda_1(\Lambda)}{-\lambda_3(\Lambda)}}\, v_\phi\, \mathrm{Re}\,\mathbf{h}^N\,, \tag{6.15}$$

where we have used (5.12) to write the masses in terms of the SM VEV v_ϕ and to work in the basis in which $\mathbf{m}_M$ is real and diagonal we require that $\mathrm{Re}\,\mathbf{h}^N = -\mathrm{Im}\,\mathbf{h}^N$. Once again we assume three degenerate heavy neutrinos, implying $\mathrm{Re}\,\mathbf{h}^N = \mathrm{Re}\,h^N \mathbf{1}_{3\times3}$, where the coupling parameter $\mathrm{Re}\,h^N < 2.06$ to be perturbative at the RG scale Λ, i.e. $\boldsymbol{\beta}_{\mathbf{h}^N}(\Lambda) \leq \mathbf{1}_{3\times3}$, and less than 0.37 or 0.33 to remain perturbative up to the GUT or Planck scale respectively.

Similar to the CP invariant scenario, the $\sigma \leftrightarrow J$ symmetric case also depends on four independent theoretical parameters; $\lambda_1(\Lambda)$, $\lambda_2(\Lambda)$, $\lambda_3(\Lambda)$ and $\mathrm{Re}\, h^N$ with $\lambda_6(\Lambda) = \frac{1}{2}\left(\lambda_2(\Lambda) - \frac{\lambda_3^2(\Lambda)}{\lambda_1(\Lambda)}\right)$ using (5.12). Due to the large number of parameters we use the same three benchmark cases as the CP invariant scenario, given in (6.12) which respect the tight theoretical constraints listed previously. The tightest constraints in this case are determined from

$$\beta_{\lambda_1}(M_{\mathrm{Planck}}) \leq 1\,, \qquad \lambda_1(M_{\mathrm{Planck}}) > 0\,, \qquad \beta > 0\,, \tag{6.16}$$

and $\alpha \leq 0$. In the numerical analysis we again apply the experimental LEP2 constraint i.e we apply the LEP2 Higgs mass limit in an identical fashion to the no-neutrino case on m_h. We have verified that even with the addition of the heavy neutrinos the oblique parameters continue to lie within their respective 95% CL limits δS_{exp}, δT_{exp} and δU_{exp} and provide no constraints on the theoretically permitted region.

In Figure 6.5 we show the dependence of the h boson mass, given in (6.14) where m_{Ni} are now given in (6.15), on the Majorana neutrino Yukawa coupling $\mathrm{Re}\, h^N(\Lambda)$, for the three cases A, B and C defined in (6.12). The area enclosed by the black lines is theoretically favoured by the perturbative and BFB conditions given in (6.16). The area above the red $\alpha = 1$ line is disfavoured, whilst the area above the grey dashed LEP lines correspond to the regions which are permitted by the LEP2 constraint. The grey shaded regions are theoretically and experimentally permitted. From Figure 6.5, we observe that the h boson mass has a similar range of values as the CP symmetric scenario discussed in the previous section.

In Figure 6.6 we display the allowed parameter space of the degenerate right-handed neutrino Majorana mass m_N and $\mathrm{Re}\, h^N(\Lambda)$, for the three different cases A, B and C. As before, we consider the following theoretical conditions given in (6.16) and $\alpha \leq 1$. The theoretically favoured regions are those enclosed by the black $\beta_{\lambda_1} = 1$, $\lambda_1 = 0$ and $\beta = 0$ lines and below the red $\alpha = 1$ line.

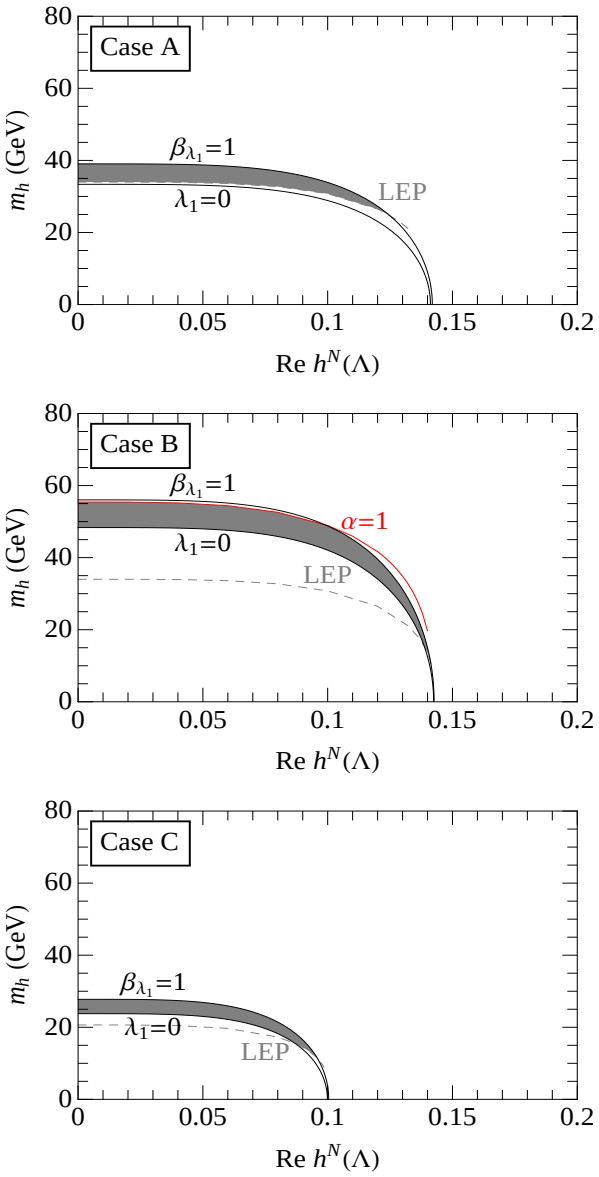

Figure 6.5: *The scalar mass m_h as a function of* $\mathrm{Re}\, h^N(\Lambda)$ *in the U(1) non-invariant MSISM with a Type II flat direction that minimally realises maximal SCPV and includes a $\sigma \leftrightarrow J$ parity symmetric right-handed neutrino sector. Cases A (top panel), B (middle panel) and C (lower panel) are defined in (6.12). The area between the black lines correspond to regions allowed by the theoretical constraints (6.16). The region above the red $\alpha = 1$ line in case B is excluded. The area below the grey dashed LEP line is excluded by LEP2 constraint so that the grey shaded areas correspond to the regions allowed by both theory, the LEP2 constraint and the oblique parameters.*

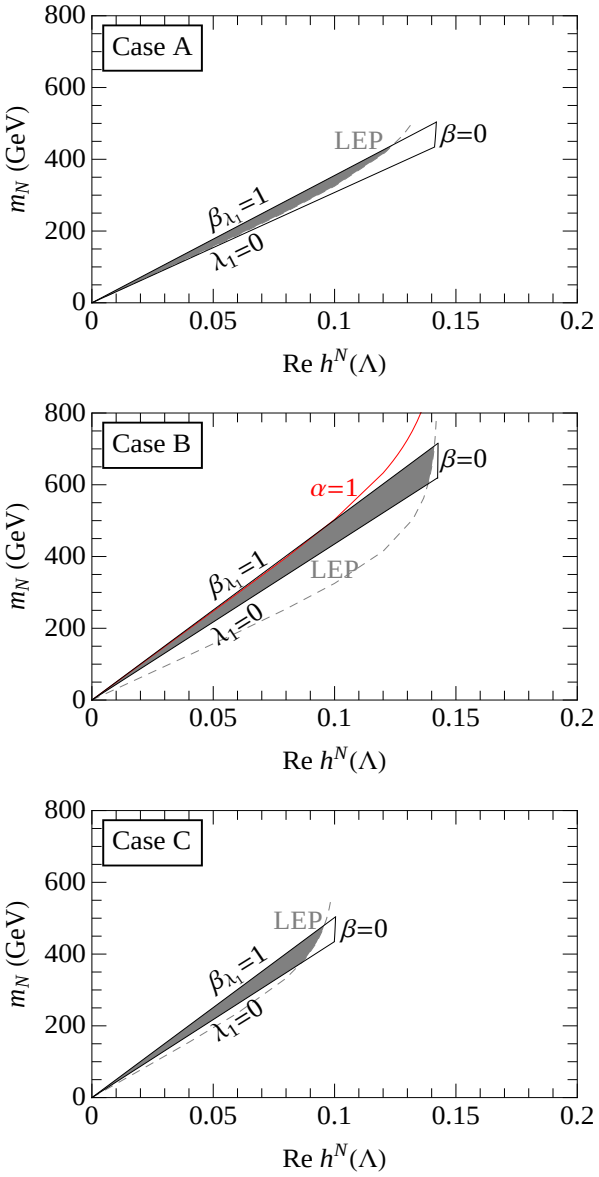

Figure 6.6: *The heavy neutrino mass m_N as a function of $\mathrm{Re}\, h^N(\Lambda)$ in the U(1) non-invariant MSISM with a Type II flat direction that minimally realises maximal SCPV and includes a $\sigma \leftrightarrow J$ parity symmetric right-handed neutrino sector. The three panels represent the three different cases A (top panel), B (middle panel) and C (lower panel), as defined in (6.12). The area between the black lines show the regions which satisfy: $\beta_{\lambda_1}(M_{\mathrm{Planck}}) < 1$, $\lambda_1(M_{\mathrm{Planck}}) > 0$ and $\beta > 0$. The regions above the red $\alpha = 1$ line and below the grey dashed LEP line are excluded by the respective limits. The grey shaded areas correspond to the regions which respect both the theoretical and the LEP2 constraints.*

The grey shaded areas correspond to the regions which are permitted by theoretical constraints, the LEP2 constraint and the oblique parameters. In all the three benchmark scenarios considered, the heavy Majorana neutrino mass scale m_N stays below the TeV scale and the value of $\mathrm{Re}\, h^N(\Lambda)$ is constrained to be: $\mathrm{Re}\, h^N \lesssim 0.15$.

In summary, the U(1) non-invariant MSISM with a Type II flat direction which minimally realises maximal SCPV and preserves the $\sigma \leftrightarrow J$ parity in the neutrino sector has a number of physically interesting properties. Firstly, it maintains the parity symmetry, such that the H_2 boson remains a stable particle even after the inclusion of right-handed neutrinos and so H_2 could play the role of cold DM in the Universe. Secondly, it can implement an electroweak seesaw mechanism which naturally provides small neutrino masses. Thirdly, it contains a new source of spontaneous CP violation, thereby enabling the model with the ability to consider addressing the problem of the baryon asymmetry in the Universe. Fourthly, the model successfully passes all obvious experimental constraints from LEP2 Higgs mass limit and other electroweak precision data, whilst the scalar H_1 lies in the region close to the Tevatron excluded region. Finally, there exists a significant region of the theoretical parameter space within which the model can stay perturbative up to Planck scale.

Chapter 7

Conclusions

In this thesis we have presented a thorough and systematic investigation of the Minimal Scale Invariant extension of the Standard Model for a number of representative scenarios along two of its three classified types of flat direction. The MSISM is an extension of the Standard Model that includes an additional complex singlet scalar field S and is classically scale invariant. Quantum corrections explicitly break the scale invariance, and their interplay with the quartic couplings can be used to trigger electroweak symmetry breaking. The SI SM suffers from a number of issues, however the inclusion of a complex singlet scalar results in a perturbative and phenomenologically viable theory.

To study the EWSSB of the MSISM we employed the perturbative approach of GW [21]. To this end, we calculated the full one-loop effective potential of the MSISM and determined a complete classification of the flat directions that can occur in the classical scalar potential of the MSISM. We have found that the flat directions can be classified into three major categories: Type I, Type II and Type III. The Type I flat direction is characterised by the singlet scalar S having a zero VEV at tree-level, whereas the Type II flat direction is defined by non-zero VEVs for both fields, S and the SM Higgs doublet Φ. The third type of flat direction, Type III, requires the VEV of Φ to be zero at tree-level, however this makes it difficult to naturally realise EWSSB without the need to introduce unnaturally

large hierarchies between the scalar potential quartic couplings, or between the VEVs of the Φ and S fields. Therefore, our analysis has focused on scenarios of the Type I or Type II flat directions.

For each of the two types of flat directions we considered two different scenarios, a U(1) invariant scenario, in which the scalar field S is invariant under a change of phase, and a scenario where the U(1) invariance has been dropped. In these scenarios we determine the permitted quartic coupling parameter space, using both theoretical and experimental constraints, and apply these limits to make numerical predictions of the scalar mass spectrum and the RG scale Λ. The theoretical constraints are derived by keeping the quartic couplings perturbative, for which we calculate the one-loop β functions of the pertinent couplings of the MSISM, and also keeping the potential BFB. The experimental constraints include the direct Higgs boson searches at LEP2 and the Tevatron, as well as phenomenological limits from electroweak precision data. We find that for all the considered scenarios the scalar masses and the RG scale Λ remain below the TeV scale, with Λ normally just higher than the EW scale.

We have found that the general Type I flat direction is perturbative only up to the EW scale and exhibits a Landau pole at energy scales $\sim 10^4$ GeV. Likewise, we have found that the U(1) invariant Type II flat direction develops a Landau pole at energy scales $\sim 10^6$ GeV. In this respect, our results are in qualitative agreement with [23]. Moving away from the constraint of U(1) invariance, we have explicitly demonstrated that a minimal U(1) non-invariant MSISM with a Type II flat direction which realises maximal SCPV can stay perturbative up to the Planck scale. This is of particular importance for suggesting that the gauge hierarchy problem is removed in this case. In [14, 15, 16] it is argued that the quadratic divergences in any SI theory are just spurious effects of the regularisation scheme provided the regularisation scheme respects the classical symmetries of the local classical action, to which scale invariance must be promoted. A further two requirements are made in [16]; that the theory has no intermediate scales between

the EW and the Planck scales and that the running couplings have neither Landau poles nor instabilities before the Planck scale. The minimal U(1) non-invariant MSISM with a Type II flat direction which realises maximal SCPV respects all these constraints.

In addition, we have discussed the phenomenological implications of the Type I and Type II flat directions, in particular, whether they realise explicit or spontaneous CP violation, contain neutrino masses or provide dark matter candidates. The key features of the different flat directions have been summarised in Table 3.1. We decided to investigate the inclusion of right-handed neutrinos to the MSISM in more detail, for the main reason that if the very small light neutrino masses were generated through the seesaw mechanism, then the corresponding heavy neutrinos could have a large impact on the one-loop effective potential, the one-loop β functions and the oblique parameters. The seesaw mechanism can only be realised in a SI way in the Type II flat direction. Our analysis shows that the additional heavy Majorana neutrino masses m_N cannot be much higher than the TeV scale.

The scenario which satisfies all the above requirements is the minimal U(1) non-invariant Type II scenario which maximally realises SCPV. It can naturally incorporate small neutrino masses via the seesaw mechanism and, provided it preserves the parity symmetry between the real and imaginary fields of the complex scalar S in the neutrino sector, produces a massive stable scalar dark matter candidate. An important feature of this model is that it can remain perturbative up to the Planck scale. As mentioned above, it can be argued that last property, along with the classical scale invariance, can potentially solve the gauge hierarchy problem for this model.

There are several issues which are beyond the scope of this thesis, but which need to be studied in greater detail. We have not discussed either the DM candidates or the CP violation in great detail, and further investigation into both areas of phenomenology is required. Additionally although we have discussed it,

a fully detailed investigation into how these scenarios could be detected at the LHC or future colliders also needs to be considered.

Appendix A

Derivation of the Ward Identity for Scale Invariance

In this appendix we present the derivation of the WI for scale invariance from Equation (2.6) to Equation (2.8). To clearly show the derivation we shall consider a single real field only, to expand to a theory containing complex fields simply include the hermitian conjugate of every term and for theories with multiple fields just sum over all the fields.

Equation (2.6) can be rewritten in terms of only one variable, x, which we will then drop for notational simplicity

$$\begin{aligned}
\delta S[\Phi(x)] &= \int d^4y \left[\delta\big(\partial_\mu\Phi(y)\big)\,\frac{\delta}{\delta\big(\partial_\mu\Phi(y)\big)} + \delta\Phi(y)\,\frac{\delta}{\delta\Phi(y)}\right]\int d^4x\,\mathcal{L}[\Phi(x)] \\
&= \int d^4y\,d^4x\left[\delta\big(\partial_\mu\Phi(y)\big)\,\frac{\delta}{\delta\big(\partial_\mu\Phi(y)\big)} + \delta\Phi(y)\,\frac{\delta}{\delta\Phi(y)}\right]\mathcal{L}[\Phi(x)]\,\delta(x-y) \\
&= \int d^4x\left[\delta\big(\partial_\mu\Phi(x)\big)\,\frac{\delta}{\delta\big(\partial_\mu\Phi(x)\big)} + \delta\Phi(x)\,\frac{\delta}{\delta\Phi(x)}\right]\mathcal{L}[\Phi(x)]\,. \qquad \text{(A.1)}
\end{aligned}$$

The first term on the right-hand side of the above equation can be replaced by

the simple manipulation

$$\begin{aligned}\delta\big(\partial_\mu\Phi\big)\,\frac{\delta}{\delta\big(\partial_\mu\Phi\big)} &= \big(\partial_\mu\delta\Phi\big)\,\frac{\delta}{\delta\big(\partial_\mu\Phi\big)} \\ &= \partial_\mu\left[\delta\Phi\frac{\delta}{\delta\big(\partial_\mu\Phi\big)}\right] - \delta\Phi\,\left(\partial_\mu\frac{\delta}{\delta\big(\partial_\mu\Phi\big)}\right)\,, \end{aligned} \tag{A.2}$$

which gives

$$\delta S[\Phi] = \int d^4x\,\left[\partial_\mu\left[\delta\Phi\frac{\delta\mathcal{L}[\Phi]}{\delta\big(\partial_\mu\Phi\big)}\right] + \delta\Phi\left\{\frac{\delta\mathcal{L}[\Phi]}{\delta\Phi} - \left(\partial_\mu\frac{\delta\mathcal{L}[\Phi]}{\delta\big(\partial_\mu\Phi\big)}\right)\right\}\right]. \tag{A.3}$$

The last two terms which are encased in the curly brackets amount to the Euler-Lagrange equation and are equal to zero. In the first term we may replace $\delta\Phi$ by the specific variation due to the scale transformation given in (2.7). Applying ∂_μ on the various terms gives

$$\begin{aligned}\delta S[\Phi] &= \epsilon\int d^4x\,\left[\Big[a(\partial_\mu\Phi) + (\partial_\mu x^\nu)(\partial_\nu\Phi) + x^\nu(\partial_\mu\partial_\nu\phi)\Big]\frac{\delta\mathcal{L}[\Phi]}{\delta\big(\partial_\mu\Phi\big)}\right. \\ &\quad \left. +\Big[a\Phi + x^\nu\partial_\nu\Phi\Big]\left(\partial_\mu\frac{\delta\mathcal{L}[\Phi]}{\delta\big(\partial_\mu\Phi\big)}\right)\right]. \end{aligned} \tag{A.4}$$

Using the Euler-Lagrange equation on the last bracket, i.e. $\partial_\mu\left(\frac{\delta\mathcal{L}[\Phi]}{\delta\left(\partial_\mu\Phi\right)}\right) = \frac{\delta\mathcal{L}[\Phi]}{\delta\Phi}$ and noting $\partial_\mu x^\nu = \delta^\nu_\mu$ we can rewrite the above equation as

$$\begin{aligned}\delta S[\Phi] &= \epsilon\int d^4x\,\left[(a+1)(\partial_\mu\Phi)\frac{\delta\mathcal{L}[\Phi]}{\delta\big(\partial_\mu\Phi\big)} + a\Phi\frac{\delta\mathcal{L}[\Phi]}{\delta\Phi}\right. \\ &\quad \left. +x^\nu\left(\partial_\nu\Phi\frac{\delta\mathcal{L}[\Phi]}{\delta\Phi} + (\partial_\mu\partial_\nu\Phi)\frac{\delta\mathcal{L}[\Phi]}{\delta\big(\partial_\mu\Phi\big)}\right)\right]. \end{aligned} \tag{A.5}$$

The last term can be simplified using the chain rule and some simple manipulation,

$$\begin{aligned} x^\nu \left(\partial_\nu \Phi \frac{\delta \mathcal{L}[\Phi]}{\delta \Phi} + (\partial_\mu \partial_\nu \Phi) \frac{\delta \mathcal{L}[\Phi]}{\delta\big(\partial_\mu \Phi\big)} \right) &= x^\nu \Big[\frac{\partial \Phi}{\partial x^\nu} \frac{\partial}{\partial \Phi} + \frac{\partial\big(\partial_\mu \Phi\big)}{\partial x^\nu} \frac{\partial}{\partial\big(\partial_\mu \Phi\big)} \Big] \mathcal{L}[\Phi] \\ &= x^\nu \left[\frac{\partial}{\partial x^\nu} \mathcal{L}[\Phi] \right] \\ &= \frac{\partial}{\partial x^\nu} \Big[x^\nu \mathcal{L}[\Phi] \Big] - \mathcal{L}[\Phi] \frac{\partial}{\partial x^\nu} x^\nu \\ &= \partial_\nu \left(x^\nu \mathcal{L}[\Phi] \right) - 4\mathcal{L}[\Phi] \,. \end{aligned} \tag{A.6}$$

Substituting this into (A.5) gives

$$\delta S[\Phi] = \epsilon \int d^4x \ \Big[(a+1)(\partial_\mu \Phi) \frac{\delta \mathcal{L}[\Phi]}{\delta\big(\partial_\mu \Phi\big)} + a\Phi \frac{\delta \mathcal{L}[\Phi]}{\delta \Phi} - 4\mathcal{L}[\Phi] + \partial_\nu \left(x^\nu \mathcal{L}[\Phi] \right) \Big] \tag{A.7}$$

which is identical to (2.8) except for the last term. The last term can be removed to give (2.8) by using Stokes theorem

$$\int_V d^4x \ \partial_\nu \left(x^\nu \mathcal{L}[\Phi] \right) \ = \ \int_\Sigma dA \ n_\nu \left(x^\nu \mathcal{L}[\Phi] \right) \tag{A.8}$$

where a finite volume V is bounded by the surface Σ, dA is the surface element and n_ν is the outward normal to the surface. This is a boundary term and therefore vanishes on field configurations that go to zero sufficiently fast at infinity.

Appendix B

The Yukawa and Gauge Sectors of the MSISM

In this appendix we briefly review the gauge-invariant, gauge-fixing and Faddeev-Popov sectors of the MSISM Lagrangian (3.1). These terms closely resemble those of the SM which has been reviewed extensively in the literature, for example see [1, 2, 3]. In this brief exposition, we introduce the notation and determine the gauge-dependent masses and couplings that enter our calculations for the effective potential and the electroweak oblique parameters.

B.1 The Gauge-Invariant Lagrangian

The gauge-invariant part of the MSISM Lagrangian (3.1) can be written as

$$\begin{aligned}\mathcal{L}_{\rm inv} &= -\frac{1}{4}G^a_{\mu\nu}G^{a,\mu\nu} - \frac{1}{4}F^i_{\mu\nu}F^{i,\mu\nu} - \frac{1}{4}B_{\mu\nu}B^{\mu\nu} \\ &\quad + \bar{\psi}i\gamma^\mu D_\mu\psi + (D^\mu\Phi)^\dagger(D_\mu\Phi) + (\partial_\mu S^*)(\partial^\mu S) \\ &\quad - \Big(\mathbf{h}^u_{ij}\bar{Q}_{iL}\tilde{\Phi}u_{jR} + \mathbf{h}^d_{ij}\bar{Q}_{iL}\Phi d_{jR} + \mathbf{h}^e_{ij}\bar{L}_{iL}\Phi e_{jR} + \text{h.c}\Big)\,. \quad \text{(B.1)}\end{aligned}$$

Field	$SU(3)_c$	$SU(2)_L$	$U(1)_Y$
$Q_{iL} = \begin{pmatrix} u_i \\ d_i \end{pmatrix}_L$	3	2	$\frac{1}{3}$
u_{iR}	3	1	$\frac{4}{3}$
d_{iR}	3	1	$-\frac{2}{3}$
$L_{iL} = \begin{pmatrix} \nu_i^0 \\ e_i \end{pmatrix}_L$	1	2	-1
e_{iR}	1	1	-2
$\Phi = \begin{pmatrix} G^+ \\ \frac{1}{\sqrt{2}}(\phi + iG) \end{pmatrix}$	1	2	1
$S = \frac{1}{\sqrt{2}}(\sigma + iJ)$	1	1	0

Table B.1: *The $SU(3)_c$, $SU(2)_L$ and $U(1)_Y$ charge assignments for the scalar and fermion fields of the MSISM.*

The field strength tensors of the $SU(3)_c$, $SU(2)_L$ and $U(1)_Y$ gauge fields G_μ^a (with $a = 1, \ldots, 8$), A_μ^i (with $i = 1, 2, 3$) and B_μ are respectively

$$\begin{aligned} G_{\mu\nu}^a &= \partial_\mu G_\nu^a - \partial_\nu G_\mu^a + g_s f^{abc} G_\mu^b G_\nu^c \,, \\ F_{\mu\nu}^i &= \partial_\mu A_\nu^i - \partial_\nu A_\mu^i + g\varepsilon^{ijk} A_\mu^j A_\nu^k \,, \\ B_{\mu\nu} &= \partial_\mu B_\nu - \partial_\nu B_\mu \,, \end{aligned} \tag{B.2}$$

where g_s, g and g' are the corresponding $SU(3)_c$, $SU(2)_L$ and $U(1)_Y$ gauge couplings, f^{abc} are the $SU(3)_c$ structure constants and ε^{ijk} is the Levi-Civita symbol; a totally antisymmetric tensor.

The covariant derivative is defined as

$$D_\mu = \partial_\mu - ig_s \frac{\lambda^a}{2} G_\mu^a - ig \frac{\tau^i}{2} A_\mu^i - i \frac{Y}{2} g' B_\mu \,, \tag{B.3}$$

where λ^a (τ^i) are the Gell-Mann (Pauli) matrices and Y is the $U(1)_Y$ weak hypercharge of the various fields. The $\mathrm{SU}(3)_c$, $\mathrm{SU}(2)_L$ and $\mathrm{U}(1)_Y$ charge assignments for the scalars and fermions fields are given in Table B.1.

After EWSSB, in which $\mathrm{SU}(2)_L \times \mathrm{U}(1)_Y \to \mathrm{U}(1)_{\mathrm{EM}}$, the massless $\mathrm{SU}(2)_L$ and $\mathrm{U}(1)_Y$ gauge bosons can be replaced by the physical gauge bosons: three massive gauge bosons,

$$W_\mu^\pm \,=\, \frac{1}{\sqrt{2}}(A_\mu^1 \,\mp\, iA_\mu^2)\,, \qquad Z_\mu \,=\, \cos\theta_W A_\mu^3 \,-\, \sin\theta_W B_\mu \tag{B.4}$$

and a fourth massless combination $A_\mu = \sin\theta_W A_\mu^3 + \cos\theta_W B_\mu$, which corresponds to the gauge boson of the remaining $\mathrm{U}(1)_{\mathrm{EM}}$ gauge group. The Weinberg angle or weak mixing angle, θ_W, is defined through $\cos^2\theta_W = \frac{g^2}{g^2+g'^2}$. EWSSB also gives rise to two-particle mixing terms between the Goldstones bosons and the gauge bosons. For practical calculations it is more convenient to eliminate these two-particle mixing terms by choosing a gauge-fixing scheme in which they naturally cancel, see Section B.2.

In (B.1), we have used ψ to collectively represent all the fermions of the model

$$\psi \,=\, \{Q_{iL},\, u_{iR},\, d_{iR},\, L_{iL},\, e_{iR}\} \tag{B.5}$$

where the subscripts L and R denote the left- and right-handed chiralities of the fermions, $\psi_{L,R} = \frac{1}{2}(1 \mp \gamma_5)\psi$. Each type of fermion has three generations, represented by $i = 1, 2, 3$. Explicitly,

$$u_i \,=\, (u,\, c,\, t)\,, \quad d_i \,=\, (d,\, s,\, b)\,, \quad e_i \,=\, (e,\, \mu,\, \tau)\,, \quad \nu_i \,=\, (\nu_e,\, \nu_\mu,\, \nu_\tau)\,. \tag{B.6}$$

The 3×3 matrices $\mathbf{h}_{ij}^{u,d,e}$ contain the Yukawa couplings for the SM up- and down-type quarks and charged leptons respectively.

Finally, in (B.1), we have denoted the hypercharge conjugate field of the Higgs doublet Φ as $\tilde{\Phi} = i\tau^2\Phi^*$.

B.2 The Gauge-Fixing and Faddeev-Popov Lagrangians

In a gauge theory with EWSSB, such as the MSISM, one has to specify a gauge-fixing scheme in order to eliminate the unphysical degrees of freedom from the gauge fields (which result from the gauge invariance). A convenient gauge-fixing scheme, which also removes the tree-level mixing terms between the Goldstone and gauge bosons, is the R_ξ class of gauges [45]. Adopting this scheme, we can write the gauge fixing Lagrangian as follows:

$$\begin{aligned}\mathcal{L}_{\rm GF} \;=\; & -\frac{1}{2\xi}\Big[(\partial_\mu G^{a\mu})^2\Big]^2 \;-\; \frac{1}{2\xi}\Big[\partial_\mu A^{i\mu} \;+\; ig\xi\big(\Phi^\dagger\frac{\tau^i}{2}\langle\Phi\rangle \;-\; \langle\Phi\rangle^\dagger\frac{\tau^i}{2}\Phi\big)\Big]^2 \\ & -\frac{1}{2\xi}\Big[\partial_\mu B^{\mu} \;+\; ig'\frac{\xi}{2}\big(\Phi^\dagger\langle\Phi\rangle \;-\; \langle\Phi\rangle^\dagger\Phi\big)\Big]^2 \end{aligned} \tag{B.7}$$

where we have linearly decomposed the neutral component of Φ about its one-loop induced VEV, $\Phi + \langle\Phi\rangle$, where

$$\langle\Phi\rangle = \begin{pmatrix} 0 \\ \frac{v_\phi}{\sqrt{2}} \end{pmatrix} . \tag{B.8}$$

At the minimum we require v_ϕ to equal the SM VEV, $v_\phi = v_{\rm SM} = 246$ GeV. The Goldstone bosons obtain gauge-dependent mass contributions given by

$$m^2_{G^\pm} \;=\; \frac{1}{4}g^2\xi v_\phi^2 \,, \qquad\qquad m^2_G \;=\; \frac{1}{4}(g^2 \;+\; g'^2)\xi v_\phi^2 \,. \tag{B.9}$$

Denoting the $\mathrm{SU}(3)_c$, $\mathrm{SU}(2)_L$ and $\mathrm{U}(1)_Y$ ghost fields as η^a $(a = 1, ..., 8)$, ω_i $(i = 1, 2, 3)$ and χ, the induced Faddeev–Popov Lagrangian is

$$\mathcal{L}_{\rm FP} \;=\; -\bar\eta^a\partial_\mu(\partial^\mu\delta^{ac} \;-\; g_s f^{abc}G^{b\mu})\eta^c \;+\; (\omega_i^\dagger, \chi^\dagger)\begin{pmatrix} M_{ij} & M_i \\ M_j & M \end{pmatrix}\begin{pmatrix} \omega_j \\ \chi \end{pmatrix} \tag{B.10}$$

where

$$\begin{aligned} M_{ij} &= -\Big[\partial^\mu(\delta_{ij}\partial_\mu - g\epsilon_{ijk}A^k_\mu) + g^2\xi\Big(\frac{1}{2}\langle\Phi\rangle^\dagger\langle\Phi\rangle\delta_{ij} + \Phi^\dagger\frac{\tau_j\tau_i}{4}\langle\Phi\rangle \\ &\quad + \langle\Phi\rangle^\dagger\frac{\tau_i\tau_j}{4}\Phi\Big)\Big] \\ M_i &= -\frac{gg'}{2}\xi\Big[\langle\Phi\rangle^\dagger\tau_i\langle\Phi\rangle + \Phi^\dagger\frac{\tau_i}{2}\langle\Phi\rangle + \langle\Phi\rangle^\dagger\frac{\tau_i}{2}\Phi\Big] \\ M_{ij} &= -\Big[\partial^\mu\partial_\mu + \frac{g'^2}{2}\xi\Big(2\langle\Phi\rangle^\dagger\langle\Phi\rangle + \Phi^\dagger\langle\Phi\rangle + \langle\Phi\rangle^\dagger\Phi\Big)\Big]\,. \end{aligned} \tag{B.11}$$

The ghosts also gain gauge-dependent mass eigenvalues;

$$m^2_{\omega_\pm} = \frac{1}{4}g^2\xi v^2_\phi\,, \qquad m^2_{\omega_Z} = \frac{1}{4}(g^2 + g'^2)\xi v^2_\phi\,, \qquad m^2_{\omega_A} = 0\,, \qquad m^2_{\eta^a} = 0\,, \tag{B.12}$$

where $\omega_\pm = \frac{1}{\sqrt{2}}(\omega_1 \mp i\omega_2)$, $\omega_Z = \cos\theta_W\omega_3 - \sin\theta_W\chi$ and $\omega_A = \sin\theta_W\omega_3 + \cos\theta_W\chi$.

We should note that after EWSSB, the ξ-dependent mass contributions appear in the one-loop effective potential $V_{\rm eff}^{1-\rm loop}$. However, when evaluated along the flat direction they cancel and leave $V_{\rm eff}^{1-\rm loop}$ gauge-invariant, for more details, see Appendix C. In the same context, we also note that the ξ-dependent mass contributions to the Goldstone bosons (B.9) contribute to the electroweak oblique parameters, S, T and U, which are conventionally calculated in the Feynman-'t Hooft gauge, $\xi = 1$, for more details, see Appendix E. However, since the one-loop anomalous dimensions and β functions can be computed in the symmetric phase of the theory, the ξ-dependent mass contributions do not influence them.

Appendix C

The One-Loop Effective Potential

To calculate the one-loop effective potential of the MSISM, we use the Feynman path integral method developed in [46]. The alternative approach of [20], which requires the summation of an infinite set of Feynman vacuum diagrams, would have been an almost impossible task in the MSISM due to the two-particle scalar mixing terms, see (C.10). Using the Feynman path integral approach, the one-loop effective potential is determined from the functional expression [46, 47]

$$V_{\rm eff}^{1-\rm loop} \;=\; -\,C_s\frac{i\hbar}{2}\Big(\mathrm{Tr}\ln H_{\varphi_1\varphi_2}(\varphi_c) \;-\; \mathrm{Tr}\ln H_{\varphi_1\varphi_2}(0)\Big)\;, \tag{C.1}$$

where φ denotes the fields of the theory, which for the MSISM are

$$\{\Phi,\, S,\, A_\mu^i,\, B_\mu,\, \omega_\pm,\, \omega_Z,\, \omega_A,\, \eta^a,\, u_i,\, d_i,\, e_i,\, \nu_i,\, N_i\},$$

and $H_{\varphi_1\varphi_2}$ is the second derivative of the classical action $S = \int d^4x\mathcal{L}$ with respect to two fields of the theory, i.e.

$$H_{\varphi_1\varphi_2}(\varphi_c) \;=\; \left.\frac{\delta^2 S}{\delta\varphi_1(x_1)\delta\varphi_2(x_2)}\right|_{\varphi=\varphi_c}. \tag{C.2}$$

The classical fields φ_c of the theory are defined such that for a vanishing source term, $J(x) = 0$, they equal the expectation value of the field φ. In (C.1), the

factor C_s takes the values, $C_s = +1$ for real fields obeying Bose–Einstein statistics, $C_s = -1$ for real fields with Fermi–Dirac statistics, and if the field is complex there is an additional factor of 2, e.g $C_s = 2$ for the complex scalars Φ and S. Finally, the trace Tr in (C.1) acts over all space and internal degrees of freedom.

To calculate $V_{\rm eff}^{1-\rm loop}$, we use the more practical representation of (C.1)

$$V_{\rm eff}^{1-\rm loop} \;=\; -\,C_s\frac{i}{2}\int_0^1 dx \mathrm{Tr}\left[\frac{H_{\varphi_1\varphi_2}(\varphi_c) \,-\, H_{\varphi_1\varphi_2}(0)}{x\,(H_{\varphi_1\varphi_2}(\varphi_c) \,-\, H_{\varphi_1\varphi_2}(0)) \,+\, H_{\varphi_1\varphi_2}(0)}\right], \quad \text{(C.3)}$$

where we have used the relation $\int_0^1 dx \frac{A}{Ax+B} = \ln(A+B) - \ln B$. Performing a Fourier transform to a momentum space of $n = 4 - 2\varepsilon$ dimension, the above expression becomes

$$V_{\rm eff}^{1-\rm loop} \;=\; -\,C_s\frac{i}{2}\int_0^1 dx \int \frac{d^n k}{(2\pi)^n}\mathrm{tr}\left[\frac{H_{\varphi_1\varphi_2}(\varphi_c) \,-\, H_{\varphi_1\varphi_2}(0)}{x\,(H_{\varphi_1\varphi_2}(\varphi_c) \,-\, H_{\varphi_1\varphi_2}(0)) \,+\, H_{\varphi_1\varphi_2}(0)}\right] \quad \text{(C.4)}$$

where tr now symbolises the trace over the internal degrees of freedom only, e.g. over the polarisations of the gauge fields, the spinor components of the fermions or over any matrices, such as the Yukawa coupling matrices.

The one-loop effective potential of the MSISM can now be calculated by individually applying (C.4) to the different field types; scalars, gauge bosons (GB), ghosts, charged fermions (CF) and neutrinos (N), i.e.

$$\begin{aligned} V_{\rm eff}^{1-\rm loop} \;=\; & V_{\rm eff}^{1-\rm loop}(\text{Scalar}) \,+\, V_{\rm eff}^{1-\rm loop}(\text{GB}) \,+\, V_{\rm eff}^{1-\rm loop}(\text{Ghost}) \\ & + V_{\rm eff}^{1-\rm loop}(\text{CF}) \,+\, V_{\rm eff}^{1-\rm loop}(\text{N})\,. \end{aligned} \quad \text{(C.5)}$$

C.1 The Scalar Contribution

The numerous interactions between the scalar fields Φ and S given in $V^{\rm tree}$ (3.2) makes determination of the scalar contribution to (C.5) a non-trivial calculation. Considering the scalar fields only, $H_{\varphi_1\varphi_2}(\varphi_c)$, as defined in (C.2), is the 6×6

matrix

$$\begin{pmatrix} H_{\Phi^\dagger\Phi} & H_{\Phi^\dagger\Phi^\dagger} & H_{\Phi^\dagger S} & H_{\Phi^\dagger S^*} \\ H_{\Phi\Phi} & H_{\Phi\Phi^\dagger} & H_{\Phi S} & H_{\Phi S^*} \\ H_{S^*\Phi} & H_{S^*\Phi^\dagger} & H_{S^*S} & H_{S^*S^*} \\ H_{S\Phi} & H_{S\Phi^\dagger} & H_{SS} & H_{SS^*} \end{pmatrix} . \tag{C.6}$$

Since Φ is a doublet whilst S is a singlet, we observe that $H_{\Phi^\dagger\Phi}$, $H_{\Phi^\dagger\Phi^\dagger}$, $H_{\Phi\Phi}$ and $H_{\Phi\Phi^\dagger}$ are 2×2 matrices, H_{SS}, H_{SS^*}, H_{S^*S} and $H_{S^*S^*}$ are complex numbers, and the remaining entries, e.g. $H_{\Phi S}$, $H_{\Phi S^*}$ etc. are two-dimensional complex vectors. This internal matrix structure must be preserved throughout the calculation, particularly when determining the matrix $[x\,(H_{\varphi_1\varphi_2}(\varphi_c) - H_{\varphi_1\varphi_2}(0)) + H_{\varphi_1\varphi_2}(0)]^{-1}$. Taking this into account, the scalar contribution is found to be

$$\begin{aligned} V_{\text{eff}}^{1-\text{loop}}(\text{Scalar}) \;&=\; \frac{1}{64\pi^2}\Bigg[\sum_{i=1}^{3} M_{H_i}^4\left(-\frac{1}{\varepsilon} - \frac{3}{2} + \ln\frac{M_{H_i}^2}{\bar\mu^2}\right) \\ &+ 2M_{G^\pm}^4\left(-\frac{1}{\varepsilon} - \frac{3}{2} + \ln\frac{M_{G^\pm}^2}{\bar\mu^2}\right) + M_G^4\left(-\frac{1}{\varepsilon} - \frac{3}{2} + \ln\frac{M_G^2}{\bar\mu^2}\right)\Bigg] , \end{aligned} \tag{C.7}$$

where $\ln\bar\mu^2 = -\gamma + \ln 4\pi\mu^2$, $\gamma \approx 0.5772$ is the Euler–Mascheroni constant and μ is 't-Hooft's renormalisation scale. The Goldstone mass terms in (C.7) are given by

$$M_G^2 \;=\; M_{G^\pm}^2 \;=\; \frac{1}{2}\lambda_1\phi^2 + \frac{1}{2}\sigma^2(\lambda_3+\lambda_4+\lambda_4^*) + \frac{1}{2}J^2(\lambda_3-\lambda_4-\lambda_4^*) + i\sigma J(\lambda_4-\lambda_4^*) . \tag{C.8}$$

Along the flat direction the Goldstone mass terms vanish because of (3.12), however, after EWSSB they obtain additional ξ-dependent contributions through the gauge fixing terms [cf. (B.9)].

The masses $M_{H_{1,2,3}}^2$ appearing in (C.7) correspond to the eigenvalues of the matrix

$$\mathcal{M}_S^2 \;=\; \begin{pmatrix} M_\phi^2 & M_{\phi\sigma} & M_{\phi J} \\ M_{\phi\sigma} & M_\sigma^2 & M_{\sigma J} \\ M_{\phi J} & M_{\sigma J} & M_J^2 \end{pmatrix} , \tag{C.9}$$

where

$$
\begin{aligned}
M_\phi^2 &= \frac{3}{2}\lambda_1\phi^2 + \frac{1}{2}(\lambda_3 + \lambda_4 + \lambda_4^*)\sigma^2 + i(\lambda_4 - \lambda_4^*)\sigma J \\
&\quad + \frac{1}{2}(\lambda_3 - \lambda_4 - \lambda_4^*)J^2 \,, \\
M_\sigma^2 &= \frac{1}{2}(\lambda_3 + \lambda_4 + \lambda_4^*)\phi^2 + \frac{3}{2}(\lambda_2 + 2\lambda_5 + 2\lambda_5^* + \lambda_6 + \lambda_6^*)\sigma^2 \\
&\quad + 3i(\lambda_5 - \lambda_5^* + \lambda_6 - \lambda_6^*)\sigma J + \frac{1}{2}(\lambda_2 - 3\lambda_6 - 3\lambda_6^*)J^2 \,, \\
M_J^2 &= \frac{1}{2}(\lambda_3 - \lambda_4 - \lambda_4^*)\phi^2 + \frac{1}{2}(\lambda_2 - 3\lambda_6 - 3\lambda_6^*)\sigma^2 \\
&\quad + 3i(\lambda_5 - \lambda_5^* - \lambda_6 + \lambda_6^*)\sigma J + \frac{3}{2}(\lambda_2 - 2\lambda_5 - 2\lambda_5^* + \lambda_6 + \lambda_6^*)J^2 \,, \\
M_{\phi\sigma} &= \phi\Big[(\lambda_3 + \lambda_4 + \lambda_4^*)\sigma + i(\lambda_4 - \lambda_4^*)J\Big] \,, \\
M_{\sigma J} &= i\Bigg[\frac{1}{2}(\lambda_4 - \lambda_4^*)\phi^2 + \frac{3}{2}(\lambda_5 - \lambda_5^* + \lambda_6 - \lambda_6^*)\sigma^2 \\
&\quad - i(\lambda_2 - 3\lambda_6 - 3\lambda_6^*)\sigma J + \frac{3}{2}(\lambda_5 - \lambda_5^* - \lambda_6 + \lambda_6^*)J^2\Bigg] \,, \\
M_{\phi J} &= \phi\Big[i(\lambda_4 - \lambda_4^*)\sigma + (\lambda_3 - \lambda_4 - \lambda_4^*)J\Big] \,. \qquad \text{(C.10)}
\end{aligned}
$$

We note that along the flat direction one of the eigenvalues of the matrix (C.9) will always vanish as it corresponds to the pseudo-Goldstone boson of scale invariance h.

C.2 The Gauge Boson Contribution

Calculated in the R_ξ gauge, the gauge-boson contribution in (C.5) reads:

$$\begin{aligned} V_{\rm eff}^{1-{\rm loop}}({\rm GB}) &= \frac{1}{64\pi^2}\Bigg[6M_W^4\left(-\frac{1}{\varepsilon}-\frac{5}{6}+\ln\frac{M_W^2}{\bar{\mu}^2}\right) \\ &+3M_Z^4\left(-\frac{1}{\varepsilon}-\frac{5}{6}+\ln\frac{M_Z^2}{\bar{\mu}^2}\right)+2\xi^2M_W^4\left(-\frac{1}{\varepsilon}-\frac{3}{2}+\ln\frac{\xi M_W^2}{\bar{\mu}^2}\right) \\ &+\xi^2M_Z^4\left(-\frac{1}{\varepsilon}-\frac{3}{2}+\ln\frac{\xi M_Z^2}{\bar{\mu}^2}\right)\Bigg], \end{aligned} \tag{C.11}$$

where

$$M_W^2 = \frac{g^2}{4}\phi^2\,, \qquad M_Z^2 = \frac{g^2+g'^2}{4}\phi^2\,. \tag{C.12}$$

C.3 The Ghost Contribution

Evaluated in the same class of R_ξ gauges, the ghost contribution after EWSSB is given by

$$\begin{aligned} V_{\rm eff}^{1-{\rm loop}}({\rm Ghost}) &= -\frac{2}{64\pi^2}\Bigg[2M_{\omega_\pm}^4\left(-\frac{1}{\varepsilon}-\frac{3}{2}+\ln\frac{M_{\omega_\pm}^2}{\bar{\mu}^2}\right) \\ &+M_{\omega_Z}^4\left(-\frac{1}{\varepsilon}-\frac{3}{2}+\ln\frac{M_{\omega_Z}^2}{\bar{\mu}^2}\right)\Bigg], \end{aligned} \tag{C.13}$$

where $M_{\omega_\pm}^2=\xi M_W^2$ and $M_{\omega_Z}^2=\xi M_Z^2$ are the field-dependent ghost masses.

C.4 The Charged Fermion Contribution

The charged fermion contribution to the effective potential (C.5) reads:

$$\begin{aligned} V_{\rm eff}^{1-{\rm loop}}({\rm CF}) &= -\frac{4}{64\pi^2}\Bigg[3\sum_{i=1}^{3}M_{ui}^4\left(-\frac{1}{\varepsilon}-1+\ln\frac{M_{ui}^2}{\bar{\mu}^2}\right) \\ &+3\sum_{i=1}^{3}M_{di}^4\left(-\frac{1}{\varepsilon}-1+\ln\frac{M_{di}^2}{\bar{\mu}^2}\right)+\sum_{i=1}^{3}M_{ei}^4\left(-\frac{1}{\varepsilon}-1+\ln\frac{M_{ei}^2}{\bar{\mu}^2}\right)\Bigg], \end{aligned} \tag{C.14}$$

where M_{fi}^2 $(f = u, d, e)$ are the eigenvalues of the background ϕ-dependent squared mass matrix for the f-type fermion: $\frac{1}{2}(\mathbf{h}^{f\dagger}\mathbf{h}^f)\,\phi^2$. The factor 3 in front of the up-type and down-type quark contributions is an $\mathrm{SU}(3)_c$ colour factor.

C.5 The Neutrino Contribution

Extending the MSISM with right-handed neutrinos to obtain a set of light ν_i and heavy N_i Majorana neutrinos, gives rise to additional contributions to the one-loop effective potential (C.5)

$$\begin{aligned} V_{\rm eff}^{1-\rm loop}(\mathrm{N}) \;=\; & -\frac{2}{64\pi^2}\Bigg\{\mathrm{Tr}\left[(\mathbf{M}_\nu\mathbf{M}_\nu^\dagger)^2\left(-\frac{1}{\varepsilon}\,-\,1\,+\,\ln\frac{\mathbf{M}_\nu\mathbf{M}_\nu^\dagger}{\bar\mu^2}\right)\right] \\ & +\,\mathrm{Tr}\left[(\mathbf{M}_N\mathbf{M}_N^\dagger)^2\left(-\frac{1}{\varepsilon}\,-\,1\,+\,\ln\frac{\mathbf{M}_N\mathbf{M}_N^\dagger}{\bar\mu^2}\right)\right]\Bigg\}\,, \end{aligned} \tag{C.15}$$

where $\mathbf{M}_\nu$ is the light-neutrino mass matrix,

$$\mathbf{M}_\nu = \frac{1}{2}\phi^2\,\mathbf{h}^\nu\,\mathbf{M}_N^{-1}\,\mathbf{h}^{\nu T}\,, \tag{C.16}$$

and $\mathbf{M}_N$ is the respective heavy-neutrino mass matrix,

$$\mathbf{M}_N \;=\; \frac{1}{\sqrt{2}}\Big[\,\sigma(\mathbf{h}^N + \tilde{\mathbf{h}}^{N\dagger}) + iJ(\mathbf{h}^N - \tilde{\mathbf{h}}^{N\dagger})\,\Big]\,. \tag{C.17}$$

Finally, we shall make an important remark regarding the gauge-dependence of the one-loop effective potential. In general $V_{\rm eff}^{1-\rm loop}$ is gauge dependent through (C.11) and, after EWSSB, through (C.13) and the Goldstone ξ-dependent mass terms in (C.7). It is known that the effective potential becomes gauge-independent when evaluated at local extrema [48, 49]. As a consistency check, we have independently verified that the ξ-dependent terms due to the gauge, Goldstone and ghost contributions cancel against each other in the one-loop effective potential (C.5) when evaluated along the flat directions as well as at the minimum.

Appendix D

The One-Loop Anomalous Dimensions and β Functions

In this appendix, we present the one-loop anomalous dimensions of the fields and the one-loop β functions of the couplings of the MSISM. For completeness we also review the approach used to determine them. This approach is compatible with dimensional regularisation [17], the $\overline{\text{MS}}$ renormalisation scheme [35] and the R_ξ class gauges [45], which have been used through this analysis of the MSISM.

D.1 Formal Analysis

To calculate the one-loop anomalous dimensions and β functions, we need to determine the one-loop wavefunction and coupling constant renormalisation constants. To do this, we use the displacement operator formalism, or D-formalism for short, that was developed in [50] as an alternative approach which enables one to systematically perform renormalisation to all orders in perturbation theory. Since it is not a common approach, we shall briefly review its main features.

In the D-formalism the renormalised one-particle irreducible n-point correlation functions $\mathbb{\Gamma}_{\varphi^n}$ are related to the unrenormalised or bare ones $\mathbb{\Gamma}^0_{\varphi^n}$ through

the relation

$$\varphi^n \; \mathbb{\Gamma}_{\varphi^n}(\lambda, m^2, \xi; \mu) \;=\; e^D \Big(\varphi^n \; \mathbb{\Gamma}^0_{\varphi^n}(\lambda, m^2, \xi; \mu, \varepsilon) \Big) \,, \tag{D.1}$$

where D is the displacement operator that takes the form

$$D \;=\; \delta\varphi \frac{\partial}{\partial \varphi} \;+\; \delta\lambda \frac{\partial}{\partial \lambda} \;+\; \delta m^2 \frac{\partial}{\partial m^2} \;+\; \delta\xi \frac{\partial}{\partial \xi} \,, \tag{D.2}$$

with φ denoting all the fields of the theory, λ all the couplings (gauge, Yukawa and quartic couplings), m^2 all the squared masses and ξ is the gauge fixing parameter. Additionally, the parameter shifts $\delta\varphi$, $\delta\lambda$ etc. are defined as

$$\begin{aligned} \delta\varphi \;&=\; \varphi^0 - \varphi \;=\; (Z_\varphi^{1/2} - 1)\varphi \,, \qquad \delta m^2 \;=\; (m^0)^2 - m^2 \;=\; (Z_{m^2} - 1) m^2 \,, \\ \delta\lambda \;&=\; \lambda^0 - \lambda \;=\; (Z_\lambda - 1)\lambda \,, \qquad \delta\xi \;=\; \xi^0 - \xi \;=\; (Z_\xi - 1)\xi \,. \end{aligned} \tag{D.3}$$

We have used the notation that all bare elements are denoted with a superscript 0 and all renormalised ones are left un-annotated.

Since (D.1) is an all-order result, we may expand it to any given order using perturbation theory. Performing a loopwise expansion of the operator e^D gives

$$e^D \;=\; 1 \;+\; D^{(1)} \;+\; \Big(D^{(2)} + \frac{1}{2} (D^{(1)})^2 \Big) \;+\; \ldots \,, \tag{D.4}$$

where the superscript (n) on D denotes the loop order, such that

$$D^{(n)} \;=\; \delta\varphi^{(n)} \frac{\partial}{\partial \varphi} \;+\; \delta\lambda^{(n)} \frac{\partial}{\partial \lambda} \;+\; (\delta m^2)^{(n)} \frac{\partial}{\partial m^2} \;+\; \delta\xi^{(n)} \frac{\partial}{\partial \xi} \,. \tag{D.5}$$

Correspondingly, the parameter shifts $\delta\varphi^{(n)}, \delta\lambda^{(n)}$ etc are defined loop-wise as

$$\begin{aligned} \delta\varphi^{(n)} \;&=\; Z_{\varphi}^{\frac{1}{2}(n)} \varphi \,, \qquad & \delta\lambda^{(n)} \;&=\; Z_\lambda^{(n)} \lambda \,, \\ (\delta m^2)^{(n)} \;&=\; Z_{m^2}^{(n)} m^2 \,, \qquad & \delta\xi^{(n)} \;&=\; Z_\xi^{(n)} \xi \,. \end{aligned} \tag{D.6}$$

Applying the D-formalism to one-loop, we have

$$\varphi^n \mathbb{\Gamma}^{(1)}_{\varphi^n}(\lambda, m^2, \xi; \mu) = D^{(1)} \left(\varphi^n \mathbb{\Gamma}^{0(0)}_{\varphi^n}(\lambda, m^2, \xi; \mu) \right) + \varphi^n \mathbb{\Gamma}^{0(1)}_{\varphi^n}(\lambda, m^2, \xi; \mu, \varepsilon) \; . \quad \text{(D.7)}$$

Rearranging the above equation and using (D.5) and (D.6), we obtain an explicit relation to calculate the one-loop wavefunction and coupling constant renormalisation constants, $Z^{(1)}_{\varphi}$ and $Z^{(1)}_{\lambda}$ of the MSISM:

$$-\varphi^n \overline{\mathbb{\Gamma}}^{0(1)}_{\varphi^n}(\lambda, \xi; \mu, \varepsilon) \;=\; \left[\frac{1}{2} \varphi Z^{(1)}_{\varphi} \frac{\partial}{\partial \varphi} + \lambda Z^{(1)}_{\lambda} \frac{\partial}{\partial \lambda} + \xi Z^{(1)}_{\xi} \frac{\partial}{\partial \xi} \right] \left(\varphi^n \mathbb{\Gamma}^{0(0)}_{\varphi^n}(\lambda, \xi; \mu) \right) \quad \text{(D.8)}$$

where the bar indicates that only the infinite part of the corresponding bare one-particle irreducible n-point correlation function $\mathbb{\Gamma}^{0}_{\varphi^n}$ should be considered.

Having obtained the one-loop wavefunction and coupling constant renormalisations using (D.8), we may compute the one-loop anomalous dimensions γ_{φ} of the fields and the β_{λ} functions of the couplings as follows:

$$\begin{aligned} \gamma_{\varphi} \;&\equiv\; -\mu \frac{d \ln \varphi}{d\mu}\Big|_{\varepsilon \to 0} \;=\; -\frac{1}{2} \lim_{\varepsilon \to 0} \sum_{\lambda_i} \varepsilon \, d_{\lambda_i} \lambda_i \, \frac{\partial}{\partial \lambda_i} Z^{(1)}_{\varphi} \; , \\ \beta_{\lambda_i} \;&\equiv\; \mu \frac{d\lambda_i}{d\mu}\Big|_{\varepsilon \to 0} \;=\; \lambda_i \lim_{\varepsilon \to 0} \sum_{\lambda_j} \varepsilon \, d_{\lambda_j} \lambda_j \, \frac{\partial}{\partial \lambda_j} Z^{(1)}_{\lambda_i} \; , \end{aligned} \quad \text{(D.9)}$$

where $\varepsilon \, d_{\lambda}$ is the tree-level scaling dimension of the generic coupling λ in $n = 4 - 2\varepsilon$ dimensions, with $d_{\lambda_i} = 2$ for the scalar quartic couplings, $d_g = d_h = 1$ for the gauge and Yukawa couplings and $d_{\xi} = 0$ for the gauge-fixing parameter. The relations given in (D.9) are based on the derivation presented in [51] where we have applied the fact that the bare coupling constants are related to their renormalised parameters through

$$\lambda^0_i \;=\; \mu^{d_{\lambda_i} \varepsilon} Z_{\lambda_i} \lambda_i \;=\; \mu^{d_{\lambda_i} \varepsilon} (1 + Z^{(1)}_{\lambda_i} + ...) \lambda_i, \quad \text{(D.10)}$$

where we have loopwise expanded Z_{λ_i}. Note that the contribution to Z_{λ_i} at n-loop is a function of order ε^{-n}, $Z_k^n = O(1/\varepsilon^n)$. Similarly, Z_φ can be expanded loop-wise as $Z_\varphi = 1 + Z_\varphi^{(1)} + ...$, where again the contribution at n-loop is a function of order ϵ^{-n}, $Z_\varphi^n = O(1/\epsilon^n)$.

D.2 The One-Loop Anomalous Dimensions and β Functions of the MSISM

We calculate the one-loop anomalous dimensions and β functions of the MSISM in the R_ξ gauge using dimensional regularisation in the $\overline{\text{MS}}$ renormalisation scheme. By employing (D.8) and (D.9) in the symmetric phase of the theory i.e. before EWSSB, we obtain the following anomalous dimensions of the fields

$$
\begin{aligned}
\gamma_\Phi &= \frac{1}{(4\pi)^2}\left[\frac{1}{4}(\xi-3)(3g^2+g'^2)+T_1\right] , \\
\gamma_S &= \frac{1}{(4\pi)^2}\,\frac{1}{2}T_2 , \\
\boldsymbol{\gamma}_{u_L} &= \frac{1}{(4\pi)^2}\left[\frac{1}{2}\Big(\mathbf{h}^u\mathbf{h}^{u\dagger}+\mathbf{h}^d\mathbf{h}^{d\dagger}\Big)+\xi\Big(\frac{4}{3}g_s^2+\frac{3}{4}g^2+\frac{1}{36}g'^2\Big)\mathbf{1}\right] , \\
\boldsymbol{\gamma}_{u_R} &= \frac{1}{(4\pi)^2}\left[\mathbf{h}^{u\dagger}\mathbf{h}^u+\frac{4}{9}\xi\Big(3g_s^2+g'^2\Big)\mathbf{1}\right] , \\
\boldsymbol{\gamma}_{d_L} &= \frac{1}{(4\pi)^2}\left[\frac{1}{2}\Big(\mathbf{h}^u\mathbf{h}^{u\dagger}+\mathbf{h}^d\mathbf{h}^{d\dagger}\Big)+\xi\Big(\frac{4}{3}g_s^2+\frac{3}{4}g^2+\frac{1}{36}g'^2\Big)\mathbf{1}\right] , \\
\boldsymbol{\gamma}_{d_R} &= \frac{1}{(4\pi)^2}\left[\mathbf{h}^{d\dagger}\mathbf{h}^d+\frac{1}{9}\xi\Big(12g_s^2+g'^2\Big)\mathbf{1}\right] ,
\end{aligned}
$$

$$
\begin{aligned}
\boldsymbol{\gamma}_{\nu_L^0} &= \frac{1}{(4\pi)^2}\left[\frac{1}{2}\Big(\mathbf{h}^e\mathbf{h}^{e\dagger}+\mathbf{h}^\nu\mathbf{h}^{\nu\dagger}\Big)+\frac{\xi}{4}\Big(3g^2+g'^2\Big)\,\mathbf{1}\right]\,,\\
\boldsymbol{\gamma}_{\nu_L^{0C}} &= \frac{1}{(4\pi)^2}\left[\frac{1}{2}\Big(\mathbf{h}^{e*}\mathbf{h}^{eT}+\mathbf{h}^{\nu*}\mathbf{h}^{\nu T}\Big)+\frac{\xi}{4}\Big(3g^2+g'^2\Big)\,\mathbf{1}\right]\,,\\
\boldsymbol{\gamma}_{\nu_R^0} &= \frac{1}{(4\pi)^2}\left(\mathbf{h}^{\nu\dagger}\mathbf{h}^{\nu}+\frac{1}{2}\mathbf{h}^{N\dagger}\mathbf{h}^{N}+\frac{1}{2}\tilde{\mathbf{h}}^{N}\tilde{\mathbf{h}}^{N\dagger}\right)\,,\\
\boldsymbol{\gamma}_{\nu_R^{0C}} &= \frac{1}{(4\pi)^2}\left(\mathbf{h}^{\nu T}\mathbf{h}^{\nu *}+\frac{1}{2}\mathbf{h}^{N}\mathbf{h}^{N\dagger}+\frac{1}{2}\tilde{\mathbf{h}}^{N\dagger}\tilde{\mathbf{h}}^{N}\right)\,,
\end{aligned}
\tag{D.11}
$$

where $T_1=\mathrm{Tr}\Big(3\mathbf{h}^u\mathbf{h}^{u\dagger}+3\mathbf{h}^d\mathbf{h}^{d\dagger}+\mathbf{h}^e\mathbf{h}^{e\dagger}+\mathbf{h}^\nu\mathbf{h}^{\nu\dagger}\Big)$ and $T_2=\mathrm{Tr}\Big(\mathbf{h}^{N\dagger}\mathbf{h}^N+\tilde{\mathbf{h}}^{N\dagger}\tilde{\mathbf{h}}^N\Big)$. Notice that $(\boldsymbol{\gamma}_{\nu_L^0})^*=\boldsymbol{\gamma}_{\nu_L^{0C}}$ and $(\boldsymbol{\gamma}_{\nu_R^0})^*=\boldsymbol{\gamma}_{\nu_R^{0C}}$, where we have used $h^N=h^{NT}$ and $\tilde{h}^N=\tilde{h}^{NT}$, which is a consequence of the Majorana constraint on the left-handed and right-handed neutrinos, ν_{iL}^0 and ν_{iR}^0.

Correspondingly, the one-loop β functions of the scalar-potential quartic couplings are

$$
\begin{aligned}
\beta_{\lambda_1} &= \frac{1}{8\pi^2}\Bigg[6\lambda_1^2+\lambda_3^2+4\lambda_4\lambda_4^*+\frac{3}{8}\left(3g^4+2g^2g'^2+g'^4\right)-T_3\\
&\quad -\lambda_1\left(\frac{3}{2}\left(3g^2+g'^2\right)-2T_1\right)\Bigg]\,,\\
\beta_{\lambda_2} &= \frac{1}{8\pi^2}\Bigg[5\lambda_2^2+2\lambda_3^2+4\lambda_4\lambda_4^*+54\lambda_5\lambda_5^*+36\lambda_6\lambda_6^*-\mathrm{Tr}\Big(\mathbf{h}^N\mathbf{h}^{N\dagger}\mathbf{h}^N\mathbf{h}^{N\dagger}\Big)\\
&\quad -2\mathrm{Tr}\Big(\tilde{\mathbf{h}}^N\tilde{\mathbf{h}}^{N\dagger}\mathbf{h}^{N\dagger}\mathbf{h}^N\Big)-2\mathrm{Tr}\Big(\tilde{\mathbf{h}}^{N\dagger}\tilde{\mathbf{h}}^N\mathbf{h}^N\mathbf{h}^{N\dagger}\Big)\\
&\quad -\mathrm{Tr}\Big(\tilde{\mathbf{h}}^{N\dagger}\tilde{\mathbf{h}}^N\tilde{\mathbf{h}}^{N\dagger}\tilde{\mathbf{h}}^N\Big)+\lambda_2T_2\Bigg]\,,\\
\beta_{\lambda_3} &= \frac{1}{8\pi^2}\Bigg[3\lambda_1\lambda_3+2\lambda_2\lambda_3+2\lambda_3^2+8\lambda_4\lambda_4^*+6\lambda_4\lambda_5^*+6\lambda_5\lambda_4^*\\
&\quad -2\mathrm{Tr}\Big(\mathbf{h}^{N\dagger}\mathbf{h}^N\mathbf{h}^{\nu\dagger}\mathbf{h}^\nu\Big)-2\mathrm{Tr}\Big(\tilde{\mathbf{h}}^N\tilde{\mathbf{h}}^{N\dagger}\mathbf{h}^{\nu\dagger}\mathbf{h}^\nu\Big)\\
&\quad -\lambda_3\left(\frac{3}{4}\left(3g^2+g'^2\right)-T_1-\frac{1}{2}T_2\right)\Bigg]\,,
\end{aligned}
$$

$$
\begin{aligned}
\beta_{\lambda_4} &= \frac{1}{8\pi^2}\Bigg[3\lambda_1\lambda_4+\lambda_2\lambda_4+4\lambda_3\lambda_4+3\lambda_3\lambda_5+6\lambda_4^*\lambda_6-2\mathrm{Tr}\Big(\tilde{\mathbf{h}}^N\mathbf{h}^N\mathbf{h}^{\nu\dagger}\mathbf{h}^{\nu}\Big) \\
&\quad -\lambda_4\left(\frac{3}{4}\left(3g^2+g'^2\right)-T_1-\frac{1}{2}T_2\right)\Bigg] , \\
\beta_{\lambda_5} &= \frac{1}{8\pi^2}\Big[9\lambda_2\lambda_5+2\lambda_3\lambda_4+18\lambda_5^*\lambda_6-\mathrm{Tr}\Big(\tilde{\mathbf{h}}^{N\dagger}\tilde{\mathbf{h}}^N\mathbf{h}^N\tilde{\mathbf{h}}^N\Big) \\
&\quad -\mathrm{Tr}\Big(\mathbf{h}^N\mathbf{h}^{N\dagger}\mathbf{h}^N\tilde{\mathbf{h}}^N\Big)+\lambda_5T_2\Big] , \\
\beta_{\lambda_6} &= \frac{1}{8\pi^2}\Big[6\lambda_2\lambda_6+2\lambda_4^2+9\lambda_5^2-\mathrm{Tr}\Big(\tilde{\mathbf{h}}^N\mathbf{h}^N\tilde{\mathbf{h}}^N\mathbf{h}^N\Big)+\lambda_6T_2\Big] ,
\end{aligned}
\tag{D.12}
$$

where $T_3=\mathrm{Tr}\Big(6\,\mathbf{h}^u\mathbf{h}^{u\dagger}\mathbf{h}^u\mathbf{h}^{u\dagger}+6\,\mathbf{h}^d\mathbf{h}^{d\dagger}\mathbf{h}^d\mathbf{h}^{d\dagger}+2\,\mathbf{h}^e\mathbf{h}^{e\dagger}\mathbf{h}^e\mathbf{h}^{e\dagger}+2\,\mathbf{h}^\nu\mathbf{h}^{\nu\dagger}\mathbf{h}^\nu\mathbf{h}^{\nu\dagger}\Big)$. Note that the one-loop β functions of the complex conjugate quartic couplings, e.g. the λ_4^* coupling, are given by $\beta_{\lambda_4^*}=(\beta_{\lambda_4})^*$ etc.

For the one-loop β functions of the $\mathrm{SU}(3)_c$, $\mathrm{SU}(2)_L$ and $\mathrm{U}(1)_Y$ gauge couplings, we use the established results

$$
\beta_{g_s} = -\frac{1}{8\pi^2}\,\frac{7}{2}g_s^3 , \qquad \beta_g = -\frac{1}{8\pi^2}\,\frac{19}{12}g^3 , \qquad \beta_{g'} = \frac{1}{8\pi^2}\,\frac{41}{12}g'^3 . \tag{D.13}
$$

We also present the known one-loop β functions of the Yukawa couplings

$$
\begin{aligned}
\boldsymbol{\beta}_{\mathbf{h}^u} &= \frac{1}{8\pi^2}\left[-\frac{17}{24}g'^2-\frac{9}{8}g^2-4g_s^2+\frac{1}{2}T_1+\frac{3}{4}\left(\mathbf{h}^u\mathbf{h}^{u\dagger}-\mathbf{h}^d\mathbf{h}^{d\dagger}\right)\right]\mathbf{h}^u , \\
\boldsymbol{\beta}_{\mathbf{h}^d} &= \frac{1}{8\pi^2}\left[-\frac{5}{24}g'^2-\frac{9}{8}g^2-4g_s^2+\frac{1}{2}T_1+\frac{3}{4}\left(\mathbf{h}^d\mathbf{h}^{d\dagger}-\mathbf{h}^u\mathbf{h}^{u\dagger}\right)\right]\mathbf{h}^d , \\
\boldsymbol{\beta}_{\mathbf{h}^e} &= \frac{1}{8\pi^2}\left[-\frac{15}{8}g'^2-\frac{9}{2}g^2+\frac{1}{2}T_1+\frac{3}{4}\left(\mathbf{h}^e\mathbf{h}^{e\dagger}-\mathbf{h}^\nu\mathbf{h}^{\nu\dagger}\right)\right]\mathbf{h}^e .
\end{aligned}
\tag{D.14}
$$

Finally, the one-loop β functions of the Dirac and Majorana neutrino Yukawa

couplings are calculated to be

$$\begin{aligned}
\boldsymbol{\beta}_{\tilde{\mathbf{h}}^N} &= \frac{1}{8\pi^2}\Bigg[\tilde{\mathbf{h}}^N\Big(\frac{5}{4}\mathbf{h}^N\mathbf{h}^{N\dagger}+\frac{1}{4}\mathbf{h}^{\tilde{\mathbf{N}}\dagger}\mathbf{h}^{\tilde{\mathbf{N}}}+\frac{1}{2}\mathbf{h}^{\nu T}\mathbf{h}^{\nu *}\Big) \\
&\quad +\Big(\frac{5}{4}\mathbf{h}^{N\dagger}\mathbf{h}^N+\frac{1}{4}\tilde{\mathbf{h}}^N\tilde{\mathbf{h}}^{N\dagger}+\frac{1}{2}\mathbf{h}^{\nu\dagger}\mathbf{h}^{\nu}\Big)\tilde{\mathbf{h}}^N+\frac{1}{4}\tilde{\mathbf{h}}^N T_2\Bigg]\,, \\
\boldsymbol{\beta}_{\mathbf{h}^N} &= \frac{1}{8\pi^2}\Bigg[\mathbf{h}^N\Big(\frac{5}{4}\tilde{\mathbf{h}}^N\tilde{\mathbf{h}}^{N\dagger}+\frac{1}{4}\mathbf{h}^{N\dagger}\mathbf{h}^N+\frac{1}{2}\mathbf{h}^{\nu\dagger}\mathbf{h}^{\nu}\Big) \\
&\quad +\Big(\frac{5}{4}\tilde{\mathbf{h}}^{N\dagger}\tilde{\mathbf{h}}^N+\frac{1}{4}\mathbf{h}^N\mathbf{h}^{N\dagger}+\frac{1}{2}\mathbf{h}^{\nu T}\mathbf{h}^{\nu *}\Big)\mathbf{h}^N+\frac{1}{4}\mathbf{h}^N T_2\Bigg]\,, \\
\boldsymbol{\beta}_{\mathbf{h}^\nu} &= \frac{1}{8\pi^2}\Bigg[\mathbf{h}^\nu\Big(-\frac{3}{8}g'^2-\frac{9}{8}g^2+\frac{1}{2}T_1\Big)+\frac{3}{4}\Big(\mathbf{h}^\nu\mathbf{h}^{\nu\dagger}-\mathbf{h}^e\mathbf{h}^{e\dagger}\Big)\mathbf{h}^\nu \\
&\quad +\frac{1}{4}\mathbf{h}^\nu\Big(\mathbf{h}^{N\dagger}\mathbf{h}^N+\tilde{\mathbf{h}}^N\tilde{\mathbf{h}}^{N\dagger}\Big)\Bigg]\,. \qquad \text{(D.15)}
\end{aligned}$$

The renormalisability of $V_{\rm eff}^{1-\rm loop}$ can be verified by using the one-loop anomalous dimensions of the scalar fields and the β functions of the λ quartic couplings. Specifically, the renormalised potential $V = V^{\rm tree} + V_{\rm eff}^{1-\rm loop}$ should be UV finite i.e. contain no $1/\varepsilon$ terms. In the $\overline{\rm MS}$ renormalisation scheme [35], the one-loop UV counter-terms for the fields and coupling constants are explicitly given by

$$\begin{aligned}
\delta\varphi^{(1)} &= Z_\varphi^{(1)\,1/2}\varphi \;=\; -\frac{1}{2}\left(\frac{1}{\varepsilon}-\gamma+\ln 4\pi\right)\gamma_\varphi\varphi\,, \\
\delta\lambda^{(1)} &= Z_\lambda^{(1)}\lambda \;=\; \frac{1}{2}\left(\frac{1}{\varepsilon}-\gamma+\ln 4\pi\right)\beta_\lambda\,. \qquad \text{(D.16)}
\end{aligned}$$

Taking these relations into account, the one-loop MSISM effective potential

can be renormalised in the $\overline{\rm MS}$ scheme and its complete analytic form is given by

$$
\begin{aligned}
V_{\rm eff}^{1-{\rm loop}} \;=\; & \frac{1}{64\pi^2}\left\{ 2M_{G^\pm}^4\left(-\frac{3}{2}+\ln\frac{M_{G^\pm}^2}{\mu^2}\right)+M_G^4\left(-\frac{3}{2}+\ln\frac{M_G^2}{\mu^2}\right)\right. \\
& +\sum_{i=1}^{3} m_{H_i}^4\left(-\frac{3}{2}+\ln\frac{m_{H_i}^2}{\mu^2}\right)+6M_W^4\left(-\frac{5}{6}+\ln\frac{M_W^2}{\mu^2}\right) \\
& +3M_Z^4\left(-\frac{5}{6}+\ln\frac{M_Z^2}{\mu^2}\right)+2\xi^2 M_W^4\left(-\frac{3}{2}+\ln\frac{\xi M_W^2}{\mu^2}\right) \\
& +\xi^2 M_Z^4\left(-\frac{3}{2}+\ln\frac{\xi M_Z^2}{\mu^2}\right)-4M_{\omega_\pm}^4\left(-\frac{3}{2}+\ln\frac{M_{\omega_\pm}^2}{\bar{\mu}^2}\right) \\
& -2M_{\omega_Z}^4\left(-\frac{3}{2}+\ln\frac{M_{\omega_Z}^2}{\bar{\mu}^2}\right)-12\sum_{i=1}^{3} M_{ui}^4\left(-1+\ln\frac{M_{ui}^2}{\mu^2}\right) \\
& -12\sum_{i=1}^{3} M_{di}^4\left(-1+\ln\frac{M_{di}^2}{\mu^2}\right)-4\sum_{i=1}^{3} M_{ei}^4\left(-1+\ln\frac{M_{ei}^2}{\mu^2}\right) \\
& -2{\rm Tr}\left[(\mathbf{M}_\nu\mathbf{M}_\nu^\dagger)^2\left(-1+\ln\frac{\mathbf{M}_\nu\mathbf{M}_\nu^\dagger}{\mu^2}\right)\right] \\
& \left.-2{\rm Tr}\left[(\mathbf{M}_N\mathbf{M}_N^\dagger)^2\left(-1+\ln\frac{\mathbf{M}_N\mathbf{M}_N^\dagger}{\mu^2}\right)\right]\right\}, \qquad \text{(D.17)}
\end{aligned}
$$

where the mass terms are defined in Appendices B and C. In general, like the unrenormalised $V_{\rm eff}^{1-{\rm loop}}$ given in Appendix C, the one-loop renormalised effective potential is gauge dependent through the ξ-dependent Goldstone boson masses $M_{G^\pm}$ and M_G, the ξ-dependent contributions from the $W^\pm$ and Z bosons and their respective ghost fields masses $M_{\omega_\pm}$ and M_{ω_Z}. However, along a stationary flat direction, where $\mu \to \Lambda$, the ξ-dependent terms cancel against each other. Hence, the complete one-loop renormalised effective potential becomes gauge independent along the flat direction, and consequently at the minimum too.

Appendix E

The Oblique Parameters

Following the formalism and notation of [32], the electroweak oblique parameters S, T and U are defined as

$$\begin{aligned} \alpha_{\rm em}\, S &= 4e^2\Big[\Pi'_{33}(0) - \Pi'_{3Q}(0)\Big] \,, \\ \alpha_{\rm em}\, T &= \frac{e^2}{\sin^2\theta_w \cos^2\theta_w m_Z^2}\Big[\Pi_{11}(0) - \Pi_{33}(0)\Big] \,, \\ \alpha_{\rm em}\, U &= 4e^2\Big[\Pi'_{11}(0) - \Pi'_{33}(0)\Big] \,, \end{aligned} \tag{E.1}$$

where e is the electric charge, $\alpha_{\rm em} = e^2/(4\pi)$ is the electromagnetic fine structure constant and θ_w is the Weinberg or weak mixing angle. The vacuum polarisation amplitudes are decomposed as follows:

$$i\Pi^{\mu\nu}_{XY}(q^2) \;=\; ig^{\mu\nu}\Pi_{XY}(q^2) \;+\; (q^\mu q^\nu \text{terms}) \,, \tag{E.2}$$

where

$$\Pi_{XY}(q^2) \;=\; \Pi_{XY}(0) \;+\; q^2\Pi'_{XY}(q^2) \,, \tag{E.3}$$

and $XY = \{11, 22, 33, 3Q, QQ\}$. The one-particle irreducible self-energies of the A, $W^{\pm}$ and Z gauge bosons are related to the vacuum polarisations through

$$\begin{aligned}
\Pi_{AA} &= e^2\Pi_{QQ} \,, \qquad \Pi_{WW} = \frac{e^2}{\sin^2\theta_w}\Pi_{11} \,, \\
\Pi_{ZA} &= \frac{e^2}{\cos\theta_w \sin\theta_w}\left(\Pi_{3Q} - \sin^2\theta_w\Pi_{QQ}\right) \,, \\
\Pi_{ZZ} &= \frac{e^2}{\cos^2\theta_w \sin^2\theta_w}\left(\Pi_{33} - 2\sin^2\theta_w\Pi_{3Q} + \sin^4\theta_w\Pi_{QQ}\right) \,. \qquad \text{(E.4)}
\end{aligned}$$

Noting the $\sin^2\theta_w$ dependence of Π_{33}, Π_{3Q} and Π_{QQ} in Π_{ZZ}, the S, T and U parameters given in (E.1) can be determined by calculating just two vacuum polarisation amplitudes: Π_{ZZ} and Π_{WW}.

Since we are interested in finding the difference between the electroweak oblique parameters in the MSISM and the corresponding ones in the SM, i.e.

$$\delta P = P_{\text{MSISM}} - P_{\text{SM}} \,, \qquad \text{(E.5)}$$

where $P = \{S, T, U\}$, we need only calculate the contributions from fields which differ between the two models. These differences arise in the scalar sector and, if the MSISM contains right-handed neutrinos, the massive Majorana neutrino sector. We shall consider each contribution separately.

E.1 The Scalar Contribution

The scalar sector of the SM and the MSISM differ by the latter containing an additional complex singlet scalar S. However, since S does not interact with the gauge bosons, it can not contribute to the WW and ZZ self-energies or electroweak oblique parameters. This implies that the difference between the SM and the MSISM contributions to the oblique parameters comes entirely from the definition of the CP-even part of the Φ doublet ϕ. In the SM $\phi = H_{SM}$, whilst, in the MSISM, ϕ is generically linearly composed of the mass eigenstates h and

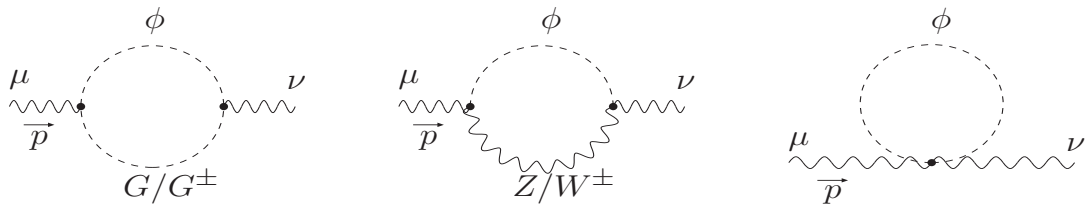

Figure E.1: *The generic Feynman diagrams of the ϕ contributions to the WW and ZZ self-energies.*

$H_{1,2}$:

$$\phi = g_h h + g_{H_1} H_1 + g_{H_2} H_2 \tag{E.6}$$

where the coupling sum rule requires $g_h^2 + g_{H_1}^2 + g_{H_2}^2 = 1$. The shift in the oblique parameters δP (E.5) due to the scalar sector can thus be written as

$$\delta P \;=\; g_h^2 \widetilde{P}(m_h) \;+\; g_{H_1}^2 \widetilde{P}(m_{H_1}) \;+\; g_{H_2}^2 \widetilde{P}(m_{H_2}) \;-\; \widetilde{P}(m_{H_{\rm SM}})\,, \tag{E.7}$$

where $\widetilde{P}(m)$ is the scalar contribution to the oblique parameters from the sum of the three Feynman diagrams for a scalar $\phi = \{H_{\rm SM}, h, H_{1,2}\}$ of mass m, given in Figure E.1. To simplify the calculations we have assumed the SM coupling of the scalars and gauge bosons when calculating the Feynman diagrams. So, to obtain the correct contributions from h and $H_{1,2}$ in (E.7), we multiply their contributions by g_h^2 and $g_{H_{1,2}}^2$ respectively, which gives the correct modified gauge coupling constants.

Explicitly, the three shifts in the oblique parameters are calculated to be

$$\begin{aligned}\widetilde{S}(m) \;=\; & \frac{1}{12\pi}\left[-\frac{1}{\epsilon} - \frac{1}{2} + \frac{m^4(m^2-3m_Z^2)}{(m^2-m_Z^2)^3}\,\ln\left(\frac{m^2}{\bar{\mu}^2}\right)\right. \\ & \left. + \frac{m_Z^4(3m^2-m_Z^2)}{(m^2-m_Z^2)^3}\,\ln\left(\frac{m_Z^2}{\bar{\mu}^2}\right) - \frac{5m^4-22m^2m_Z^2+5m_Z^4}{6\,(m^2-m_Z^2)^2}\right],\end{aligned}$$

$$
\begin{aligned}
\widetilde{T}(m) &= \frac{3}{16\pi \sin^2\theta_w \cos^2\theta_w m_Z^2}\left[\left(\frac{1}{\epsilon}+1\right)(m_Z^2-m_W^2)\right. \\
&+ \frac{m^2 m_W^2}{m^2-m_W^2}\ln\left(\frac{m^2}{\bar{\mu}^2}\right) - \frac{m^2 m_Z^2}{m^2-m_Z^2}\ln\left(\frac{m^2}{\bar{\mu}^2}\right) \\
&\left. - \frac{m_W^4}{m^2-m_W^2}\ln\left(\frac{m_W^2}{\bar{\mu}^2}\right) + \frac{m_Z^4}{m^2-m_Z^2}\ln\left(\frac{m_Z^2}{\bar{\mu}^2}\right)\right], \\
\widetilde{U}(m) &= \frac{1}{12\pi}\left[\frac{m^4(m^2-3m_W^2)}{(m^2-m_W^2)^3}\ln\left(\frac{m^2}{\bar{\mu}^2}\right) - \frac{m^4(m^2-3m_Z^2)}{(m^2-m_Z^2)^3}\ln\left(\frac{m^2}{\bar{\mu}^2}\right)\right. \\
&+ \frac{m_W^4(3m^2-m_W^2)}{(m^2-m_W^2)^3}\ln\left(\frac{m_W^2}{\bar{\mu}^2}\right) + \frac{m_Z^4(m_Z^2-3m^2)}{(m^2-m_Z^2)^3}\ln\left(\frac{m_Z^2}{\bar{\mu}^2}\right) \\
&\left. - \frac{5m^4-22m^2m_W^2+5m_W^4}{6\,(m^2-m_W^2)^2} + \frac{5m^4-22m^2m_Z^2+5m_Z^4}{6\,(m^2-m_Z^2)^2}\right], \qquad \text{(E.8)}
\end{aligned}
$$

where we have applied the standard convention and calculated the electroweak oblique parameters in the Feynman-'t Hooft $\xi = 1$ gauge, in which $m_G = m_Z$ and $m_{G^\pm} = m_{W^\pm}$. Moreover, it is important to note that δS, δT and δU are UV finite and independent of $\bar{\mu}$, which can easily be checked by means of the coupling sum rule.

E.2 The Neutrino Contribution

The inclusion of right handed neutrinos in the MSISM provides another contribution to the electroweak oblique parameters from the light and heavy Majorana neutrinos, $\nu_{1,2,3}$ and $N_{1,2,3}$ respectively. However, these contributions are suppressed, either by the smallness of the light neutrino masses or because they are proportional to $\mathrm{Tr}\,(\mathbf{h}^\nu\,\mathbf{h}^{\nu\,\dagger})^2$, i.e. they are suppressed by the fourth power of the small neutrino Yukawa couplings. Therefore, compared to the dominant scalar-loop effects on the S, T and U parameters, the neutrino contributions can be safely neglected.

E.3 Experimental Values

Since the neutrino contribution is negligible compared to the scalar contribution, the shifts in the electroweak oblique parameters δS, δT and δU are determined from (E.7) and (E.8). To obtain constraints on the values of the parameters of the MSISM from the oblique parameters, the theoretical relations for δS, δT and δU are equated with their experimental values. The experimental values $\delta S_{\rm exp}$, $\delta T_{\rm exp}$ and $\delta U_{\rm exp}$ are presented in [6] as

$$\begin{aligned} \delta S_{\rm exp} &= -0.10 \pm 0.10 \ (-0.08) \ , \\ \delta T_{\rm exp} &= -0.08 \pm 0.11 \ (+0.09) \ , \\ \delta U_{\rm exp} &= 0.15 \pm 0.11 \ (+0.01) \ , \end{aligned} \tag{E.9}$$

where the first uncertainty is evaluated by assuming that $m^{\rm ref}_{H_{\rm SM}} = 117$ GeV, whilst the second one, given in parenthesis, should be added to the first to give the uncertainty for assuming $m^{\rm ref}_{H_{\rm SM}} = 300$ GeV. Since the LEP2 Higgs mass limit as presented in Fig. 10(a) of Ref. [9] is at 95% C.L, we adjust the experimental limits on $\delta S_{\rm exp}$, $\delta T_{\rm exp}$ and $\delta U_{\rm exp}$ to give a corresponding 95% CL interval. The following 95% CL interval limits have been implemented throughout our analysis:

$$\begin{aligned} -0.296 \ &< \ \delta S_{\rm exp} \ < \ 0.096 \ , \\ -0.296 \ &< \ \delta T_{\rm exp} \ < \ 0.136 \ , \\ -0.066 \ &< \ \delta U_{\rm exp} \ < \ 0.366 \ . \end{aligned} \tag{E.10}$$

For clarity, we have chosen the Higgs mass reference value, $m^{\rm ref}_{H_{\rm SM}} = 117$ GeV, even though the derived constraints on the electroweak oblique parameters are independent of the choice of $m^{\rm ref}_{H_{\rm SM}}$.

Bibliography

[1] Ta-Pei Cheng and Ling-Fong Li, "Gauge Theory of Elementary Particle Physics", (1984), Oxford University Press, Great Clarendon Street, Oxford, UK.

[2] I. J. R. Aitchison and A. J. G. Hey, "Gauge Theories in Particle Physics", (1989), Adam Hilger, Bristol.

[3] Michael E. Peskin and Daniel V. Schroeder, "An Introduction to Quantum Field Theory", (1995), Westview Press.

[4] S.L. Glashow, "Partial-symmetries of weak interactions", Nucl. Phys. **22** (1961) 579;
A. Salam and J. C. Ward, "Electromagnetic and weak interactions", Phys. Lett. **13** (1964) 168;
S. Weinberg, "A Model of Leptons", Phys. Rev. Lett. **19** (1967) 1264;
A. Salam, "Weak And Electromagnetic Interactions", *In the Proceedings of 8th Nobel Symposium, Lerum, Sweden, 19-25 May 1968, pp 367-377.*

[5] M. Gell-Mann, "A Schematic Model Of Baryons And Mesons", Phys. Lett. **8** (1964) 214;
G. Zweig, "An SU(3) Model For Strong Interaction Symmetry And Its Breaking", CERN-TH-401;
D. J. Gross and F. Wilczek, "Ultraviolet Behavior Of Non-Abelian Gauge Theories", Phys. Rev. Lett. **30** (1973) 1343;

H. D. Politzer, "Reliable Perturbative Results For Strong Interactions?", Phys. Rev. Lett. **30** (1973) 1346;
H. Fritzsch, M. Gell-Mann and H. Leutwyler, "Advantages Of The Color Octet Gluon Picture", Phys. Lett. B **47** (1973) 365.

[6] C. Amsler *et al.* [Particle Data Group], "Review of particle physics", Phys. Lett. B **667** (2008) 1.

[7] For an example of a prediction of the top quark mass see
U. Amaldi *et al.*, "A Comprehensive Analysis of Data Pertaining to the Weak Neutral Current and the Intermediate Vector Boson Masses", Phys. Rev. D **36** (1987) 1385;
For the first experimental detections of the top quark mass see
F. Abe *et al.* [CDF Collaboration], "Observation of top quark production in $\bar{p}p$ collisions", Phys. Rev. Lett. **74** (1995) 2626 [arXiv:hep-ex/9503002];
S. Abachi *et al.* [D0 Collaboration], "Observation of the top quark", Phys. Rev. Lett. **74** (1995) 2632 [arXiv:hep-ex/9503003].

[8] P. W. Higgs, "Broken symmetries, massless particles and gauge fields", Phys. Lett. **12** (1964) 132;
F. Englert and R. Brout, "Broken symmetry and the mass of gauge vector mesons", Phys. Rev. Lett. **13** (1964) 321;
P. W. Higgs, "Broken symmetries and the masses of gauge bosons", Phys. Rev. Lett. **13** (1964) 508;
G. S. Guralnik, C. R. Hagen and T. W. B. Kibble, "Global conservation laws and massless particles", Phys. Rev. Lett. **13** (1964) 585;
P. W. Higgs, "Spontaneous Symmetry Breakdown without Massless Bosons", Phys. Rev. **145** (1966) 1156;
T. W. B. Kibble, "Symmetry breaking in non-Abelian gauge theories", Phys. Rev. **155** (1967) 1554.

[9] R. Barate *et al.* (the ALEPH Collaboration, the DELPHI Collaboration, the

L3 Collaboration and the OPAL Collaboration, The LEP Working Group for Higgs Boson Searches) "Search for the standard model Higgs boson at LEP", Phys. Lett. B **565** (2003) 61. [arXiv:hep-ex/0306033].

[10] The TEVNPH Working Group of the CDF and D0 Collaborations, "Combined CDF and D0 Upper Limits on Standard Model Higgs-Boson Production with up to 6.7 fb^{-1} of Data", arXiv:1007.4587 [hep-ex].

[11] B. W. Lee, C. Quigg and H. B. Thacker, "Weak Interactions At Very High-Energies: The Role Of The Higgs Boson Mass", Phys. Rev. D **16** (1977) 1519;
W. J. Marciano, G. Valencia and S. Willenbrock, "Renormalization Group Improved Unitarity Bounds On The Higgs Boson And Top Quark Masses", Phys. Rev. D **40** (1989) 1725.

[12] T. Hambye and K. Riesselmann, "Matching conditions and Higgs mass upper bounds revisited", Phys. Rev. D **55** (1997) 7255 [arXiv:hep-ph/9610272].

[13] S. Weinberg, "Implications Of Dynamical Symmetry Breaking", Phys. Rev. D **13** (1976) 974;
E. Gildener, "Gauge Symmetry Hierarchies", Phys. Rev. D **14** (1976) 1667;
S. Weinberg, "Implications Of Dynamical Symmetry Breaking: An Addendum", Phys. Rev. D **19** (1979) 1277;
L. Susskind, "Dynamics Of Spontaneous Symmetry Breaking In The Weinberg-Salam Theory", Phys. Rev. D **20** (1979) 2619.

[14] W. A. Bardeen, "On naturalness in the standard model", preprint FERMILAB-CONF-95-391-T.

[15] K. A. Meissner and H. Nicolai, "Conformal symmetry and the standard model", Phys. Lett. B **648** (2007) 312. [arXiv:hep-th/0612165].

[16] K. A. Meissner and H. Nicolai, "Effective Action, Conformal Anomaly

and the Issue of Quadratic Divergences", Phys. Lett. B **660** (2008) 260. [arXiv:0710.2840 [hep-th]].

[17] G. 't Hooft, "Renormalization Of Massless Yang-Mills Fields", Nucl. Phys. B **33** (1971) 173;
G. 't Hooft and M. J. G. Veltman, "Regularization And Renormalization Of Gauge Fields", Nucl. Phys. B **44** (1972) 189.

[18] R. Foot, A. Kobakhidze, K. L. McDonald and R. R. Volkas, "A solution to the hierarchy problem from an almost decoupled hidden sector within a classically scale invariant theory", Phys. Rev. D **77** (2008) 035006. [arXiv:0709.2750 [hep-ph]].

[19] K. A. Meissner and H. Nicolai, "Conformal invariance from non-conformal gravity", Phys. Rev. D **80** (2009) 086005. [arXiv:0907.3298 [hep-th]].

[20] S. R. Coleman and E. Weinberg, "Radiative Corrections As The Origin Of Spontaneous Symmetry Breaking", Phys. Rev. D **7** (1973) 1888.

[21] E. Gildener and S. Weinberg, "Symmetry Breaking And Scalar Bosons", Phys. Rev. D **13** (1976) 3333.

[22] R. Hempfling, "The Next-to-minimal Coleman-Weinberg model", Phys. Lett. B **379** (1996) 153. [arXiv:hep-ph/9604278].

[23] R. Foot, A. Kobakhidze and R. R. Volkas, "Electroweak Higgs as a pseudo-Goldstone boson of broken scale invariance", Phys. Lett. B **655** (2007) 156. [arXiv:0704.1165 [hep-ph]].

[24] W. F. Chang, J. N. Ng and J. M. S. Wu, "Shadow Higgs from a scale-invariant hidden U(1)s model", Phys. Rev. D **75** (2007) 115016. [arXiv:hep-ph/0701254].

[25] R. Foot, A. Kobakhidze, K. L. McDonald and R. R. Volkas, "Neutrino mass in radiatively-broken scale-invariant models", Phys. Rev. D **76** (2007) 075014. [arXiv:0706.1829 [hep-ph]].

[26] K. A. Meissner and H. Nicolai, "Neutrinos, Axions and Conformal Symmetry", Eur. Phys. J. C **57** (2008) 493. [arXiv:0803.2814 [hep-th]].

[27] S. Iso, N. Okada and Y. Orikasa, "Classically conformal B–L extended Standard Model", Phys. Lett. B **676** (2009) 81. [arXiv:0902.4050 [hep-ph]];
S. Iso, N. Okada and Y. Orikasa, "The minimal B-L model naturally realized at TeV scale", Phys. Rev. D **80** (2009) 115007 [arXiv:0909.0128 [hep-ph]].

[28] R. Foot, A. Kobakhidze and R. R. Volkas, "Stable mass hierarchies and dark matter from hidden sectors in the scale-invariant standard model", Phys. Rev. D **82** (2010) 035005 [arXiv:1006.0131 [hep-ph]].

[29] L. Alexander-Nunneley and A. Pilaftsis, "The Minimal Scale Invariant Extension of the Standard Model", JHEP **1009** (2010) 021 [arXiv:1006.5916 [hep-ph]].

[30] D. O'Connell, M. J. Ramsey-Musolf and M. B. Wise, "Minimal Extension of the Standard Model Scalar Sector", Phys. Rev. D **75** (2007) 037701. [arXiv:hep-ph/0611014].

[31] V. Barger, P. Langacker, M. McCaskey, M. J. Ramsey-Musolf and G. Shaughnessy, "LHC Phenomenology of an Extended Standard Model with a Real Scalar Singlet", Phys. Rev. D **77** (2008) 035005 [arXiv:0706.4311 [hep-ph]];
V. Barger, P. Langacker, M. McCaskey, M. Ramsey-Musolf and G. Shaughnessy, "Complex Singlet Extension of the Standard Model", Phys. Rev. D **79** (2009) 015018. [arXiv:0811.0393 [hep-ph]].

[32] M. E. Peskin and T. Takeuchi, "A New constraint on a strongly interacting Higgs sector", Phys. Rev. Lett. **65** (1990) 964;

M. E. Peskin and T. Takeuchi, "Estimation of oblique electroweak corrections", Phys. Rev. D **46** (1992) 381.

[33] For an alternative formulation, see
G. Altarelli and R. Barbieri, "Vacuum polarization effects of new physics on electroweak processes", Phys. Lett. B **253** (1991) 161;
G. Altarelli, R. Barbieri and S. Jadach, "Toward a model independent analysis of electroweak data", Nucl. Phys. B **369** (1992) 3.

[34] P. Minkowski, "$\mu \to e\gamma$ At A Rate Of One Out Of 1-Billion Muon Decays?", Phys. Lett. B **67** (1977) 421;
M. Gell-Mann, P. Ramond and R. Slansky, "Complex Spinors And Unified Theories" in *Supergravity*, eds. D.Z. Freedman and P. van Nieuwenhuizen (North-Holland, Amsterdam, 1979);
T. Yanagida, "Horizontal Symmetry And Masses Of Neutrinos" in proceedings of the *Workshop on the Unified Theory and the Baryon Number in the Universe*, eds. O. Sawada and A. Sugamoto, Tsukuba, Japan, 1979;
R. N. Mohapatra and G. Senjanović, "Neutrino mass and spontaneous parity nonconservation", Phys. Rev. Lett. **44**, 912 (1980).

[35] G. 't Hooft, "Dimensional regularization and the renormalization group", Nucl. Phys. B **61** (1973) 455;
S. Weinberg, "New approach to the renormalization group", Phys. Rev. D **8** (1973) 3497.

[36] V. Elias, R. B. Mann, D. G. C. McKeon and T. G. Steele, "Radiative electroweak symmetry breaking beyond leading logarithms", Can. J. Phys. **84** (2006) 545 [arXiv:hep-ph/0508107].

[37] F. A. Chishtie, T. Hanif, J. Jia, R. B. Mann, D. G. C. McKeon, T. N. Sherry

and T. G. Steele, "Can the Renormalization Group Improved Effective Potential be used to estimate the Higgs Mass in the Conformal Limit of the Standard Model?", arXiv:1006.5887 [hep-ph].

[38] A. D. Sakharov, "Violation of CP Invariance, c Asymmetry, and Baryon Asymmetry of the Universe", Pisma Zh. Eksp. Teor. Fiz. **5** (1967) 32, [JETP Lett. **5** (1967) 24], [Sov. Phys. Usp. **34** (1991) 392], [Usp. Fiz. Nauk **161** (1991) 61].

[39] M. Kobayashi and T. Maskawa, "CP Violation In The Renormalizable Theory Of Weak Interaction", Prog. Theor. Phys. **49** (1973) 652.

[40] G. C. Branco, J. M. Gerard and W. Grimus, "Geometrical T Violation", Phys. Lett. B **136** (1984) 383.

[41] V. Silveira and A. Zee, "Scalar Phantoms", Phys. Lett. B **161** (1985) 136;
J. McDonald, "Gauge Singlet Scalars as Cold Dark Matter", Phys. Rev. D **50** (1994) 3637 [arXiv:hep-ph/0702143].

[42] A. Djouadi, W. Kilian, M. Muhlleitner and P. M. Zerwas, "Testing Higgs Self-couplings at e^+e^- Linear Colliders", Eur. Phys. J. C **10** (1999) 27 [arXiv:hep-ph/9903229];
D. J. . Miller and S. Moretti, "Can the trilinear Higgs self-coupling be measured at future linear colliders?", Eur. Phys. J. C **13** (2000) 459 [arXiv:hep-ph/9906395];
T. Binoth, S. Karg, N. Kauer and R. Ruckl, "Multi-Higgs boson production in the standard model and beyond", Phys. Rev. D **74** (2006) 113008 [arXiv:hep-ph/0608057].

[43] G. Aad *et al.* [The ATLAS Collaboration], "Expected Performance of the ATLAS Experiment - Detector, Trigger and Physics", arXiv:0901.0512 [hep-ex].

[44] A. Pilaftsis, "Radiatively induced neutrino masses and large Higgs neutrino couplings in the standard model with Majorana fields", Z. Phys. C **55** (1992) 275 [arXiv:hep-ph/9901206].

[45] K. Fujikawa, B. W. Lee and A. I. Sanda, "Generalized Renormalizable Gauge Formulation Of Spontaneously Broken Gauge Theories", Phys. Rev. D **6** (1972) 2923;
Y. P. Yao, "Quantization and gauge freedom in a theory with spontaneously broken symmetry", Phys. Rev. D **7** (1973) 1647.

[46] R. Jackiw, "Functional evaluation of the effective potential", Phys. Rev. D **9** (1974) 1686.

[47] J. Zinn-Justin, "Quantum Field Theory and Critical Phenomena", Fourth Edition (2002), Oxford University Press, Great Clarendon Street, Oxford, UK.

[48] N. K. Nielsen, "Gauge Invariance And Broken Conformal Symmetry", Nucl. Phys. B **97** (1975) 527;
N. K. Nielsen, "On The Gauge Dependence Of Spontaneous Symmetry Breaking In Gauge Theories", Nucl. Phys. B **101** (1975) 173.

[49] L. P. Alexander and A. Pilaftsis, "The One-Loop Effective Potential in Non-Linear Gauges", J. Phys. G **36** (2009) 045006 [arXiv:0809.1580 [hep-ph]].

[50] D. Binosi, J. Papavassiliou and A. Pilaftsis, "Displacement operator formalism for renormalization and gauge dependence to all orders", Phys. Rev. D **71** (2005) 085007. [arXiv:hep-ph/0501259].

[51] M. E. Machacek and M. T. Vaughn, "Two Loop Renormalization Group Equations In A General Quantum Field Theory. 1. Wave Function Renormalization", Nucl. Phys. B **222** (1983) 83.